High-Energy Emission from Star Forming Regions

Gustavo E. Romero

Instituto Argentino de Radio Astronomía (IAR-CCT CONICET)
FCAG, Universidad Nacional de La Plata

Dublin Summer School on High Energy Astrophysics
4th - 15th July 2011

Contact: romero@iar-conicet.gov.ar

The Life Cycle of Stars

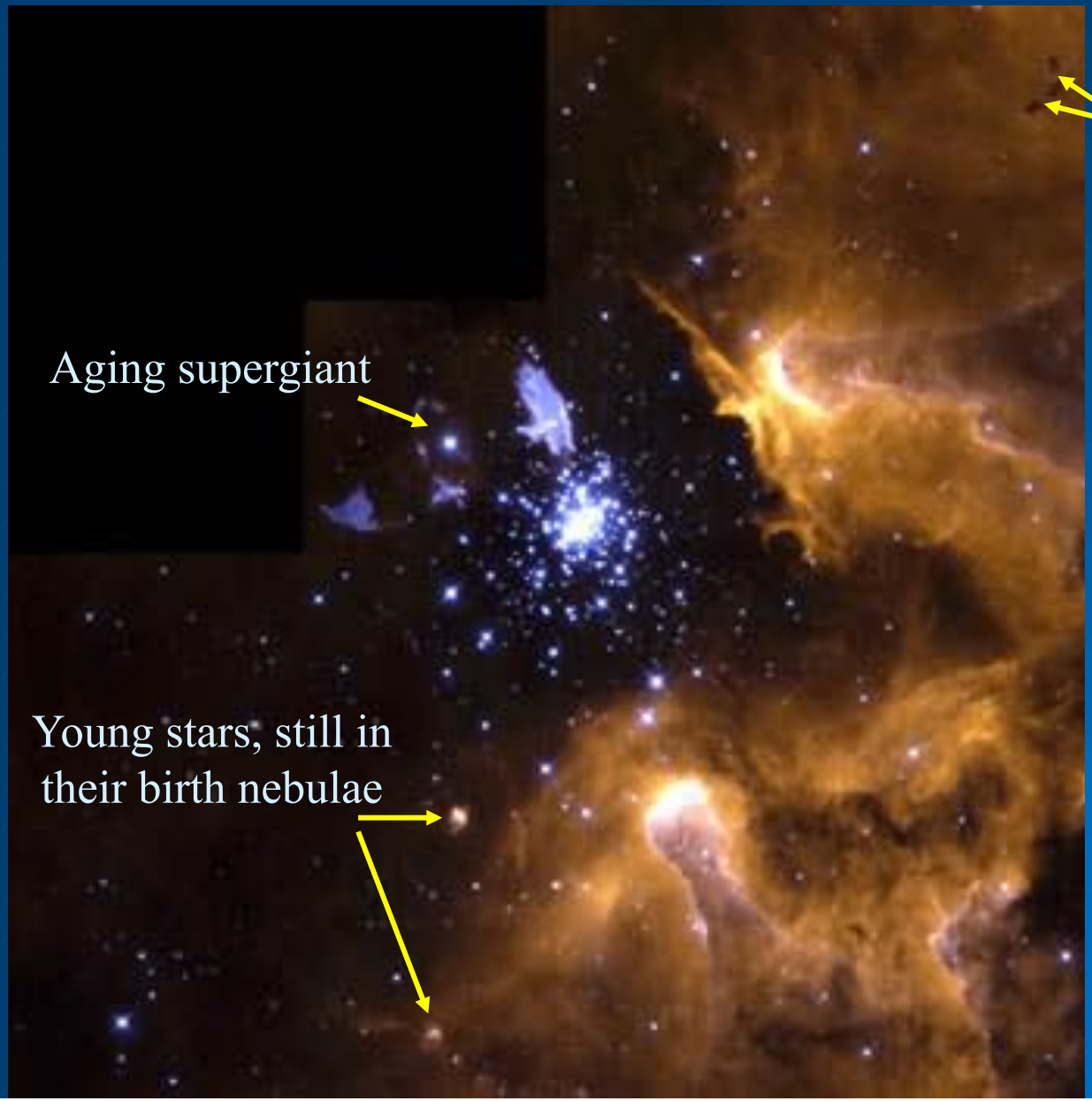

Giant Molecular Clouds

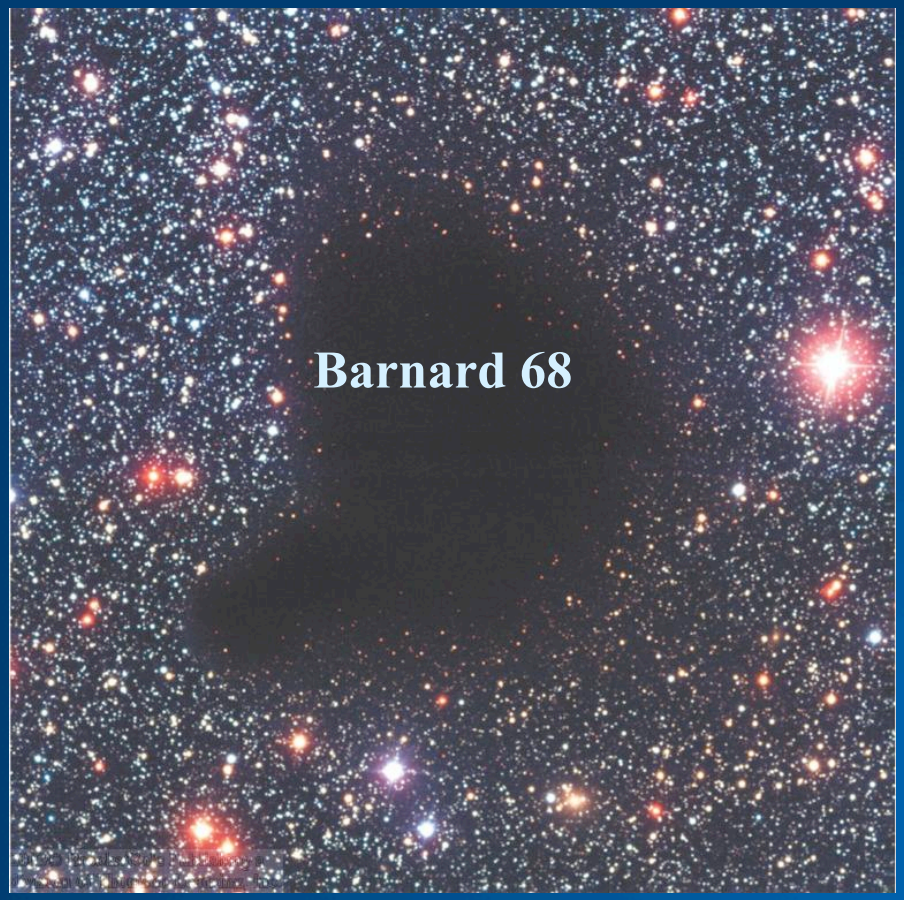

Visible

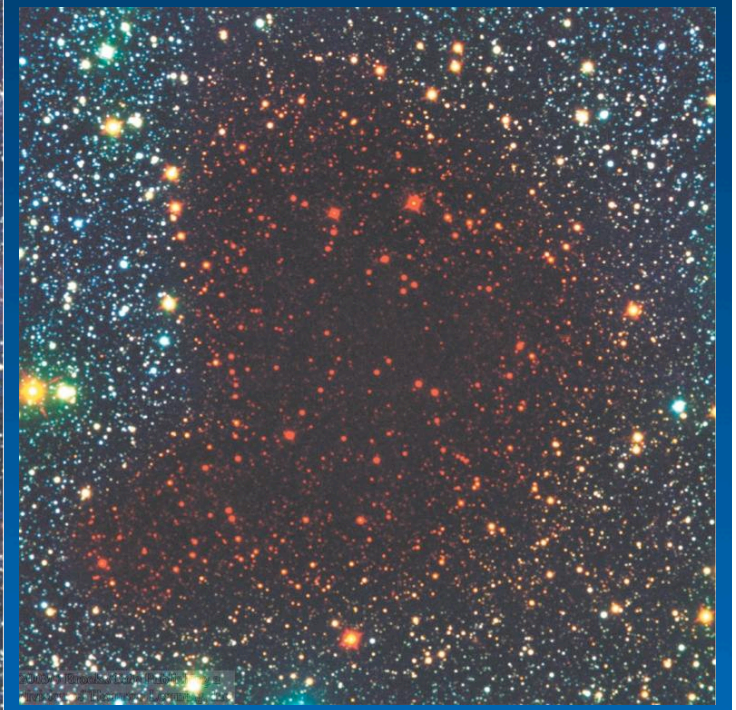

Infrared

Star formation → collapse of the cores of *giant molecular clouds*: Dark, cold, dense clouds obscuring the light of stars behind them.

(More transparent in infrared light)

Parameters of Giant Molecular Clouds

Size: r ~ 50 pc

Mass: > 100,000 M_{sun}

Temp.: a few K

Dense cores:

R ~ 0.1 pc

M ~ 10 M_{sun}

Much too cold and too low density to ignite thermonuclear processes

Clouds need to contract and heat up in order to form stars.

Contraction of Giant Molecular Cloud Cores

- Gravity
- Thermal Energy (pressure)
- Magnetic Fields
- Rotation (angular momentum)
- Turbulence

→ External trigger required to initiate the collapse of clouds to form stars.

Shocks Triggering Star Formation

Globules = sites where stars are being born *right now!*

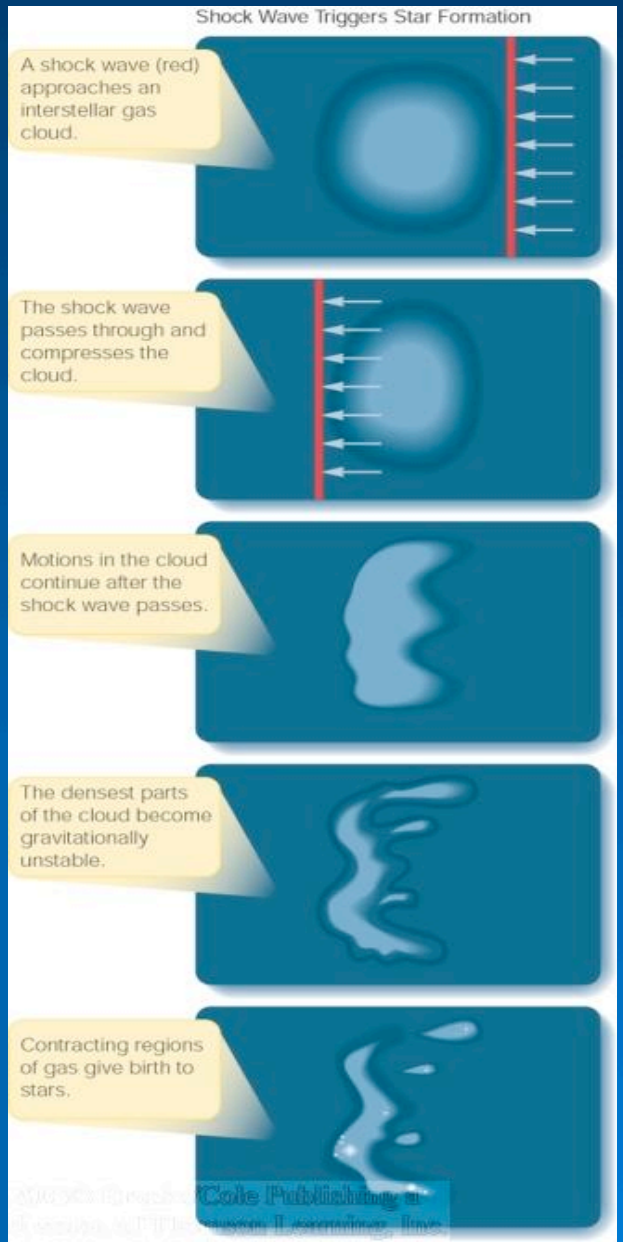

Jeans instability

$$\lambda_J = \sqrt{\frac{\pi c_s^2}{G\rho}} \propto \left(\frac{T}{\rho}\right)^{1/2}.$$

$$M_J \equiv \frac{\pi\rho}{6}\left(\frac{\pi s^2}{G\rho}\right)^{3/2} < M_{\text{ref}}$$

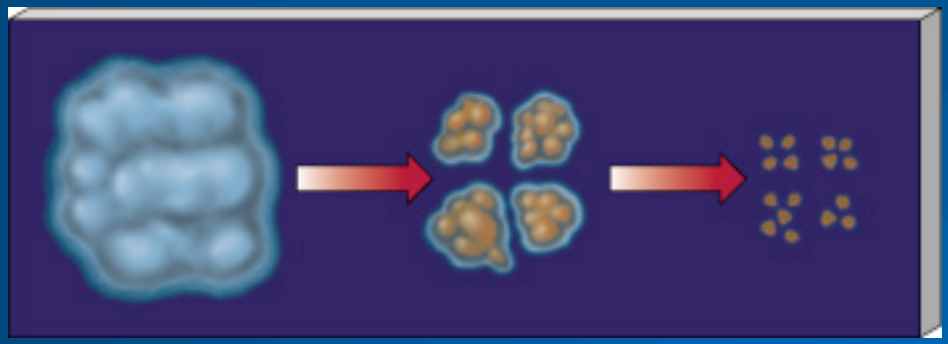

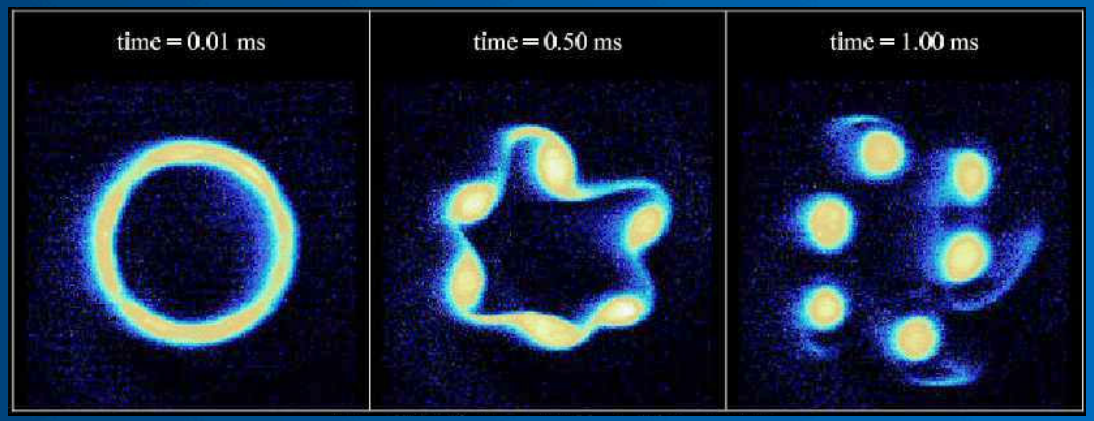

Sources of Shock Waves Triggering Star Formation (1)

Previous star formation can trigger further star formation through:

a) Shocks from supernovae (explosions of massive stars):

Massive stars die young => Supernovae tend to happen near sites of recent star formation

Sources of Shock Waves Triggering Star Formation (2)

Previous star formation can trigger further star formation through:

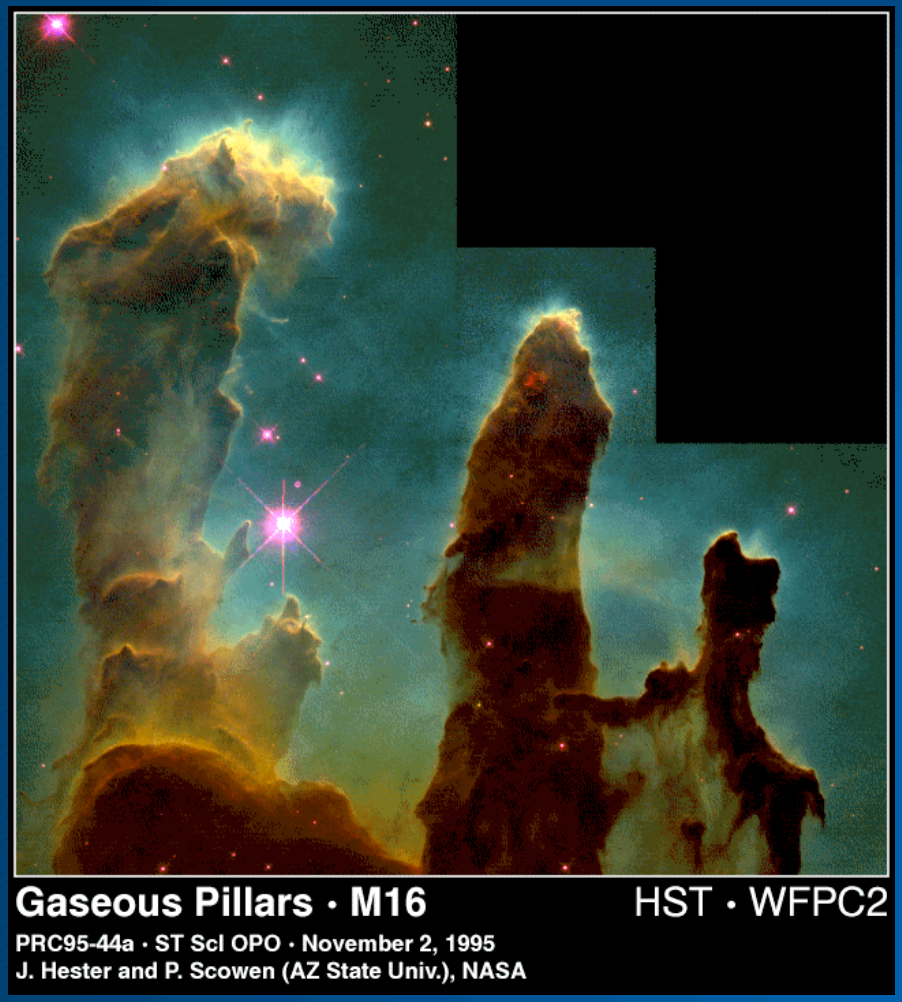

b) Ionization fronts and winds of hot, massive O or B stars.

Massive stars live fast and furiously => O and B stars only exist near sites of recent star formation

Sources of Shock Waves Triggering Star Formation (3)

c) Collisions of giant molecular clouds.

Sources of Shock Waves Triggering Star Formation (4)

d) Spiral arms in galaxies like our Milky Way:

Spirals' arms are probably rotating shock wave patterns.

Protostars

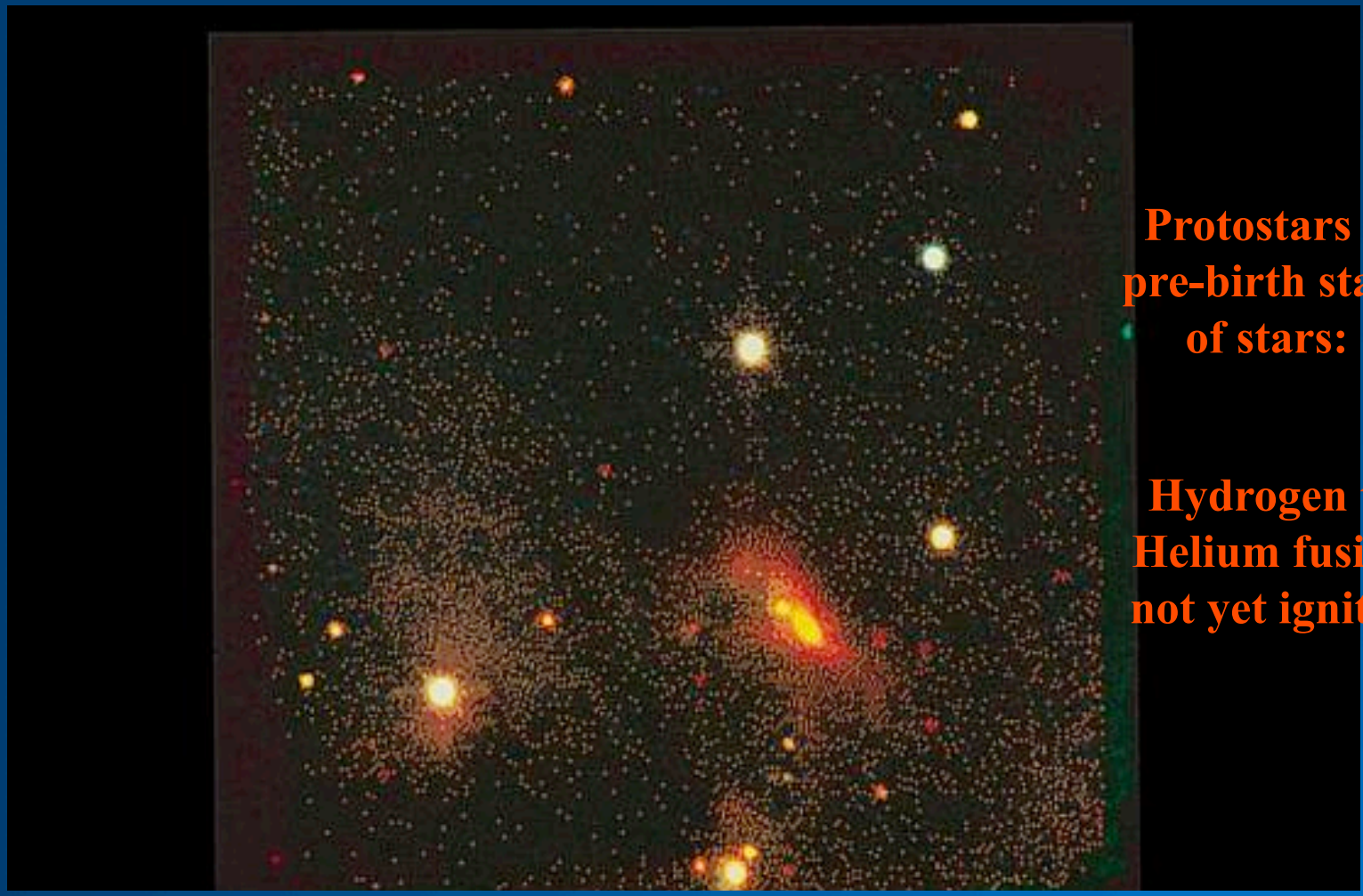

Protostars = pre-birth state of stars:

Hydrogen to Helium fusion not yet ignited

Still enshrouded in opaque “cocoons” of dust => barely visible in the optical, but bright in the infrared.

Protostellar Disks and Jets – Herbig Haro Objects

Disks of matter accreted onto the protostar ("accretion disks") often lead to the formation of jets (directed outflows; bipolar outflows): Herbig Haro Objects

Protostellar Disks and Jets – Herbig Haro Objects (2)

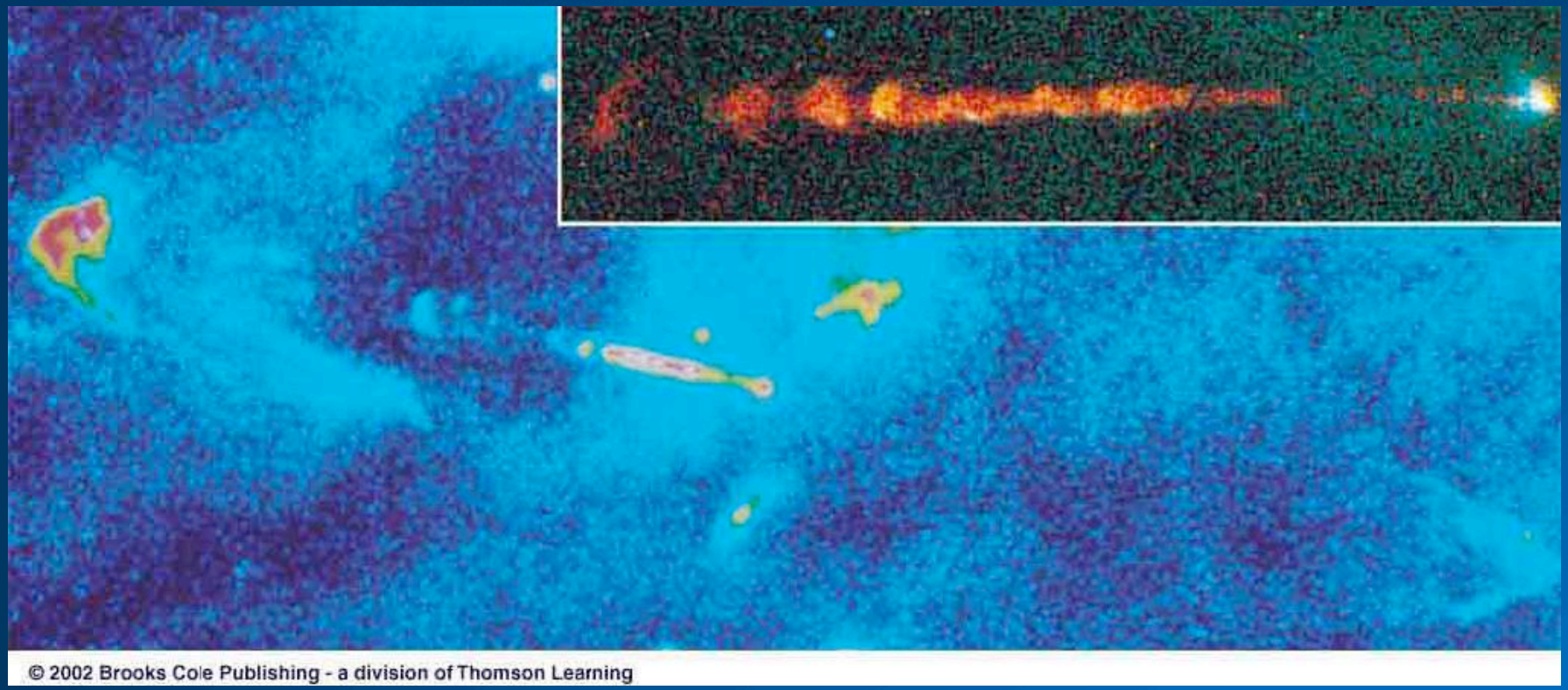

Herbig Haro Object HH34

Protostellar Disks and Jets – Herbig Haro Objects (3)

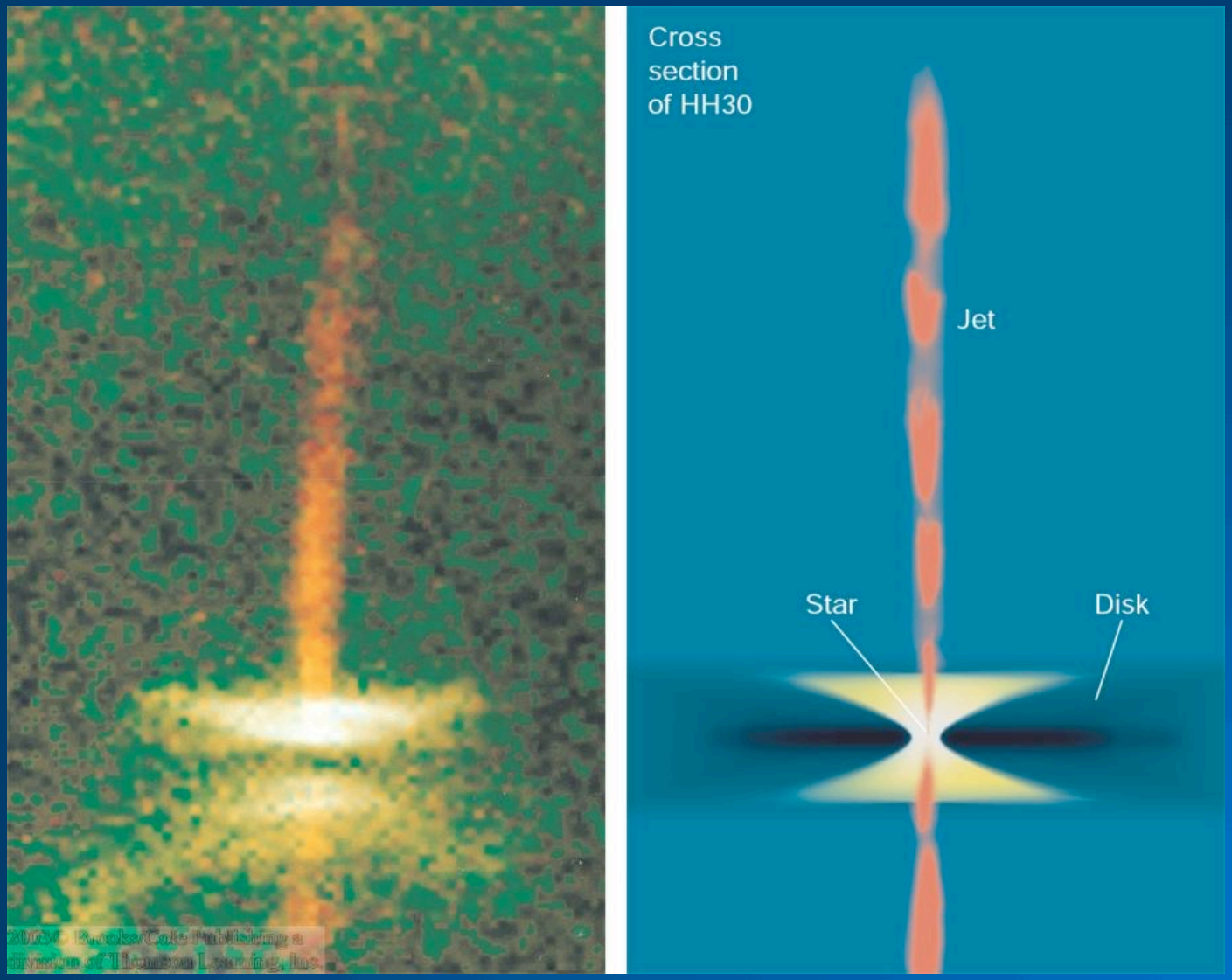

Herbig Haro Object HH30

Protostellar Disks and Jets – Herbig Haro Objects (4)

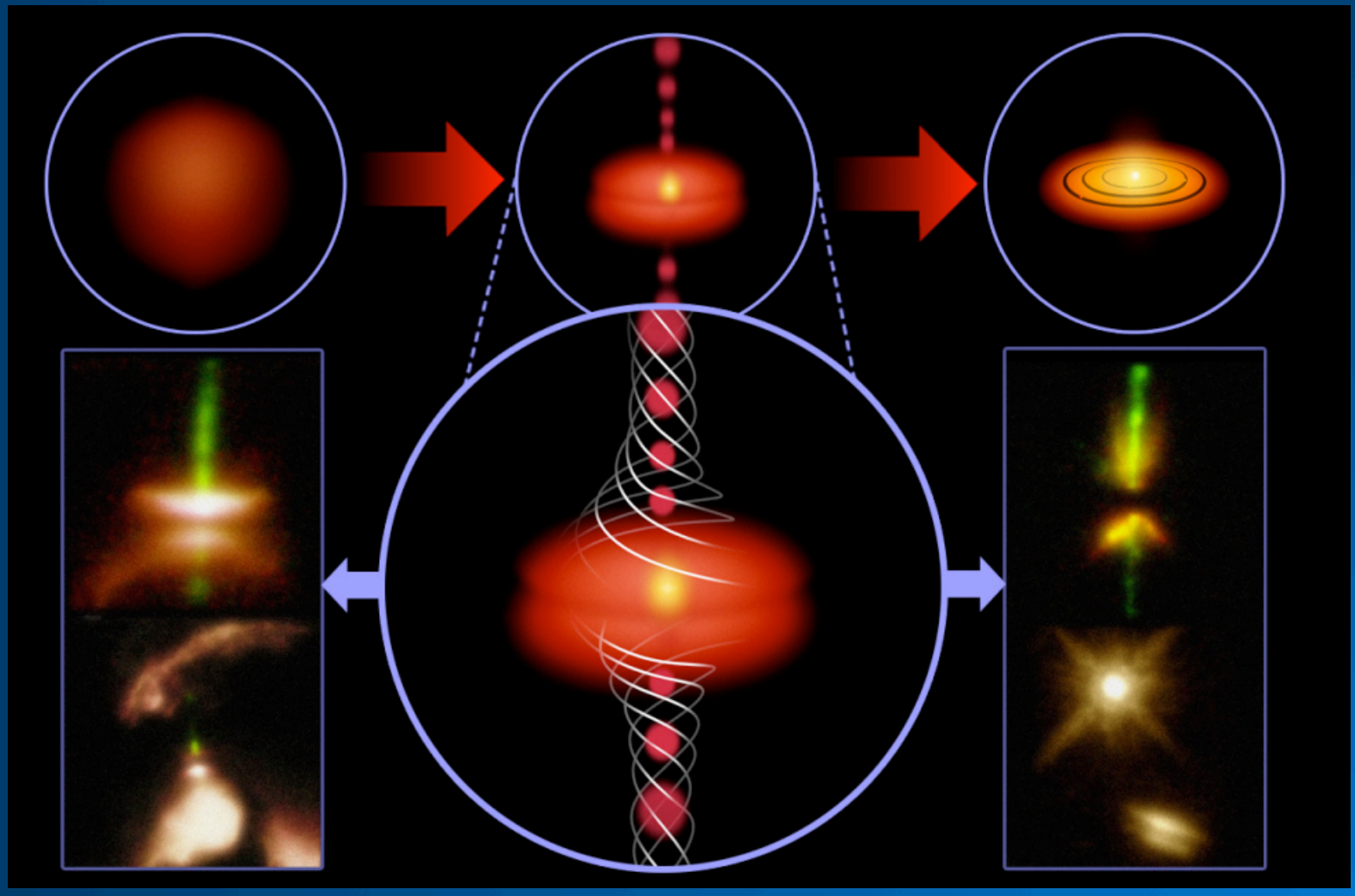

Herbig-Haro objects (5)

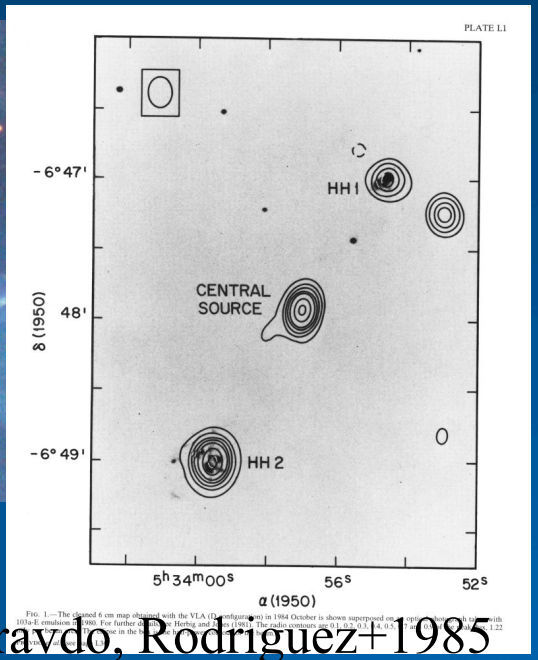

Pravdo, Rodriguez+1985

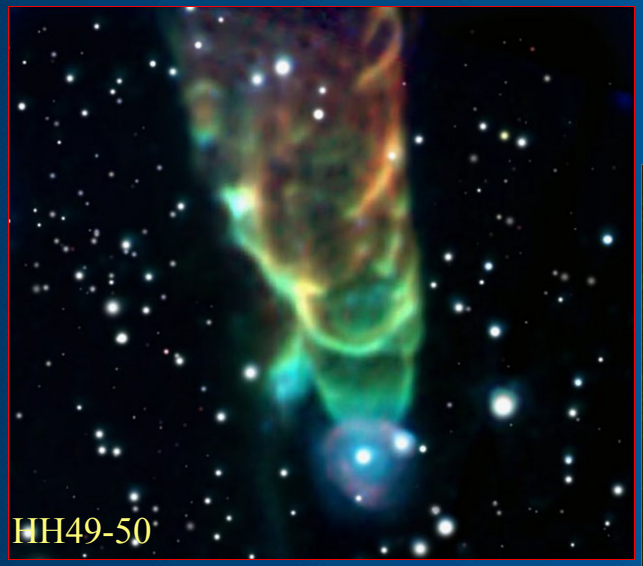

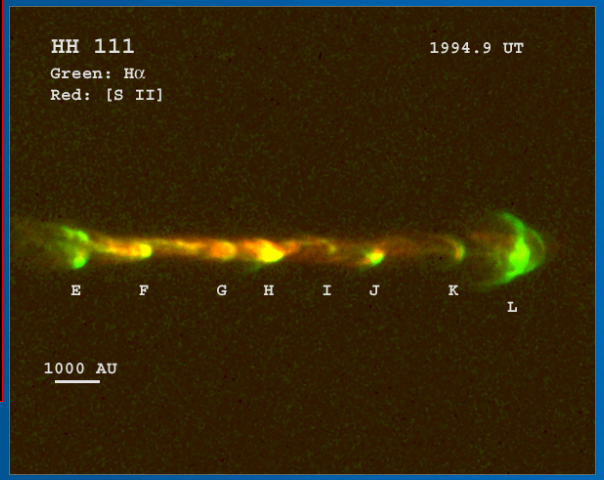

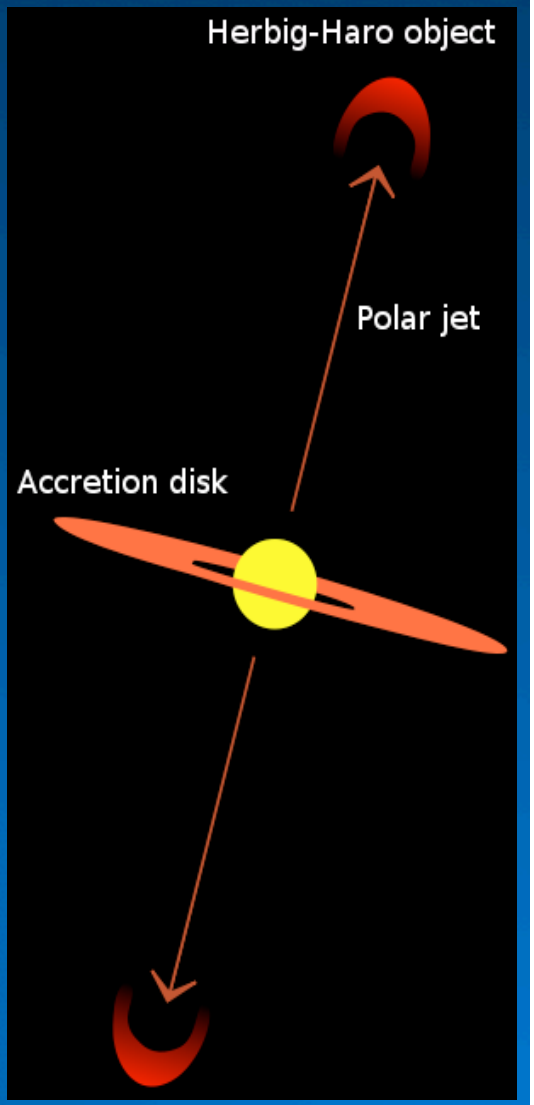

HH Disks

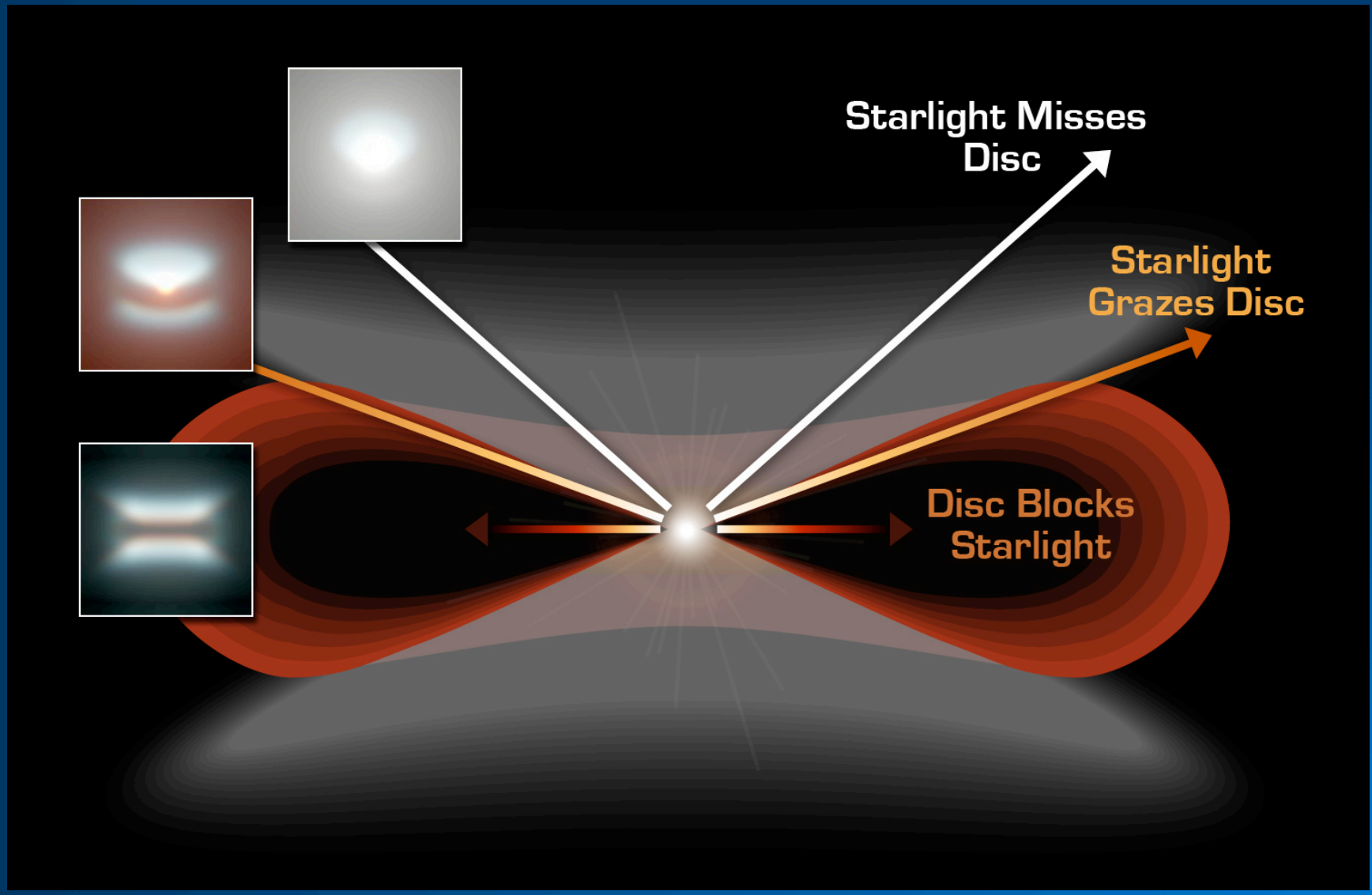
Starlight Misses Disc
Starlight Grazes Disc
Disc Blocks Starlight

Evidence of Star Formation

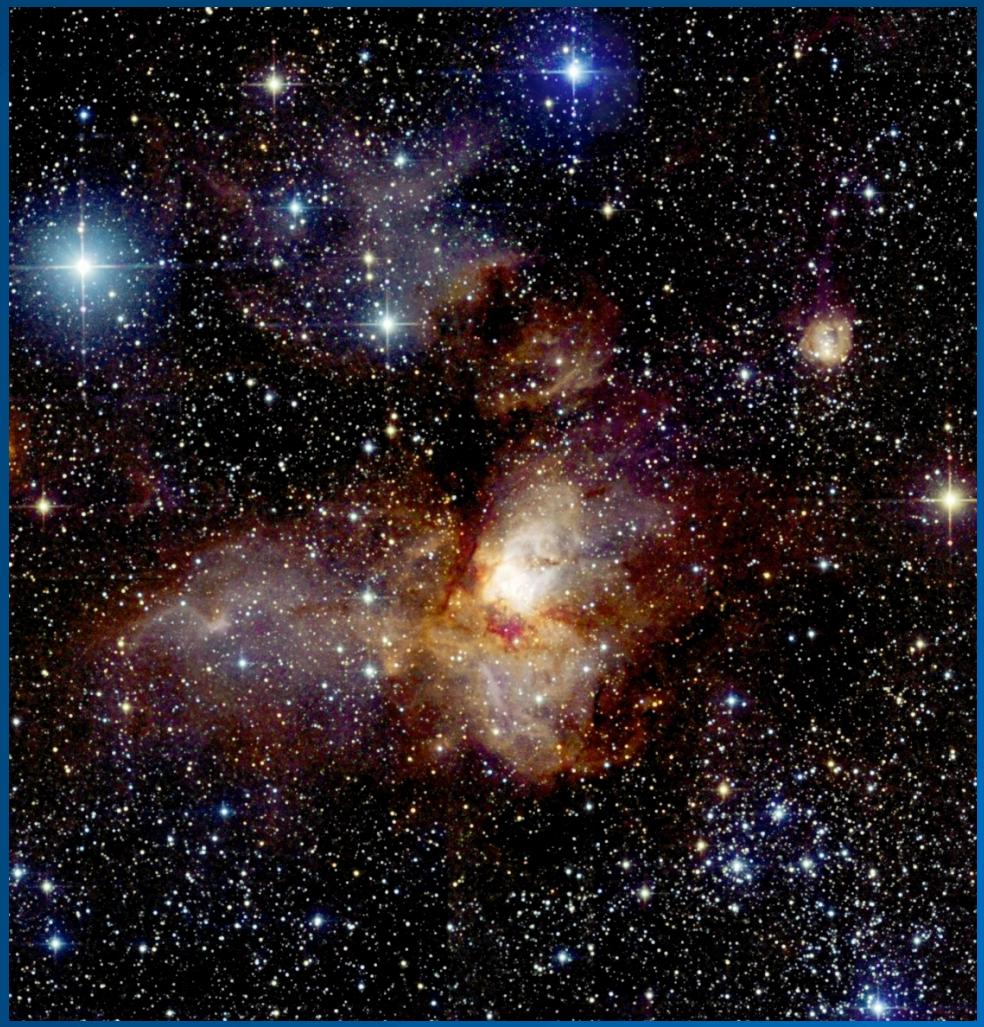

Star Forming Region RCW 38

Globules

Bok Globules:

~ 10 to 1000 solar masses;

contracting to form protostars

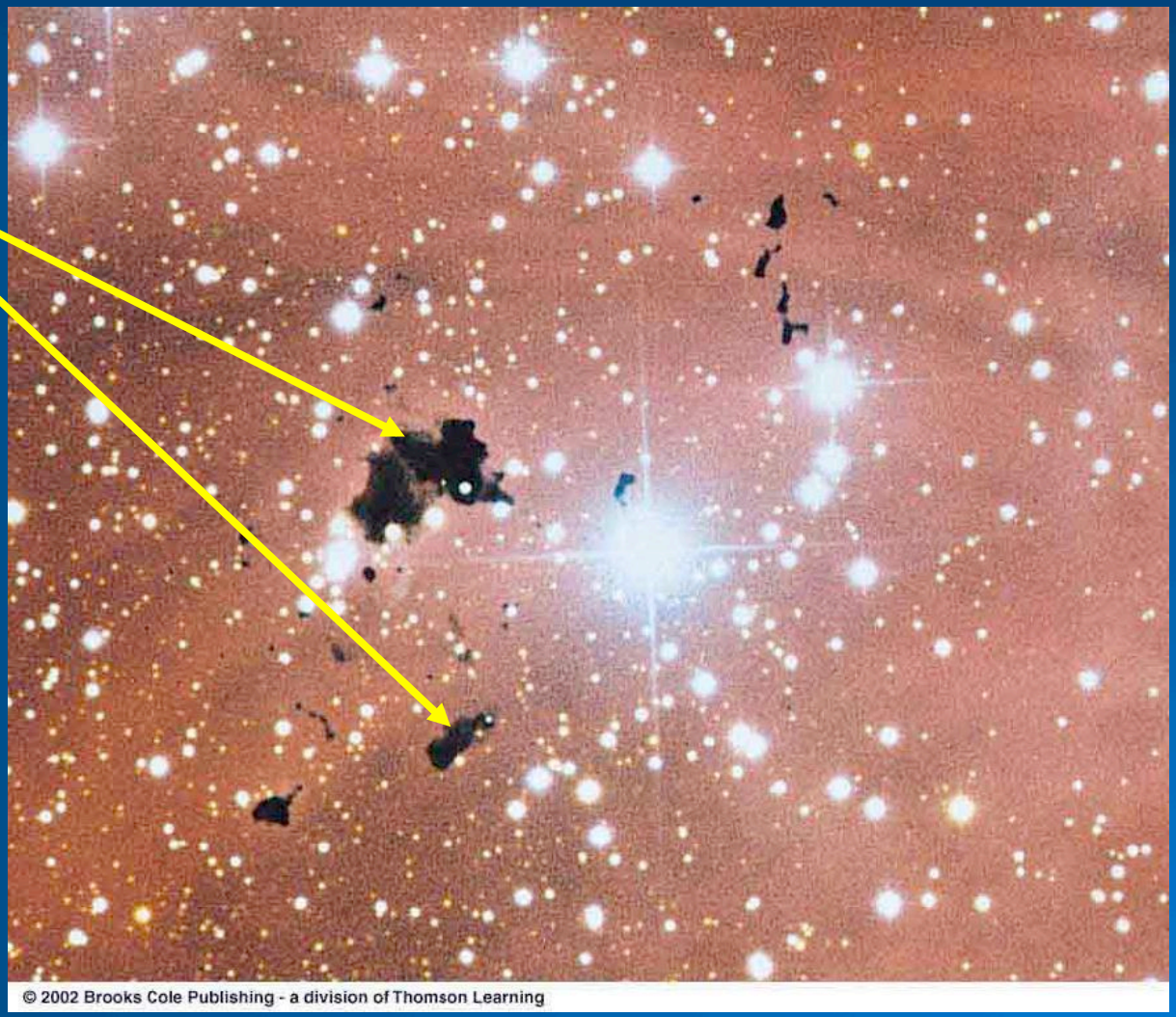

Globules (2)

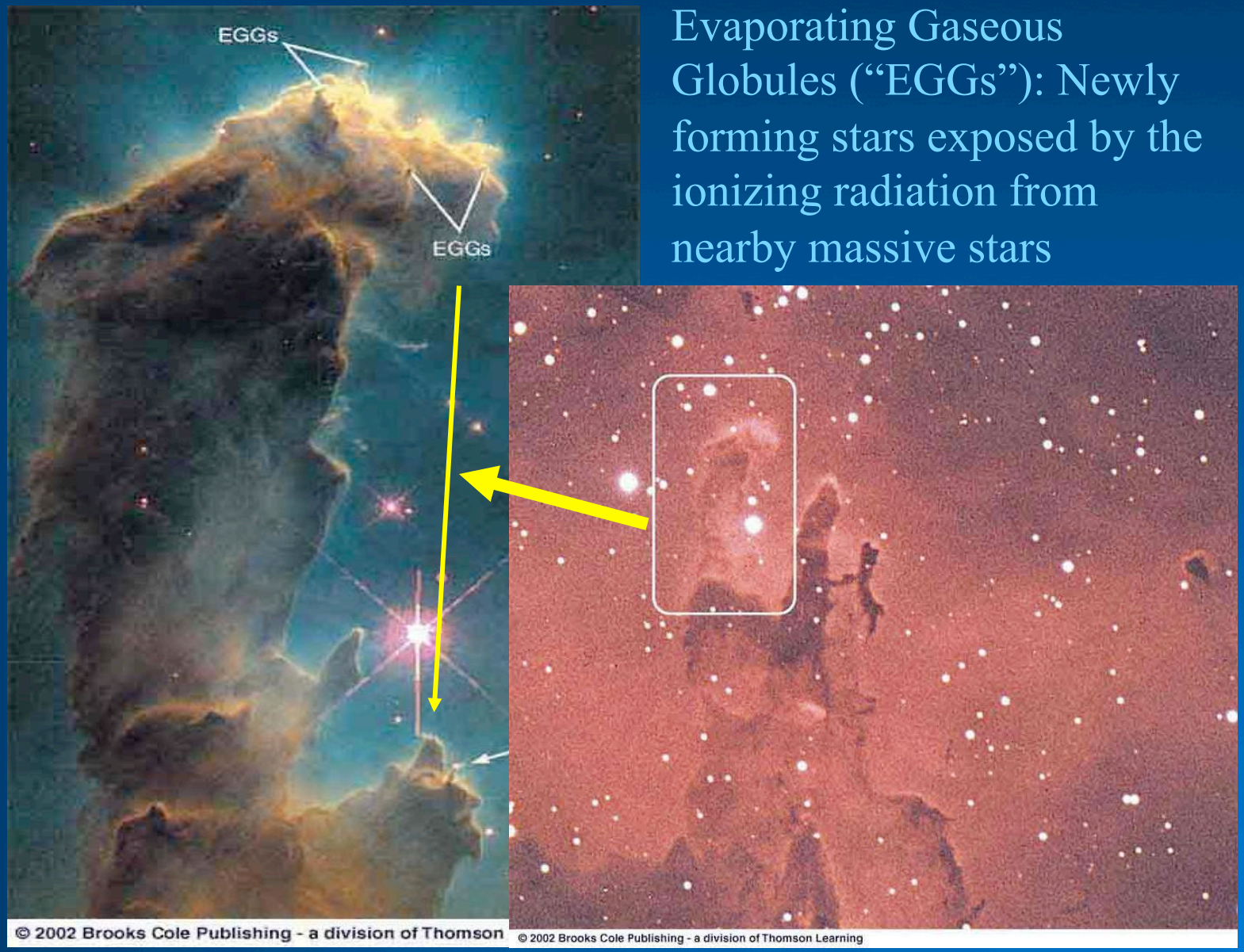

Evaporating Gaseous Globules ("EGGs"): Newly forming stars exposed by the ionizing radiation from nearby massive stars

Open Clusters of Stars

Open Cluster M7

Large masses of Giant Molecular Clouds => Stars do not form isolated, but in large groups, called *Open Clusters of Stars*.

Open Clusters of Stars (2)

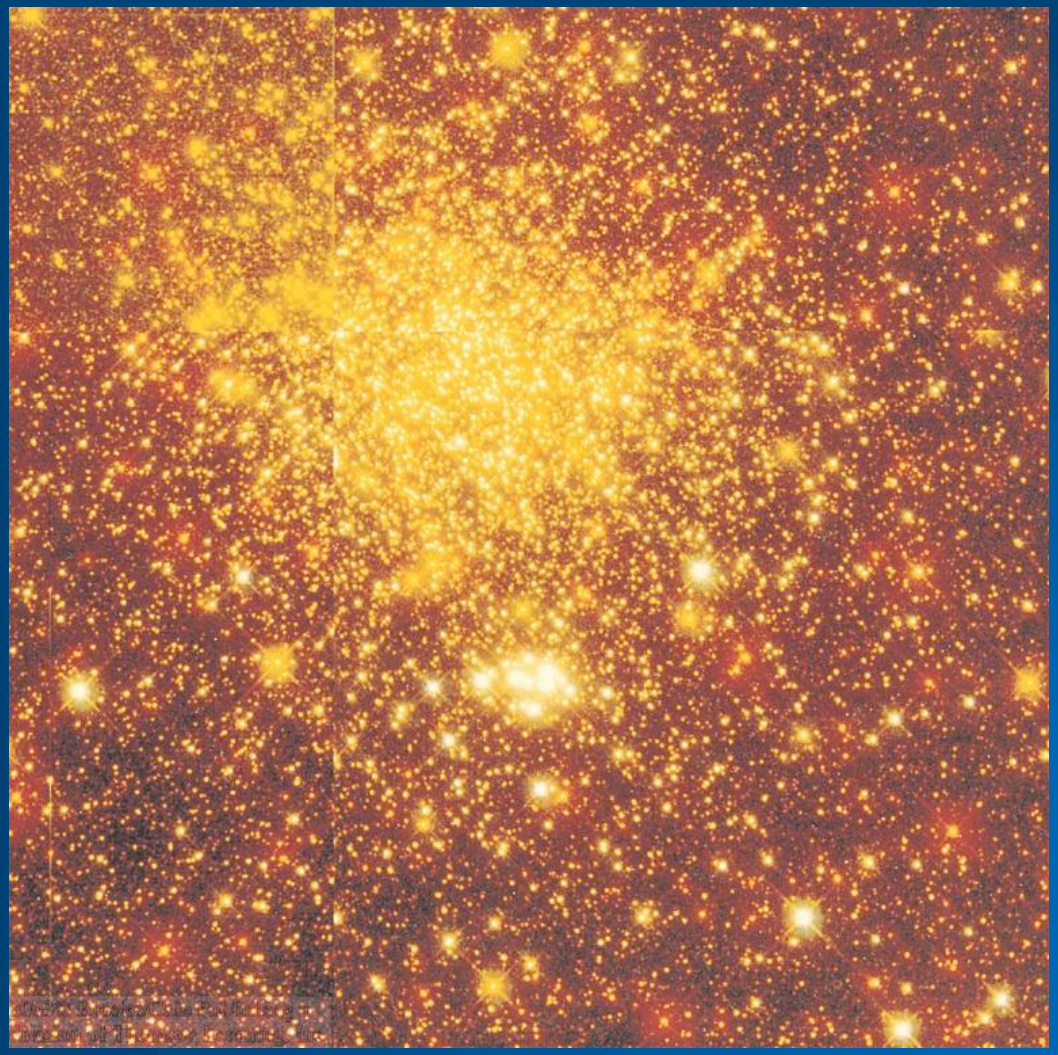

Large, dense cluster of (yellow and red) stars in the foreground; ~ 50 million years old

Scattered individual (bright, white) stars in the background; only ~ 4 million years old

Luminosity versus Mass

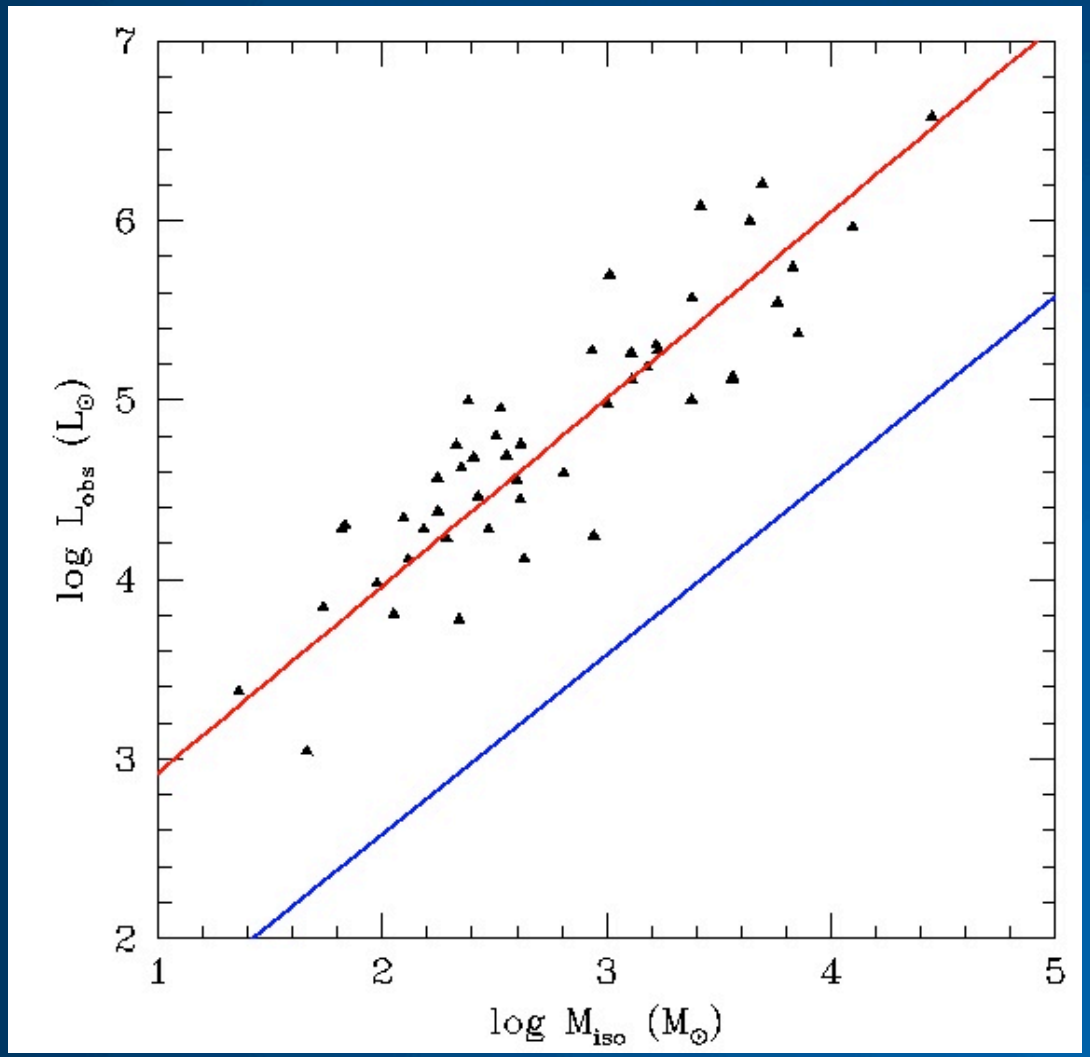

Log Luminosity vs. Log M

red line: masses of dense cores from dust
Log L = 1.9 + log M

blue line: masses of GMCs from CO
Log L = 0.6 + log M

L/M much higher for dense cores than for whole GMCs.

Mueller et al. (2002)

Low Mass vs. High Mass

- Low Mass star formation
  - "Isolated" (time to form < time to interact)
  - Low turbulence (less than thermal support)
  - Slow infall
  - Nearby (~ 100 pc)
- High Mass star formation
  - "Clustered"
  - Time to form may exceed time to interact
  - Turbulence >> thermal
  - Fast infall?
  - More distant (>400 pc)

Properties of Molecular Clouds

Type	n [cm^{-3}]	Size [pc]	T [K]	Mass [M_{sun}]
Giant Molecular Cloud	10^2	50	15	10^5
Dark Cloud Complex	$5x10^2$	10	10	10^4
Individual Dark Cloud	10^3	2	10	30
Dense low-mass cores	10^4	0.1	10	10
Dense high-mass cores	$>10^5$	0.1-1	10-30	100-1000

Discovery of outflows I

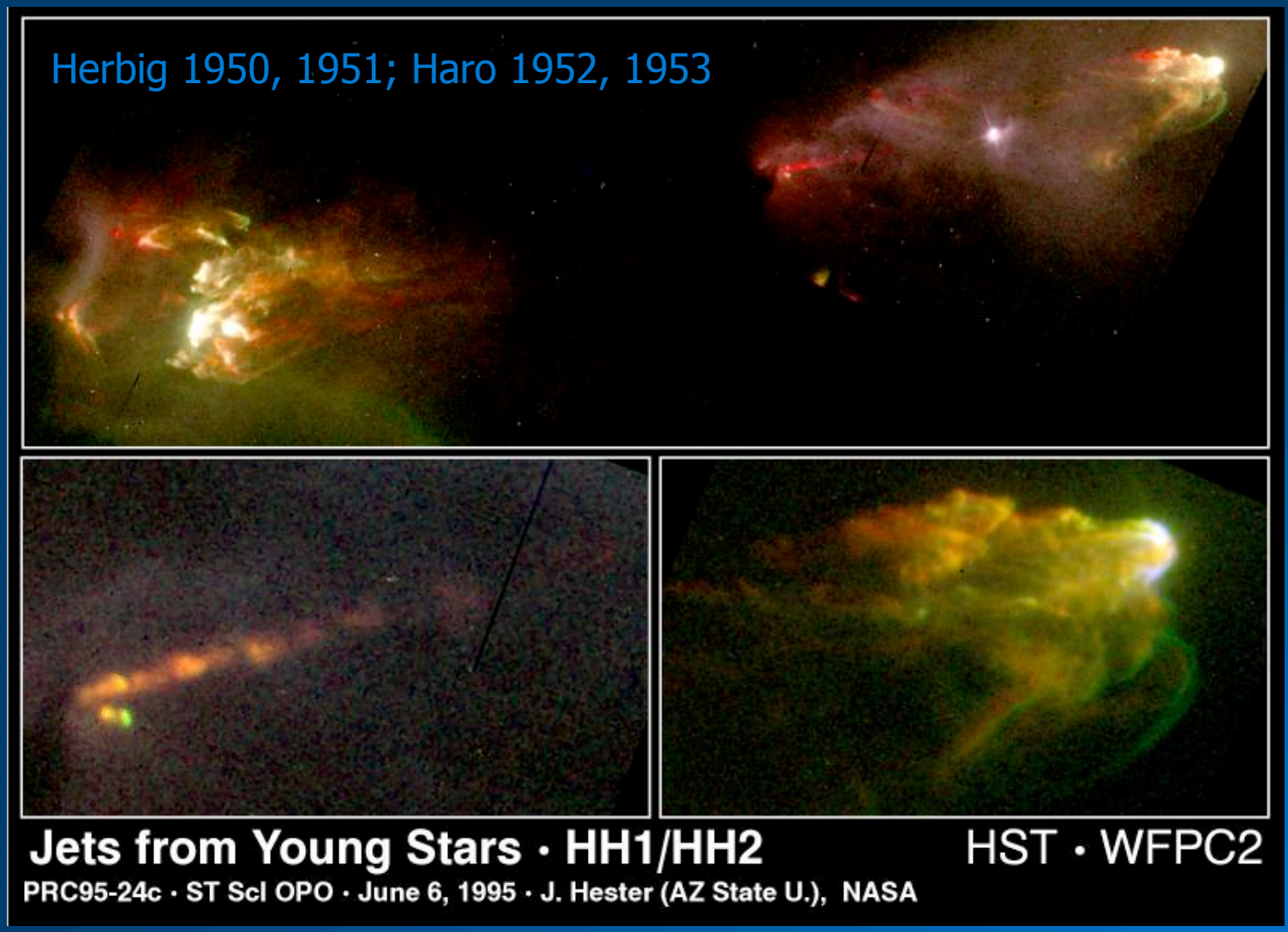

Initially thought to be embedded protostars but soon spectra were recognized as caused by shock waves --> jets and outflows

Discovery of outflows II

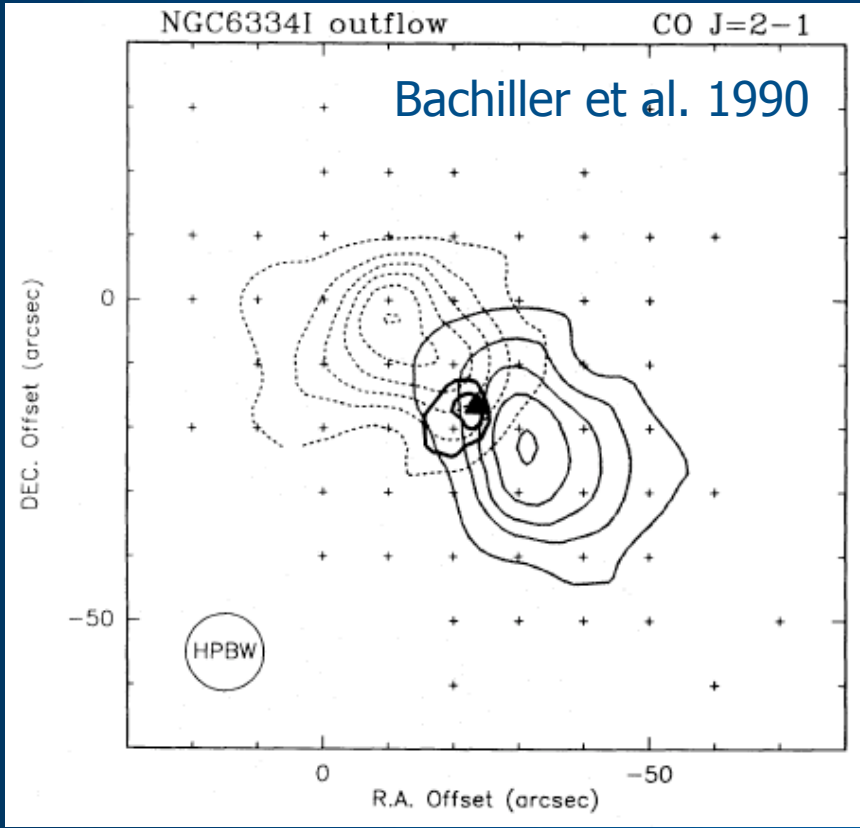

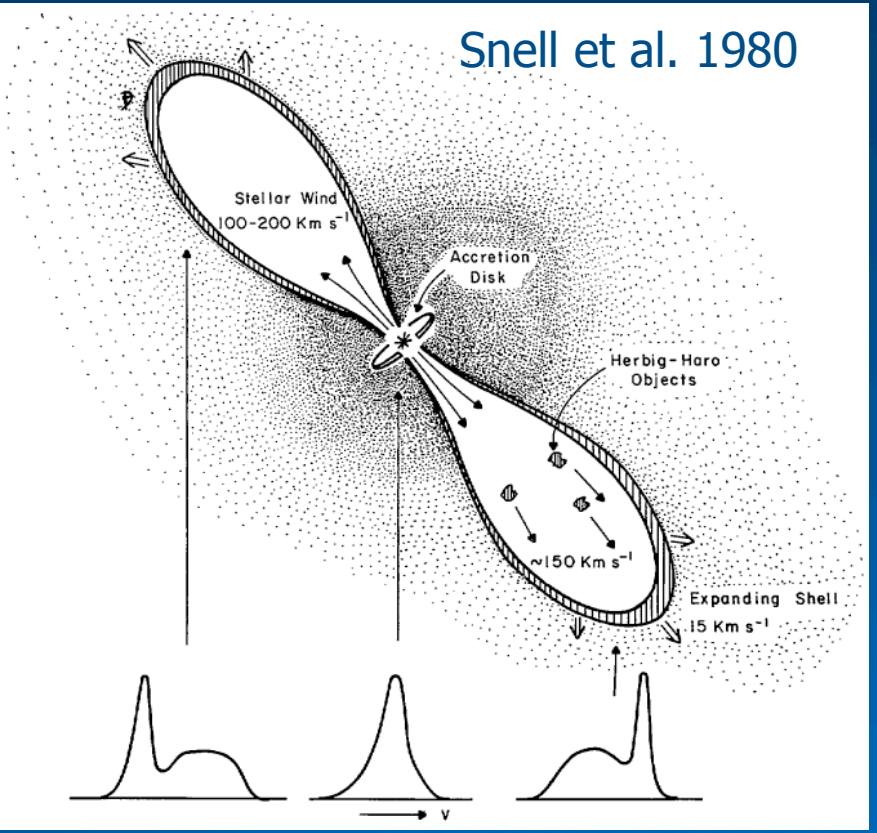

- In the mid to late 70th, first CO non-Gaussian line wing emission detected (Kwan & Scovile 1976).
- Bipolar structures, extremely energetic, often associated with HH objects

The prototypical molecular outflow HH211

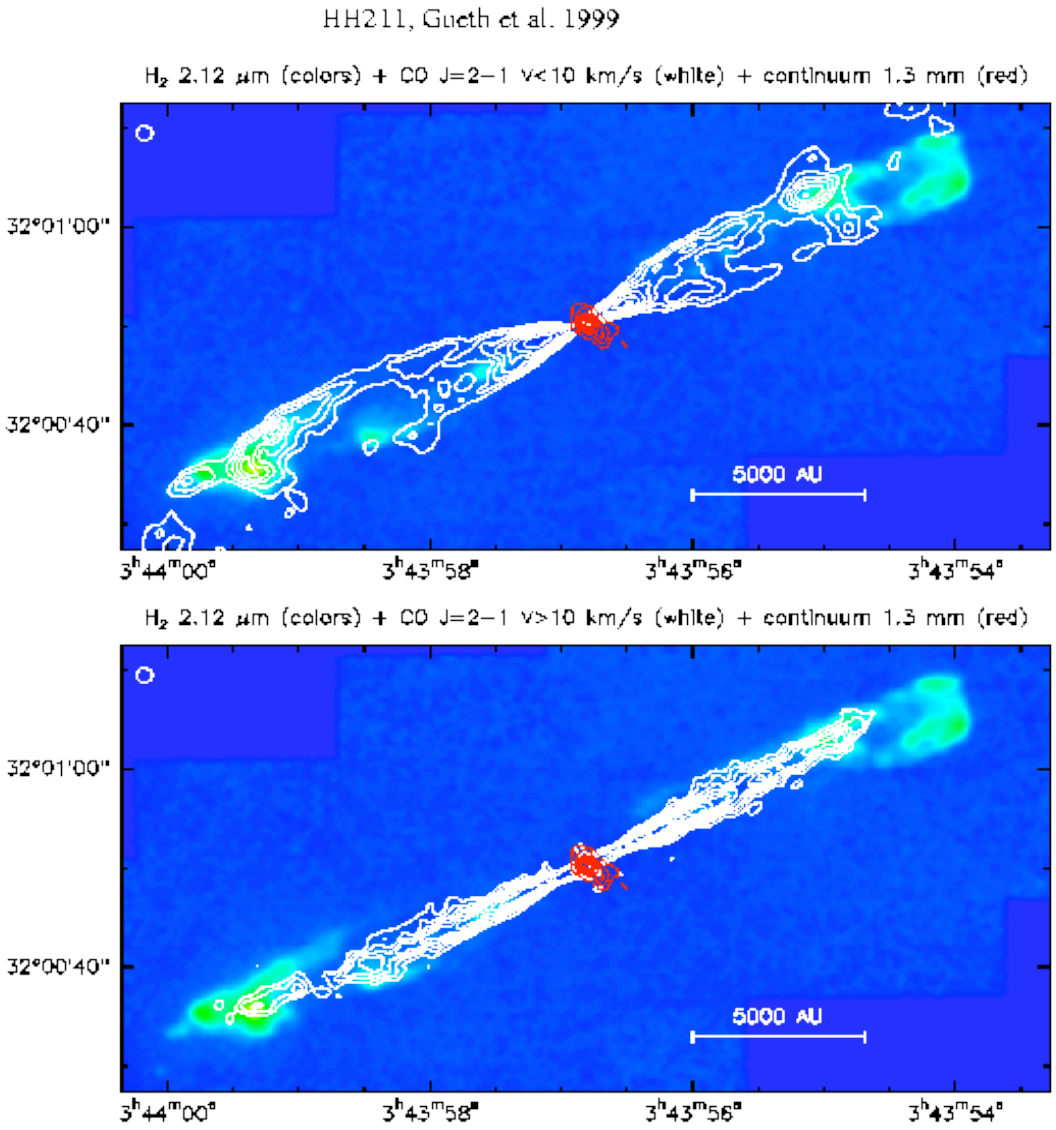

Jet launching

- Large consensus that outflows are likely driven by magneto-centrifugal winds from open magnetic field lines anchored on rotating circumstellar accretion disks.

- Two main competing theories: disk winds <==> X-winds

- Are they launched from a very small area of the disk close to the truncation radius (X-wind), or over larger areas of the disk (disk wind)?

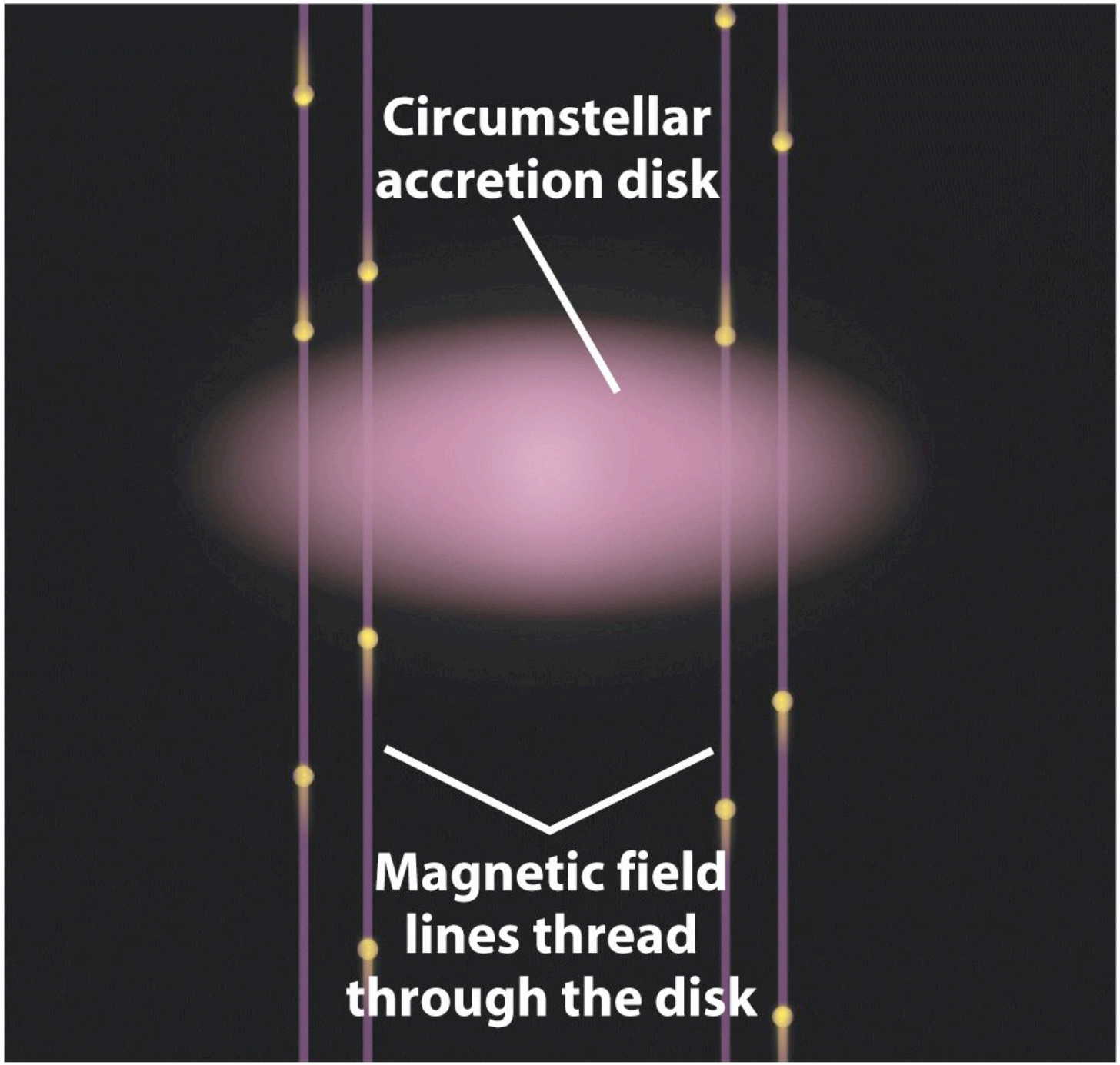
Circumstellar
accretion disk
Magnetic field
lines thread
through the disk

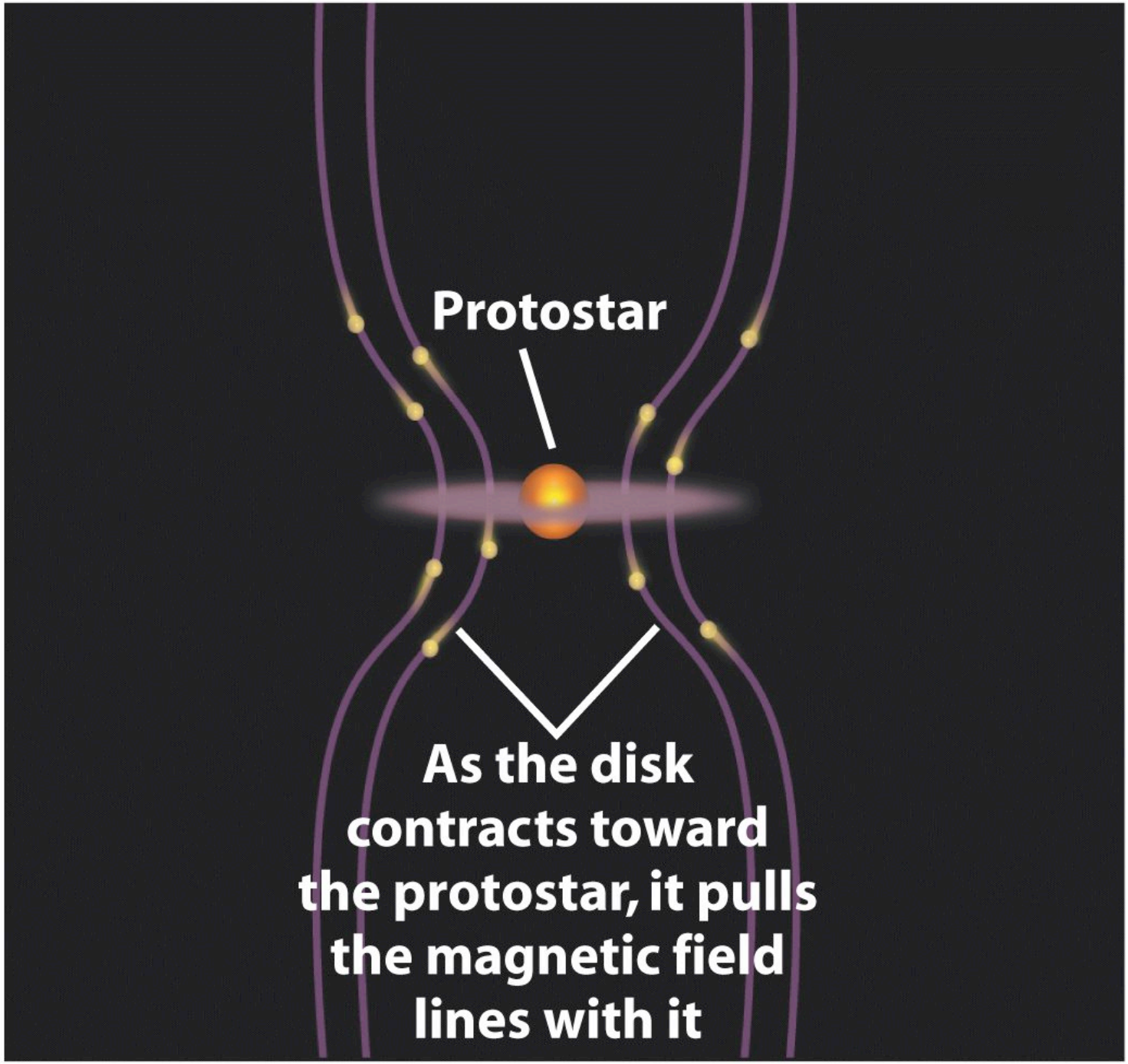
Protostar
As the disk contracts toward the protostar, it pulls the magnetic field lines with it

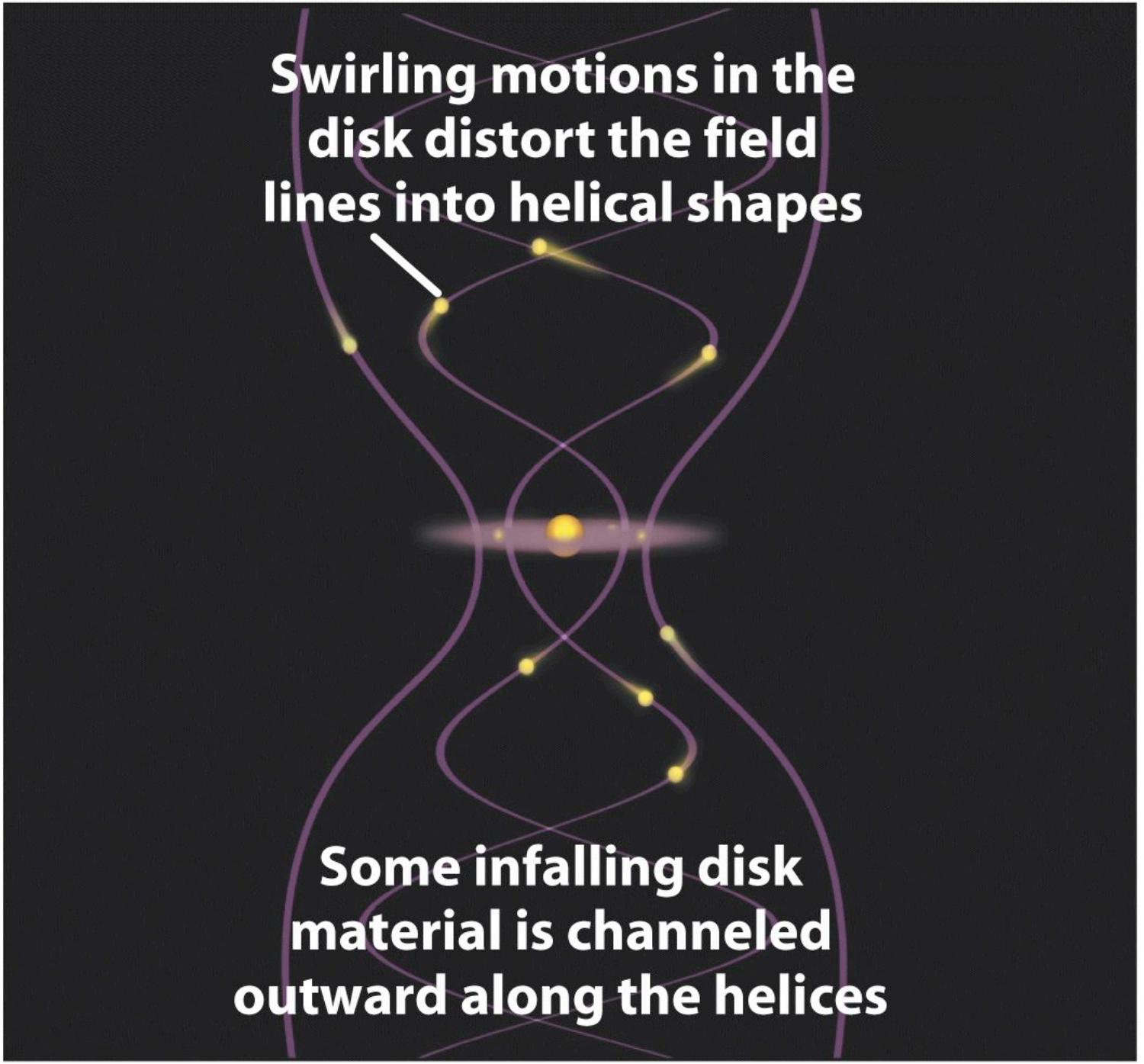
Swirling motions in the disk distort the field lines into helical shapes
Some infalling disk material is channeled outward along the helices

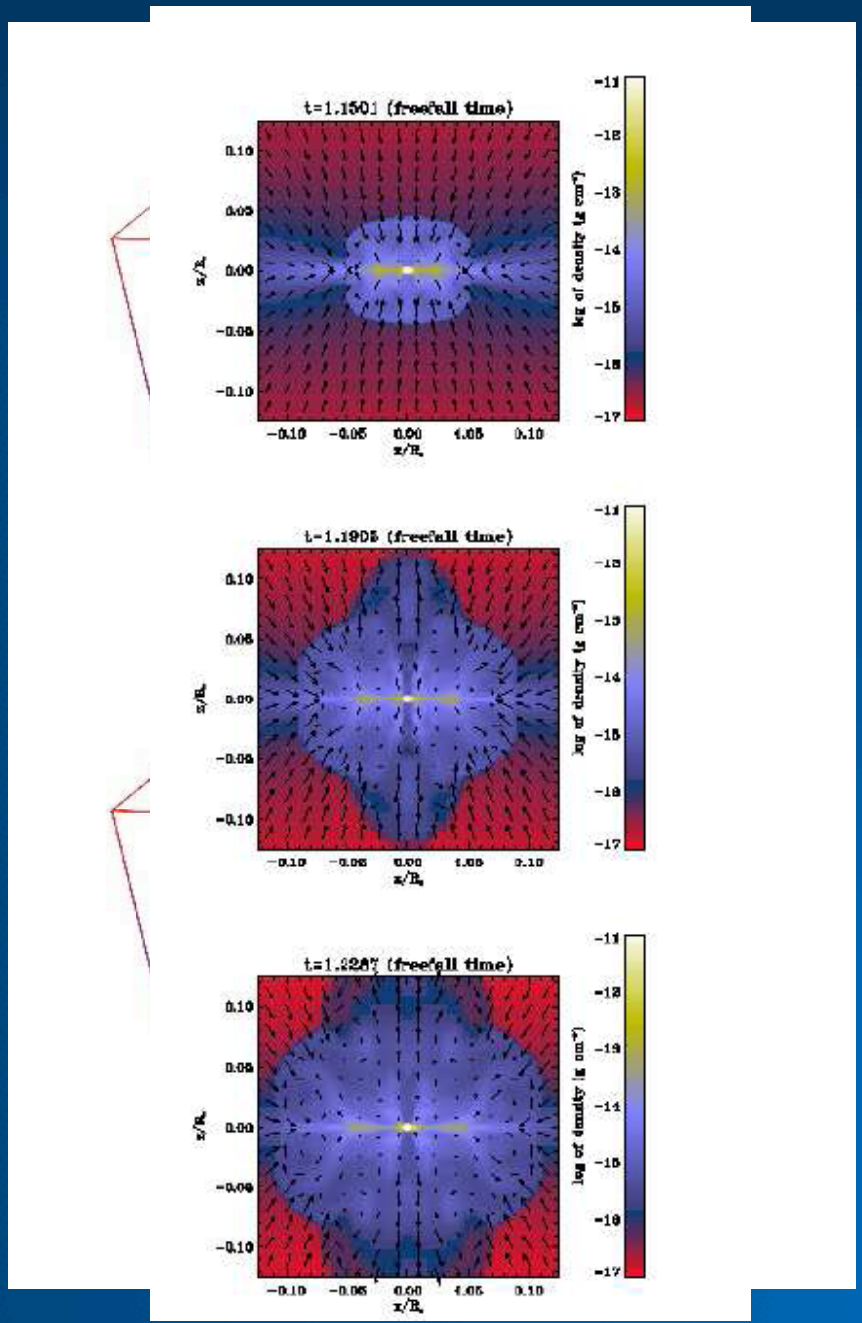

Hennebelle & Fromang (2008)

Banerjee & Pudritz (2006, 2007

Jet-launching: Disk winds

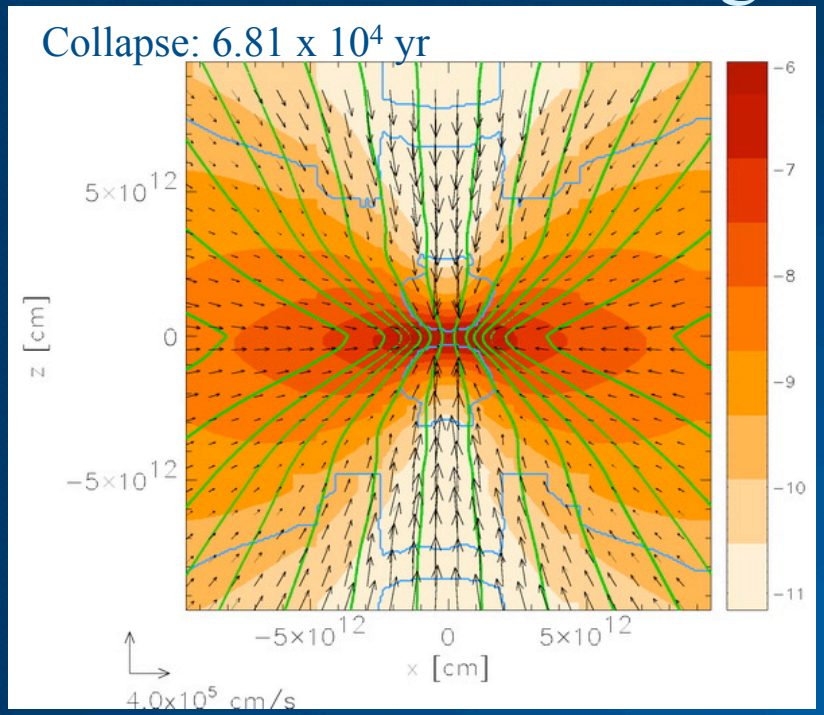

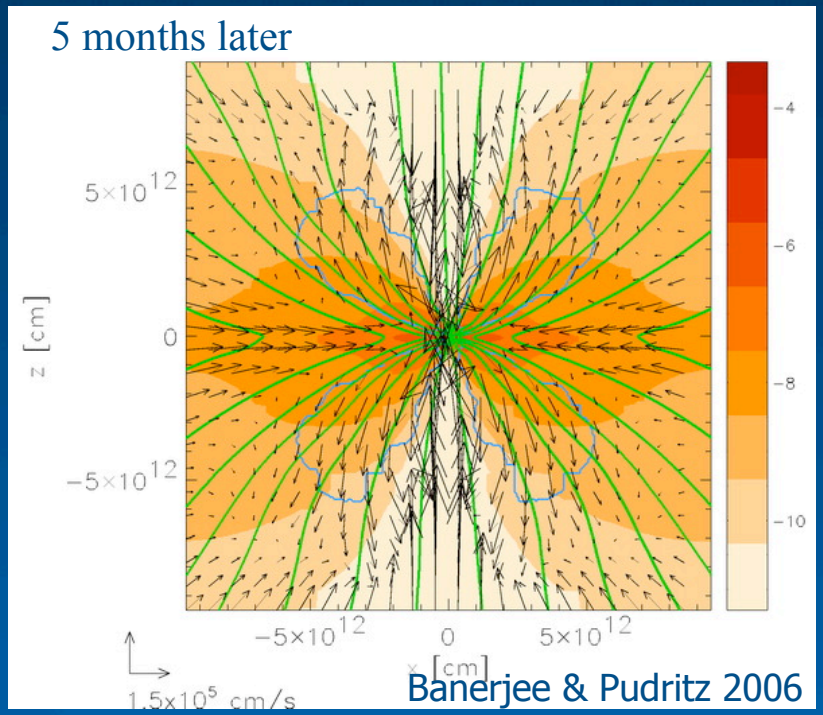

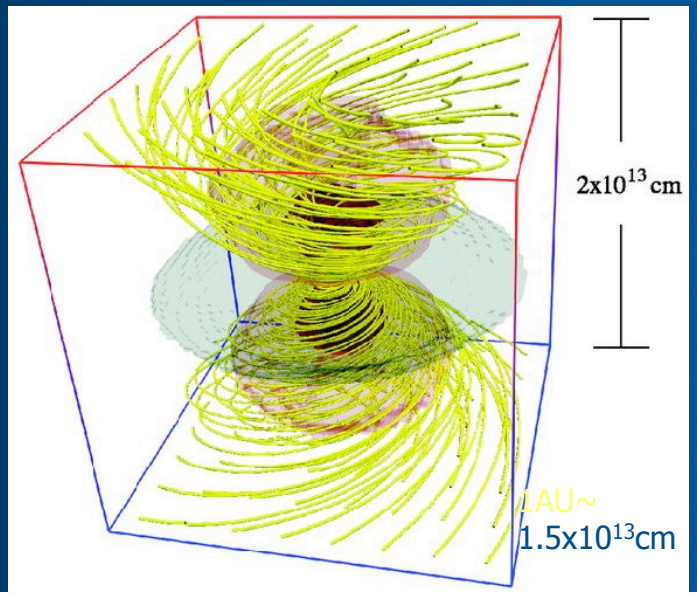

- Infalling core pinches magnetic field.
- If poloidal magnetic field component has angle larger 30˚ from vertical, centrifugal forces can launch matter-loaded wind along field lines from disk surface.
- Wind transports away from 60 to 100% of disk angular momentum.

Review: Pudritz et al. 2006

X-winds

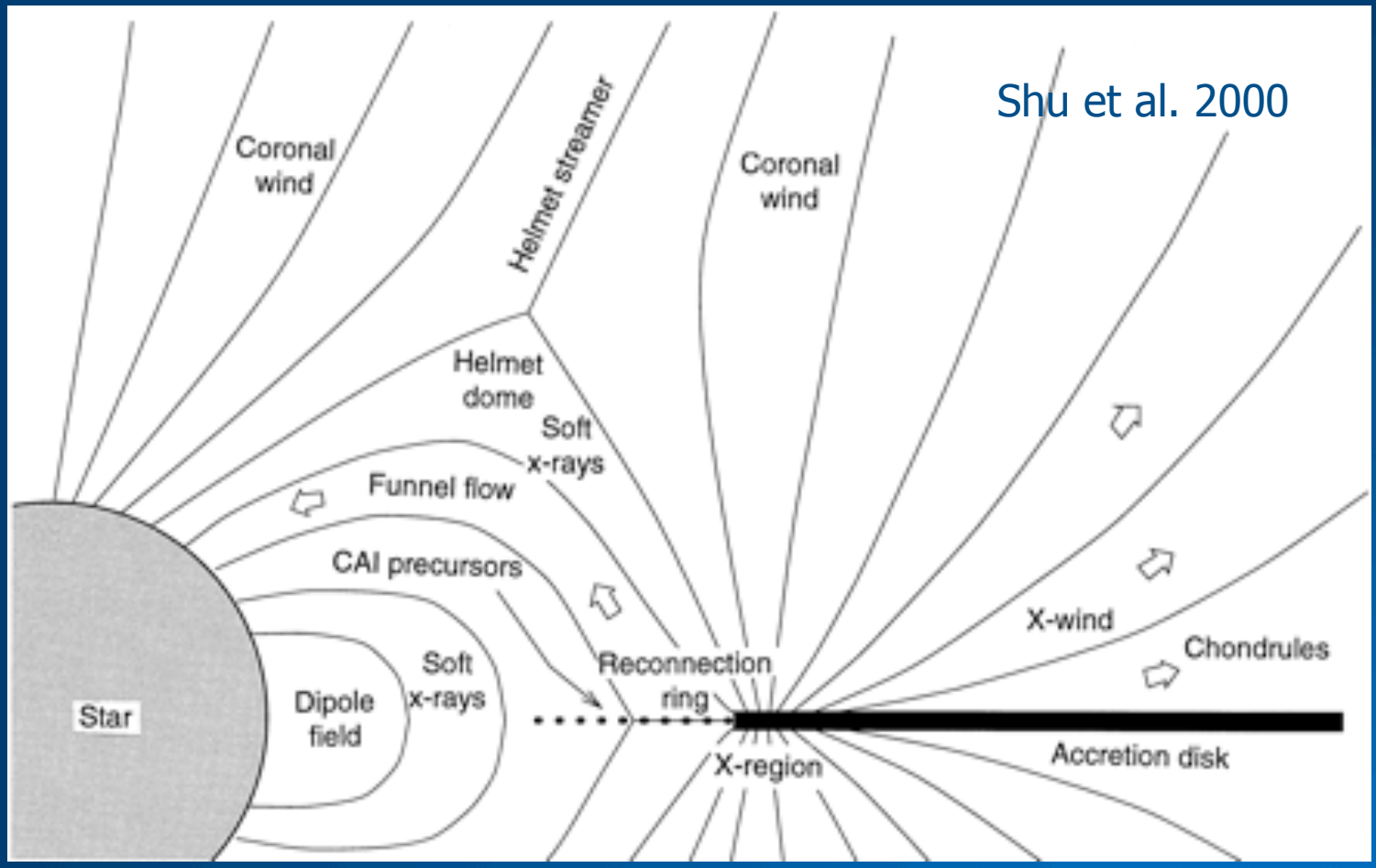

- The episodic wind is magnetically launched by fast reconnection from the inner co-rotation radius of the accretion disk (~0.03AU)

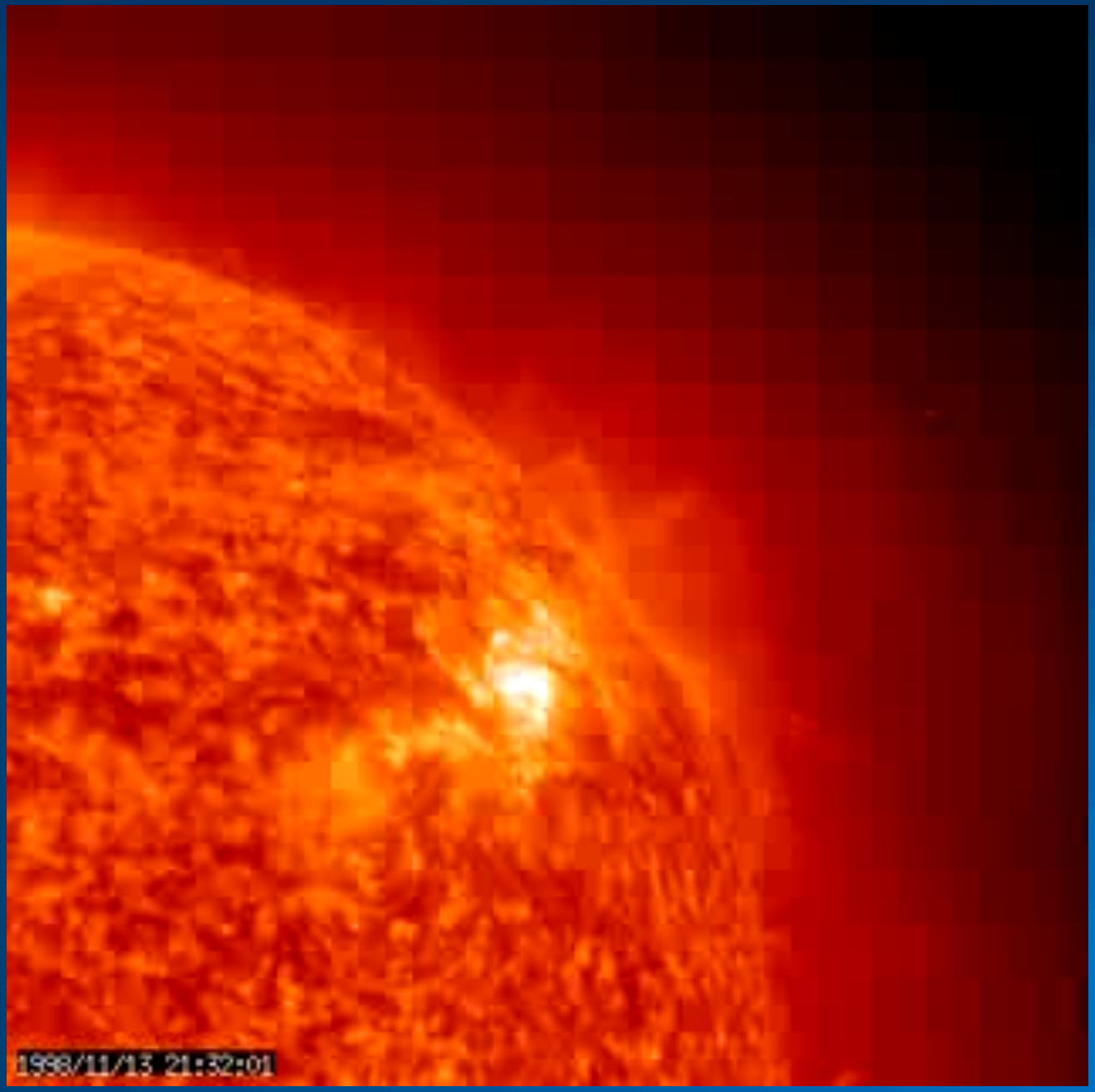
1998/11/13 21:32:01

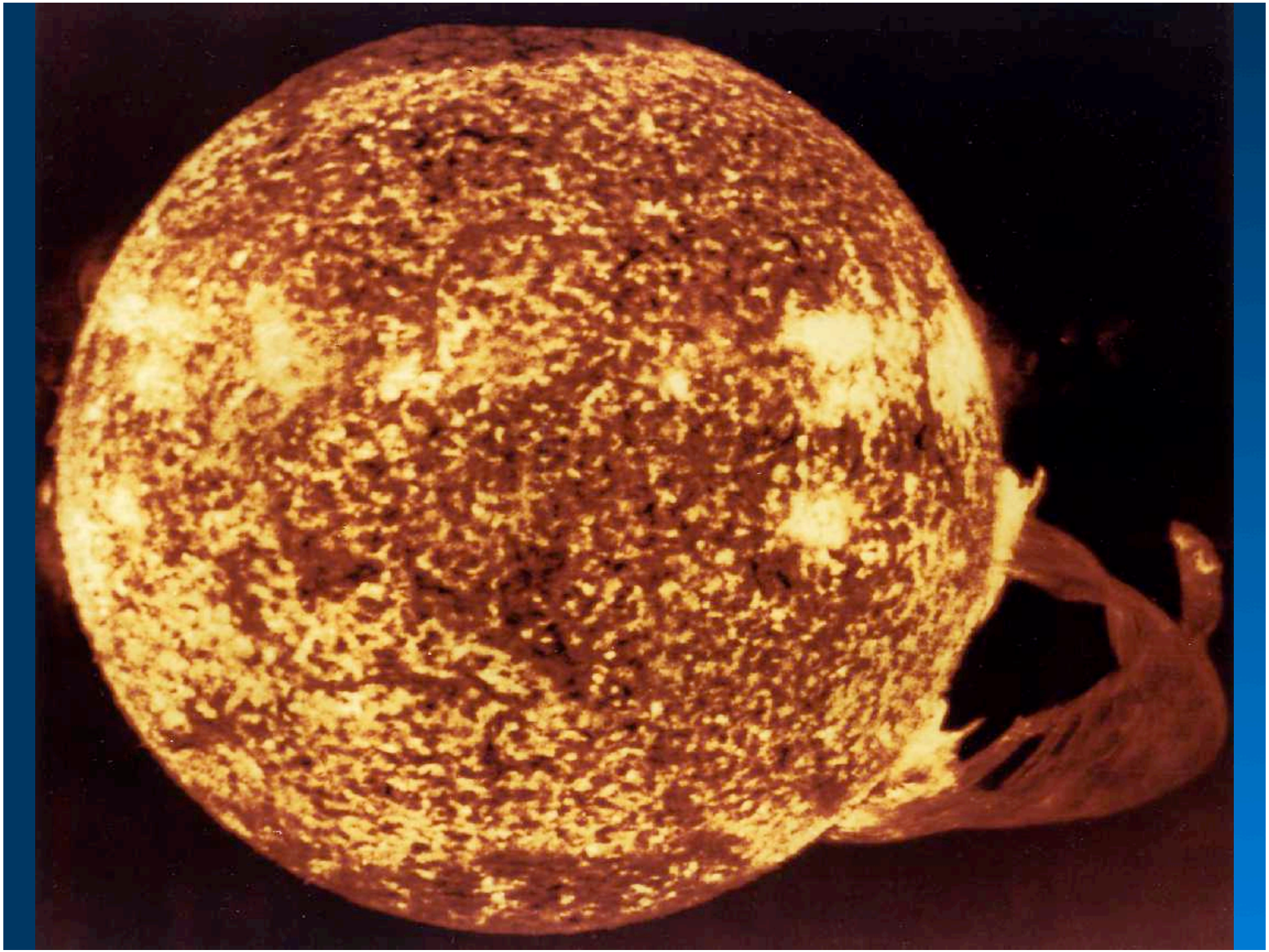

Jet-launching points and angular momenta

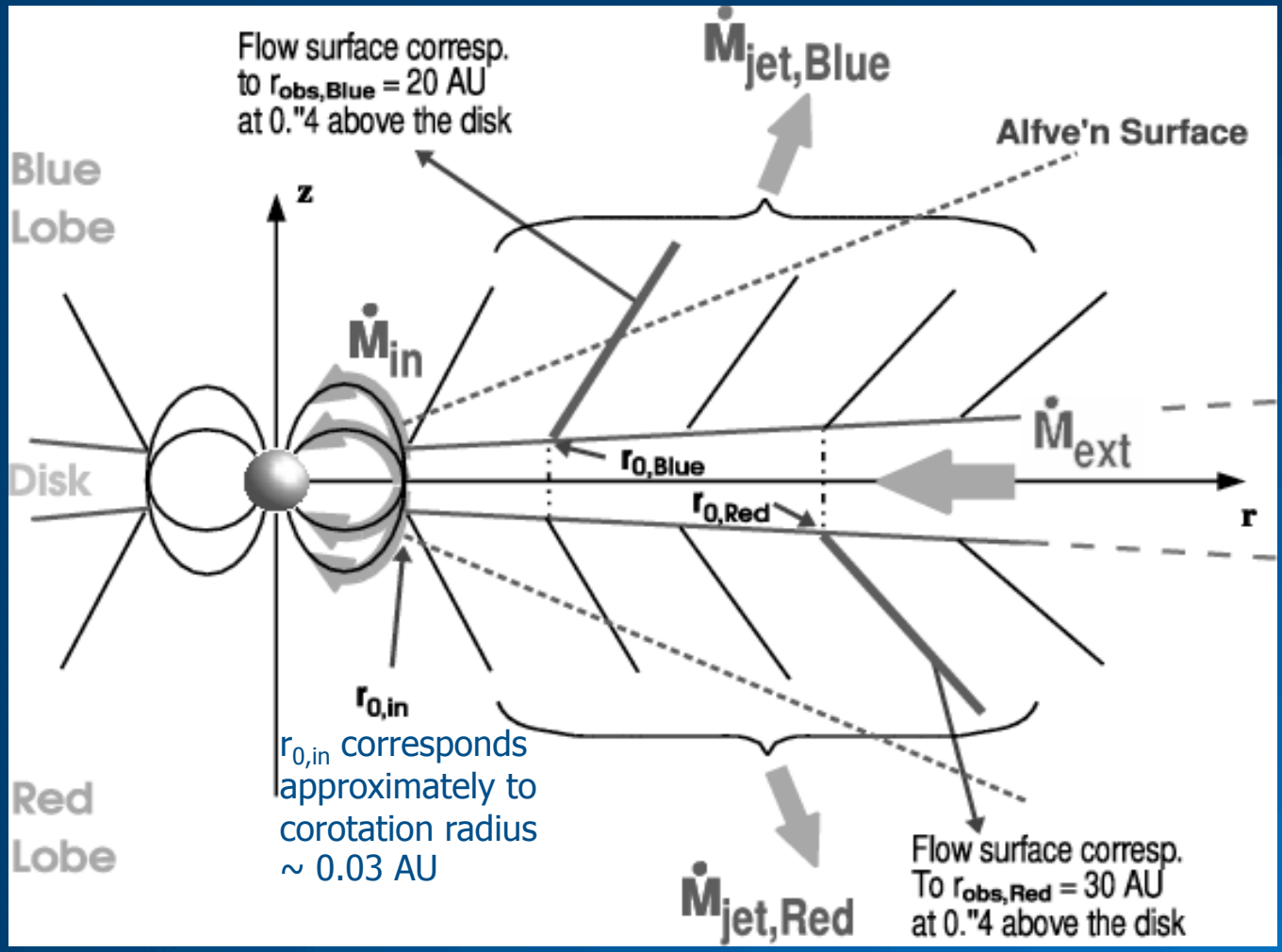

- About 2/3 of the disk angular momentum may be carried away by jet.

Woitas et al. 2005

Starforming Region in the Carina Nebula

HST•ACS/WFC

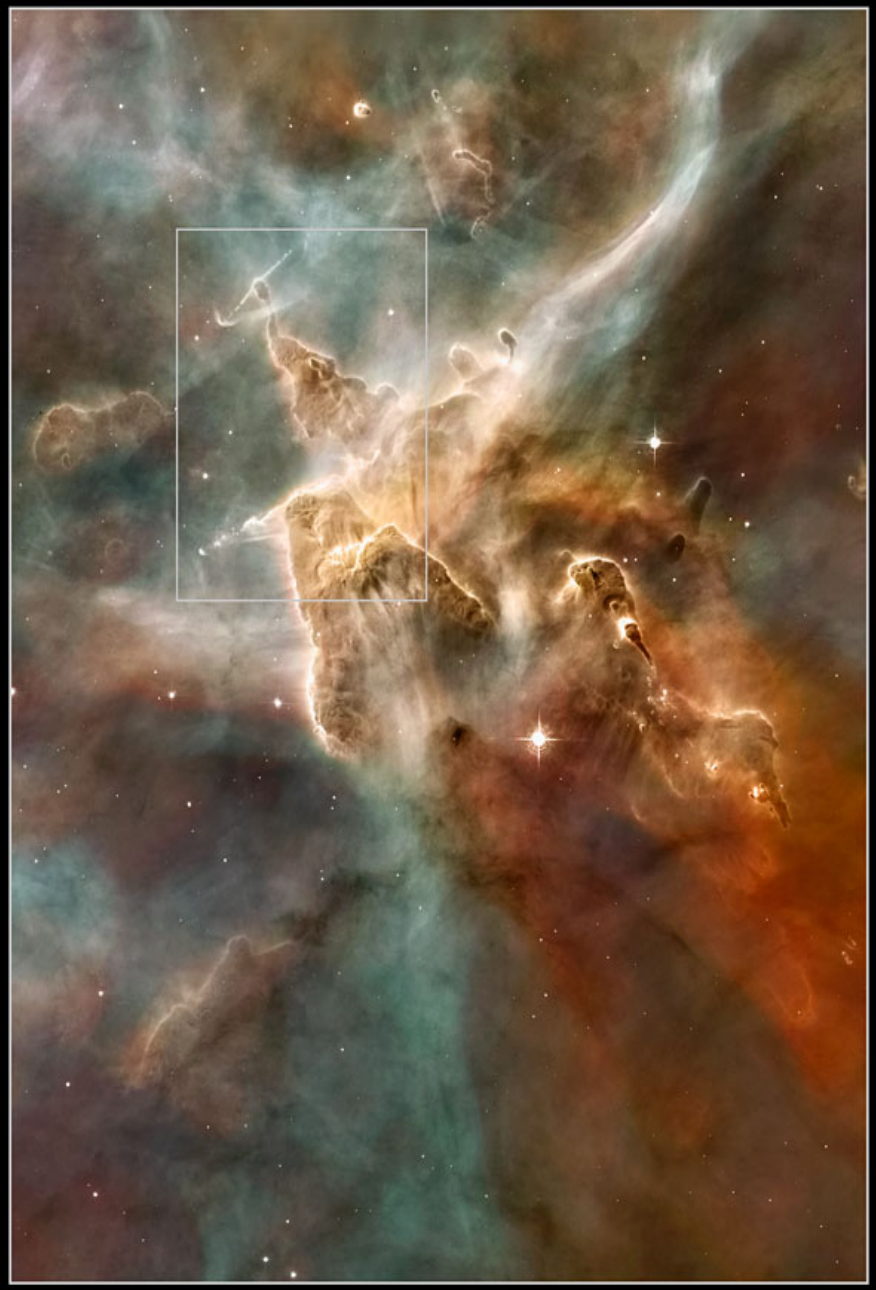

Impact of the jet on surrounding cloud

- Entrain large amounts of cloud mass with high energies.
- Partly responsible to maintain turbulence in cloud.
- Can finally disrupt the cores to stop any further accretion.
- Can erode the clouds and alter their structure.
- May trigger collapse in neighboring cores.
- Via shock interactions heat the cloud.
- Alter the chemical properties.

Highlights part I

-Stars are formed through the collapse of massive clouds of gas.

- Shocks are necessary to trigger star formation and the collapse and fragmentation of the cloud.

-Outflows and jets are ubiquitous phenomena in star formation.

- Jets transport angular momentum away from protostar.

- Jets are likely formed by magneto-centrifugal disk-winds and rapid reconnection events.

- Collimation is both due to the external medium and the magnetic field.

- Gas entrainment can be due to various processes: turbulent entrainment, bow-shocks, wide-angle winds, circulation …

- They inject significant amounts of energy in the ISM, may be important to maintain turbulence.

- Disrupt at some stage their maternal clouds.

High-energy processes in star formation

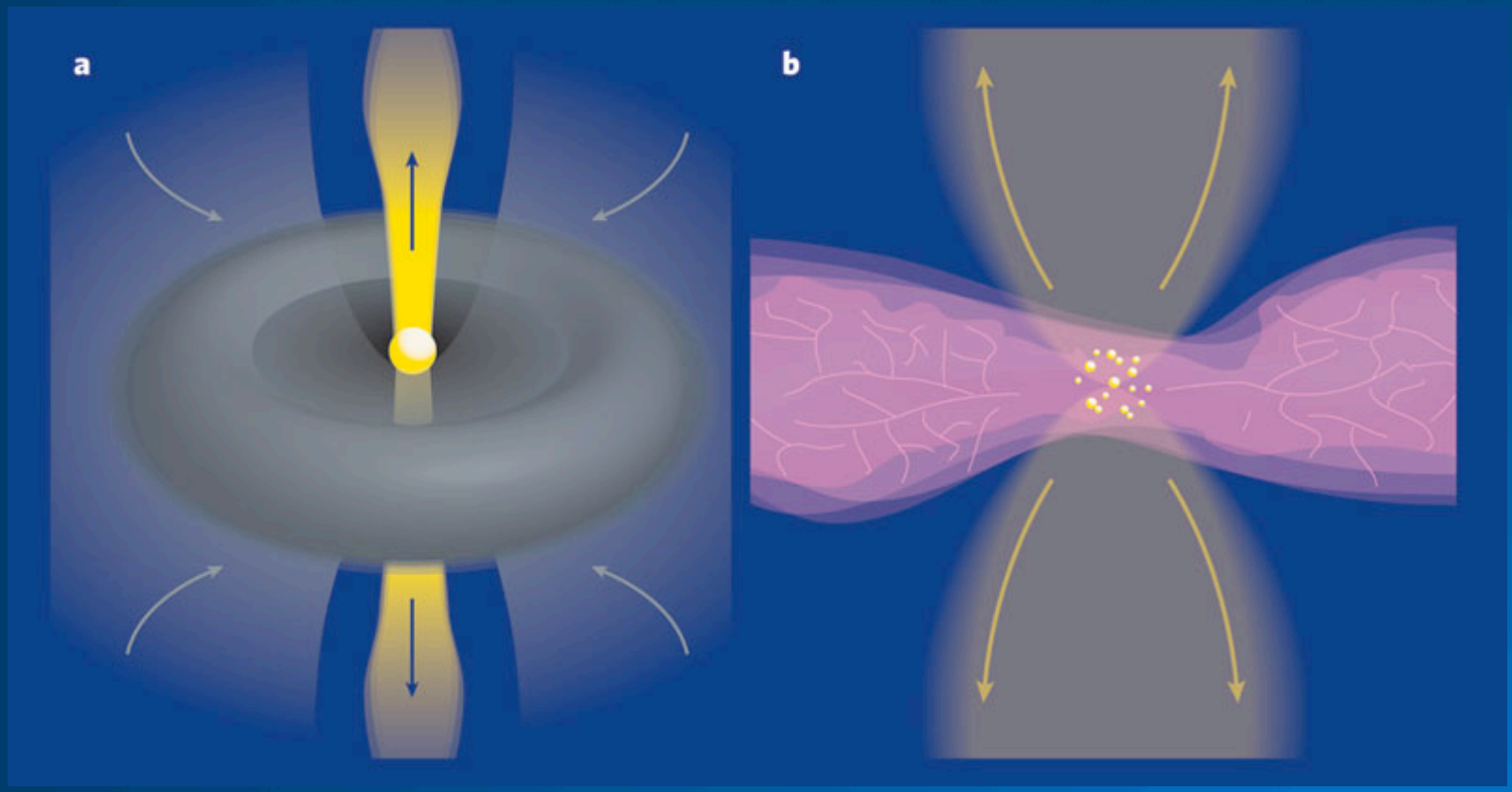

Massive protostars

Some problems in the formation to massive stars:

Radiation pressure acting on dust grains can become large enough to reverse the infall of matter:

$F_{grav} = GM_{*}m/r^2$

$F_{rad} = L\sigma/4\pi r^2 c$

Above 10 M_{sun} radiation pressure could reverse infall

So, how do stars with $M_* > 10M$ form?

Two scenarios:

- Accretion:
  - Need to reduce the effective luminosity by making the radiation field anisotropic (accretion disk and jets)
- Form massive stars through collisions of intermediate-mass stars in clusters
  - May be explained by observed cluster dynamics
  - Possible problem with cross section for coalescence
  - Observational consequences of such collisions?

Three evolutionary stages

- Massive, prestellar cold cores: Star has not formed yet, but molecular gas available (a few of these cores are known).
- Massive hot cores: Star has formed already, but accretion so strong that quenches ionization => no HII region (tens are known). Powerful jets can be produced (few detected).
- Ultracompact HII region: Accretion has ceased and detectable HII region exists (many are known).

Non-thermal emission from massive protostars:HH 80-81, (Martí et al. 1993)

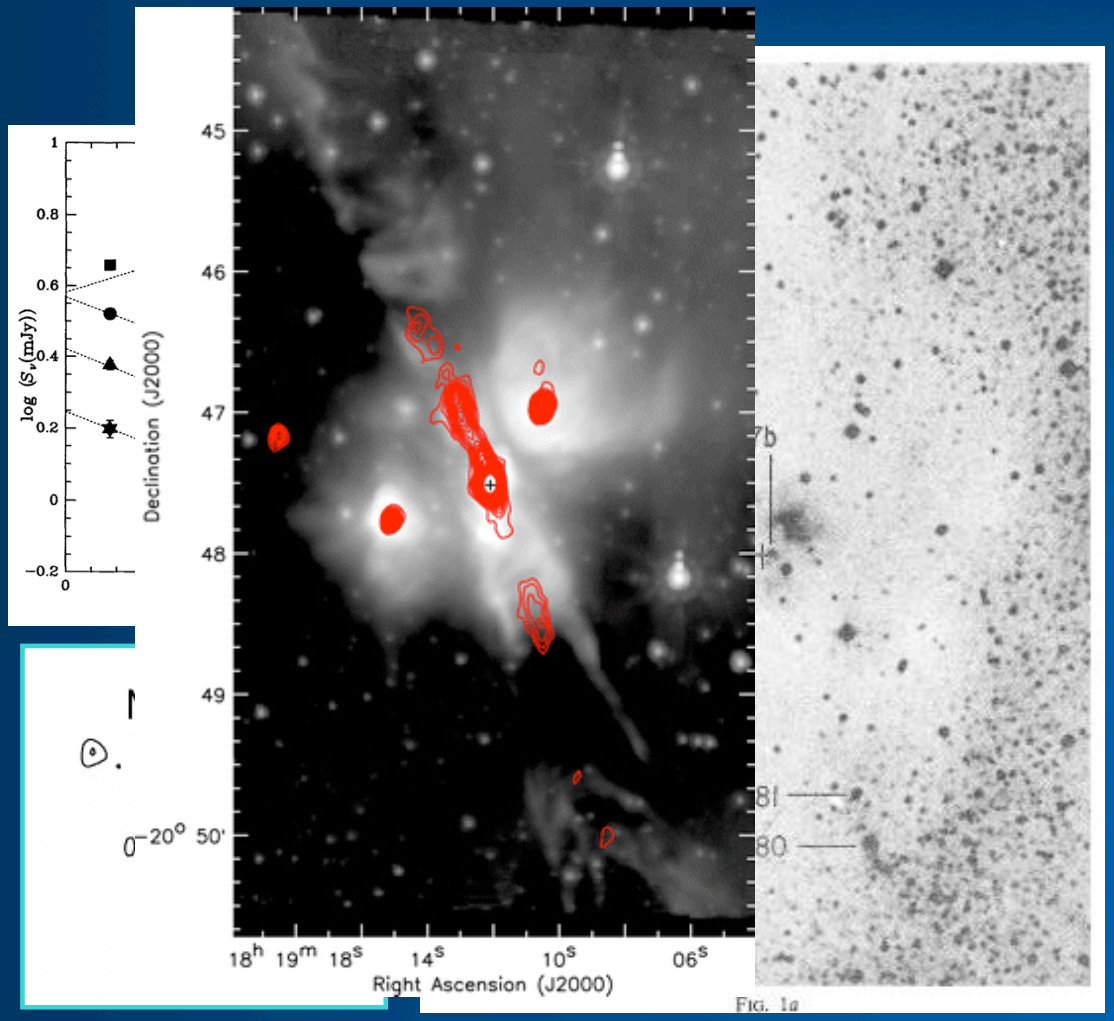

2x10^4 Lsun, 1.7kpc

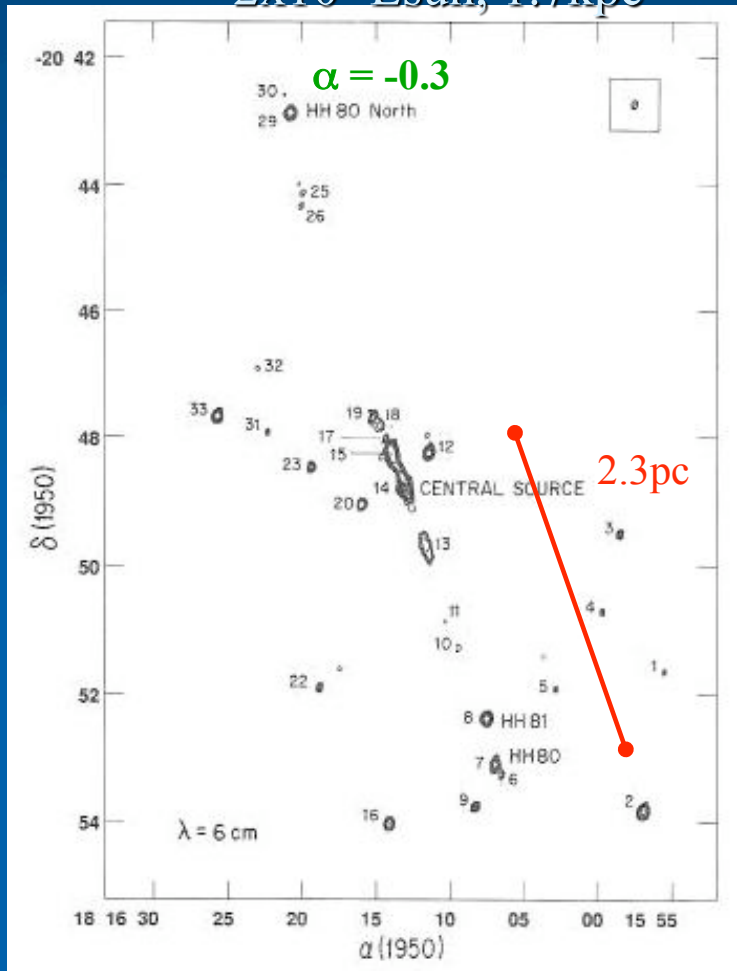

Qiu et al. 2009: episodic molecular bullets (100 km/s) ejected close to central source

Non-thermal emission from jets

- Alcolea et al. 1992: H_2O masers proper motions
- Reid et al. 1995: $\alpha_{1.4\text{-}15GHz} = -0.6$
- Wilner et al. 1999; 8.5Ghz, 0.2”

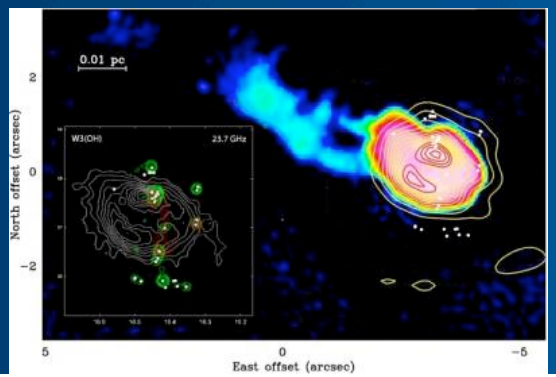

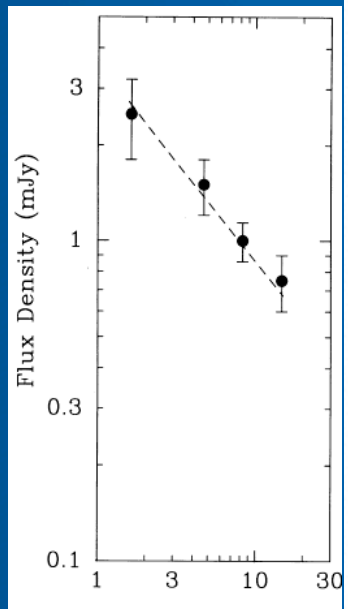

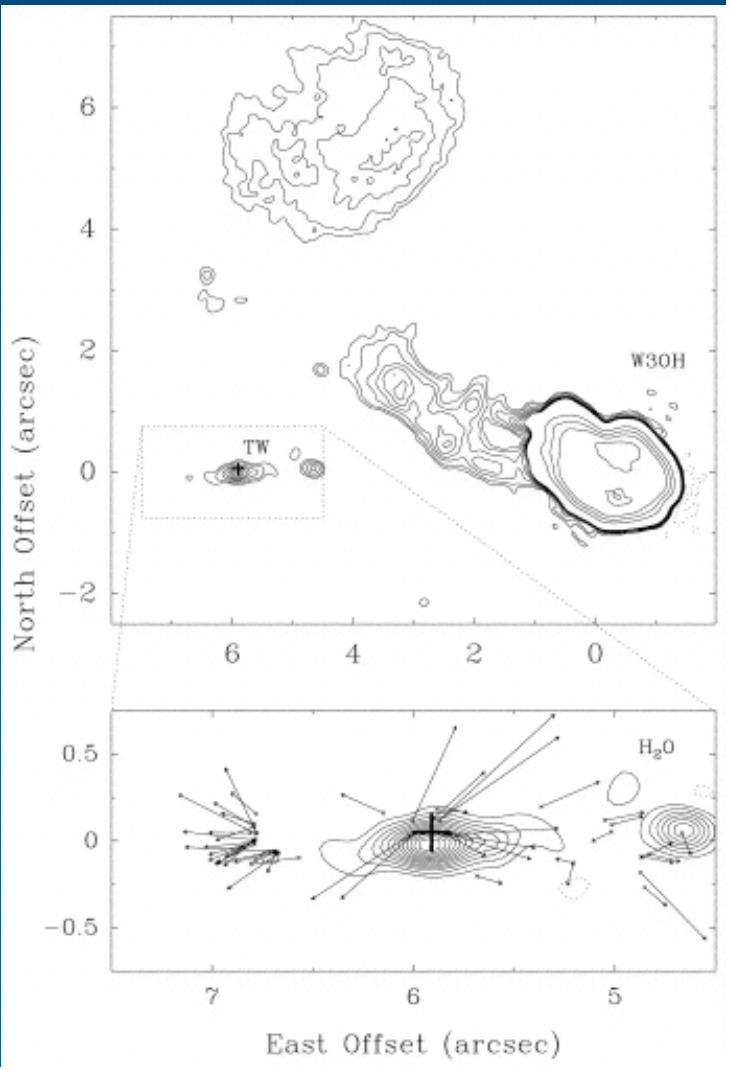

Proper motions of masers
(Torrelles et al. 2010)

Five epoch VLBI obs (0.4”, 0.3 AU at 700 pc)
Masers: static at 1” scale;
Masers at <0.1” : draw ellipse
=> Unseen YSO ?

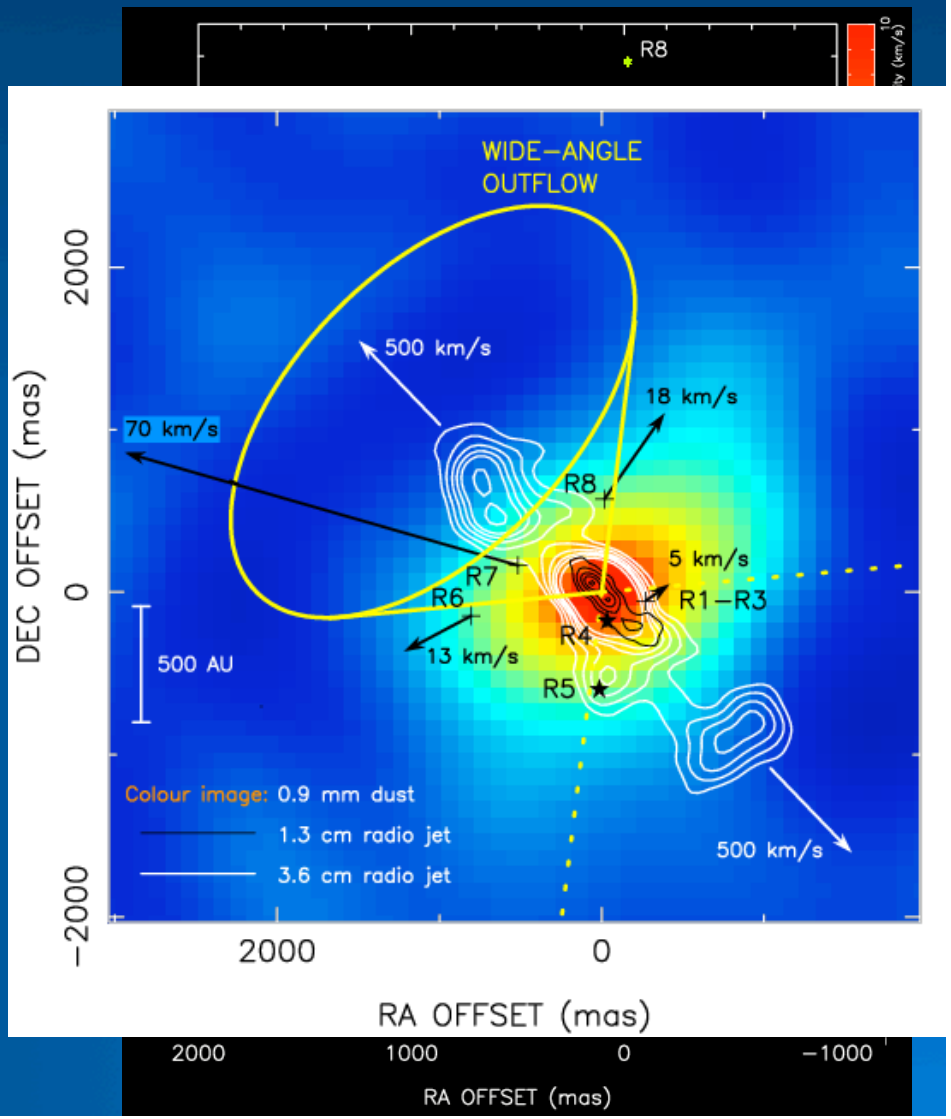

- Wide angle slow molecular outflow (50 km/s, 100º),
- Collimated fast gas jet (500 km/s, 20º)
- Hint of rotating wind
- Central mass: 20 Msun

IRAS 16547-4247 (Garay et al. 2003, …)

Brooks+2009

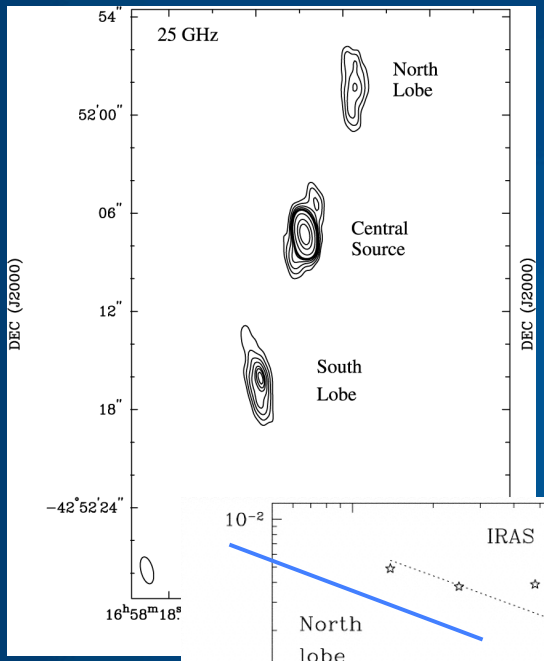

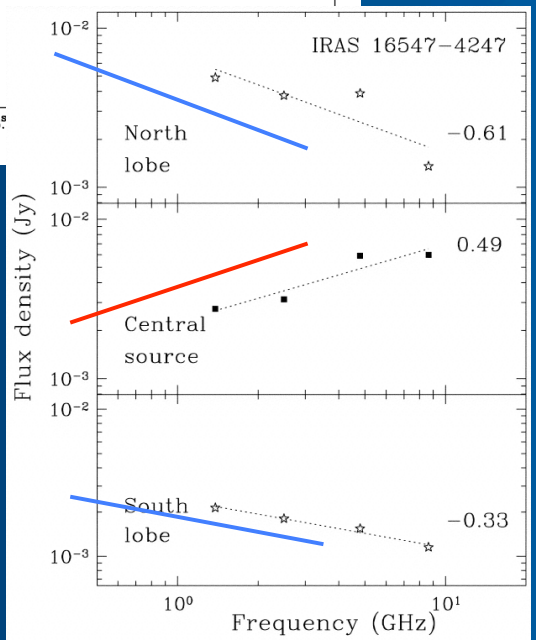

D = 2.9 kpc

L_{bol} = 62 000 L_{sun} (O8)

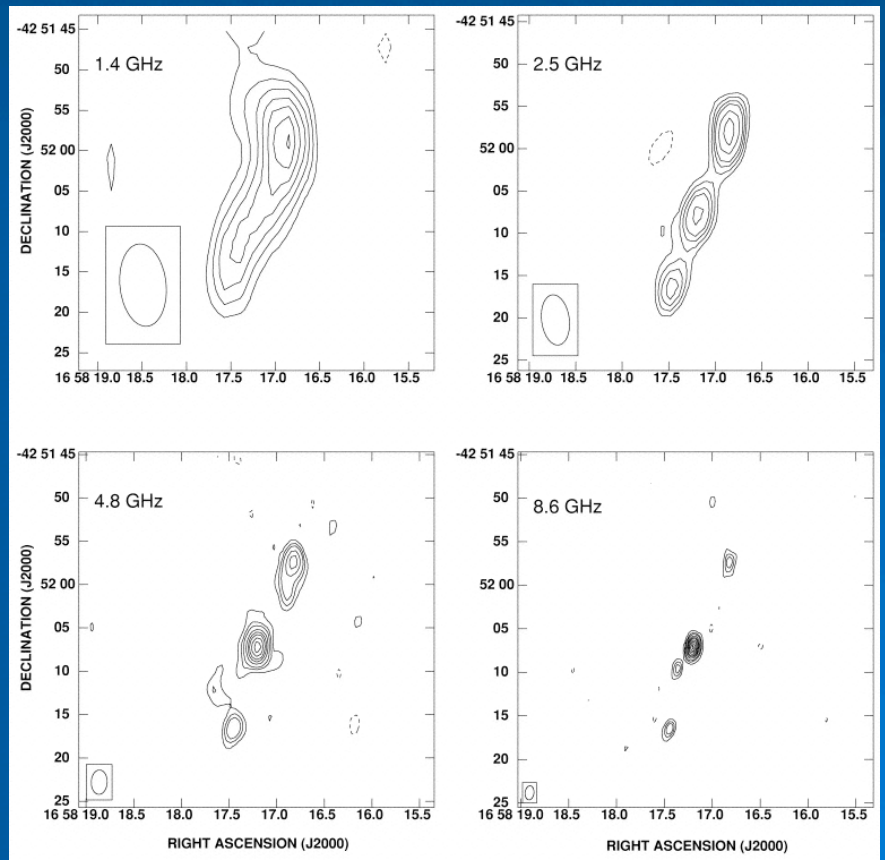

IRAS 16547-4247 (Garay et al. 2003, …)

- 1000 Msun core
- 100 Msun CO outflow

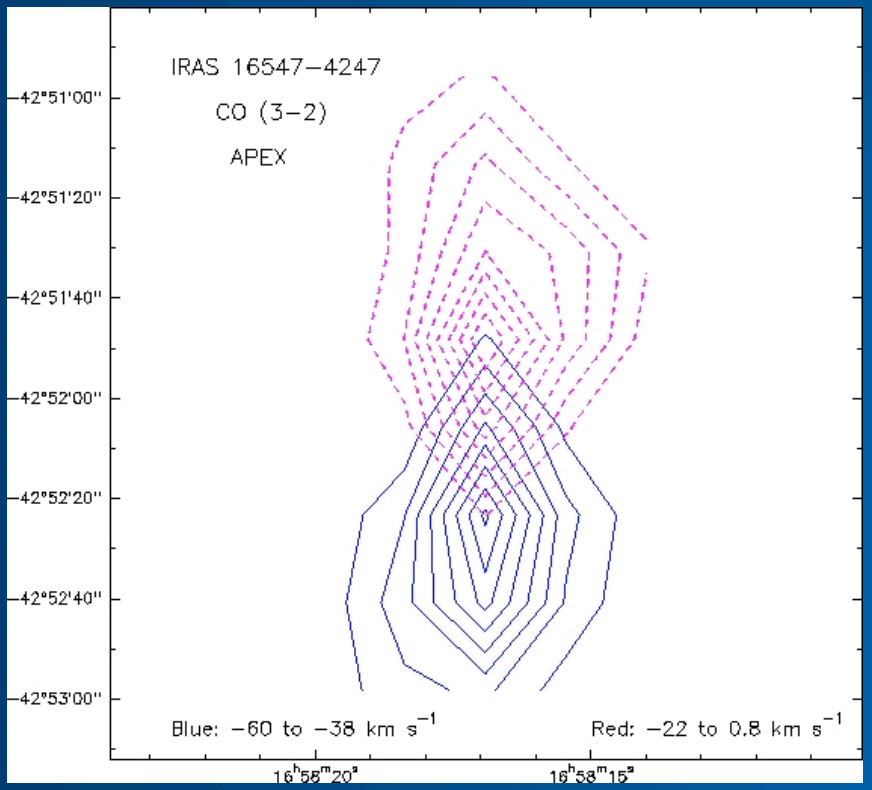

Rodriguez+2008

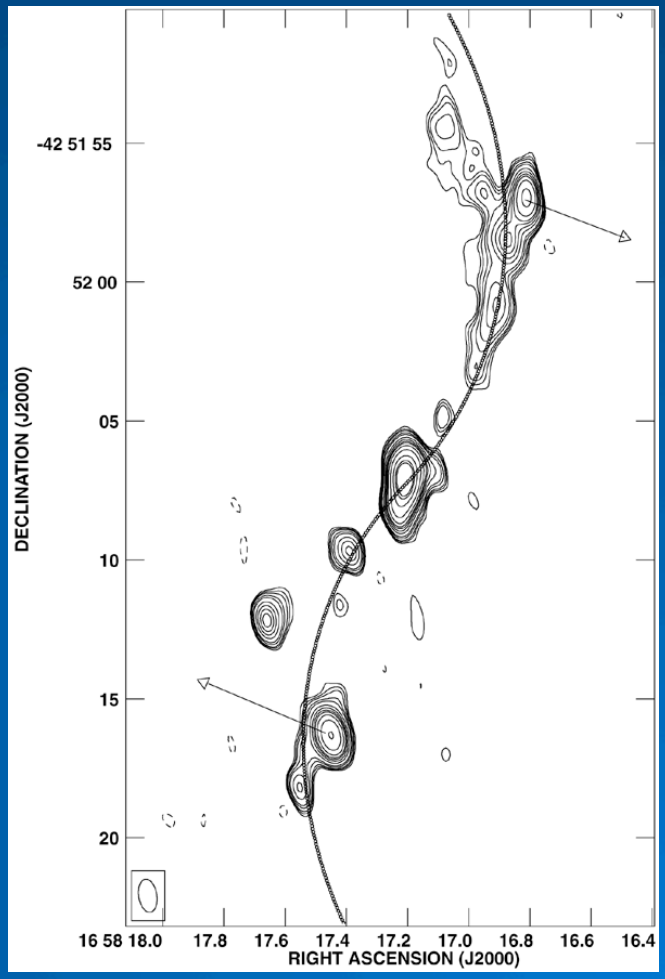

Polarization in jets!

Carrasco-González, Rodríguez et al. 2010

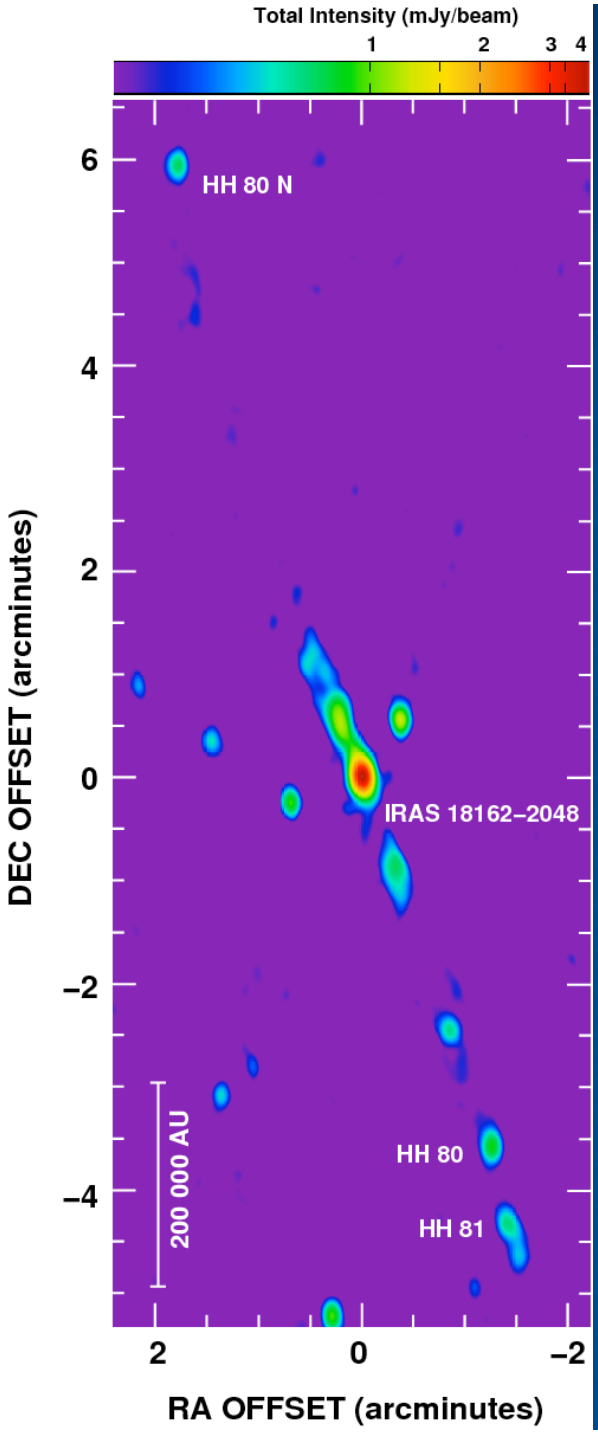

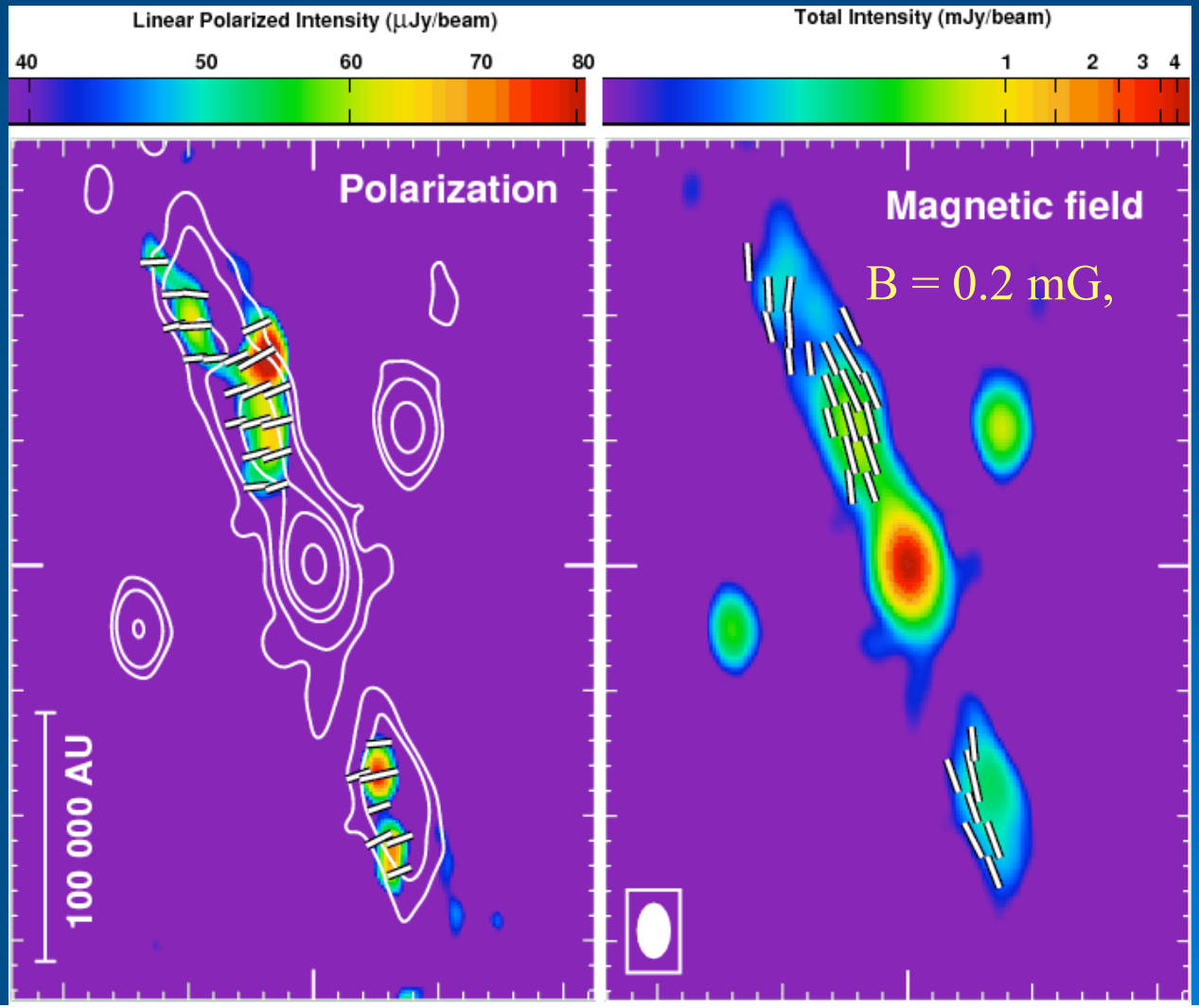

IRAS 16353-4636

FIELD

L = 6 x 10^4 erg/s, d = 8 kpc

- ATCA 1.4 to 20 GHz obs (0.5")
- NTT J, H, Ks (photometry + spectroscopy)

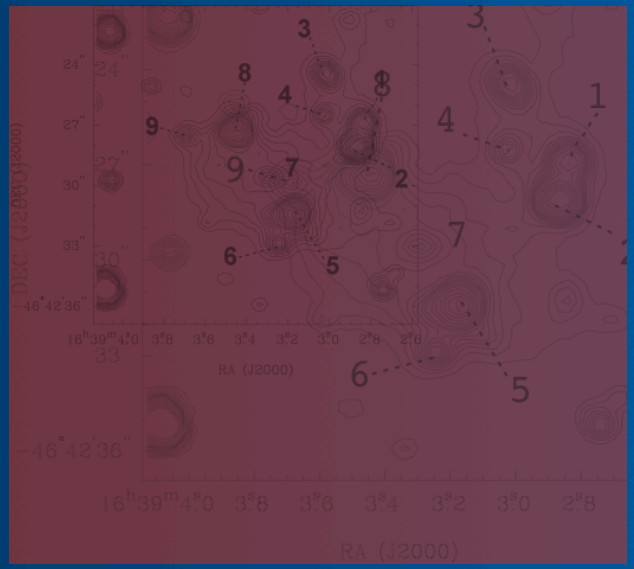

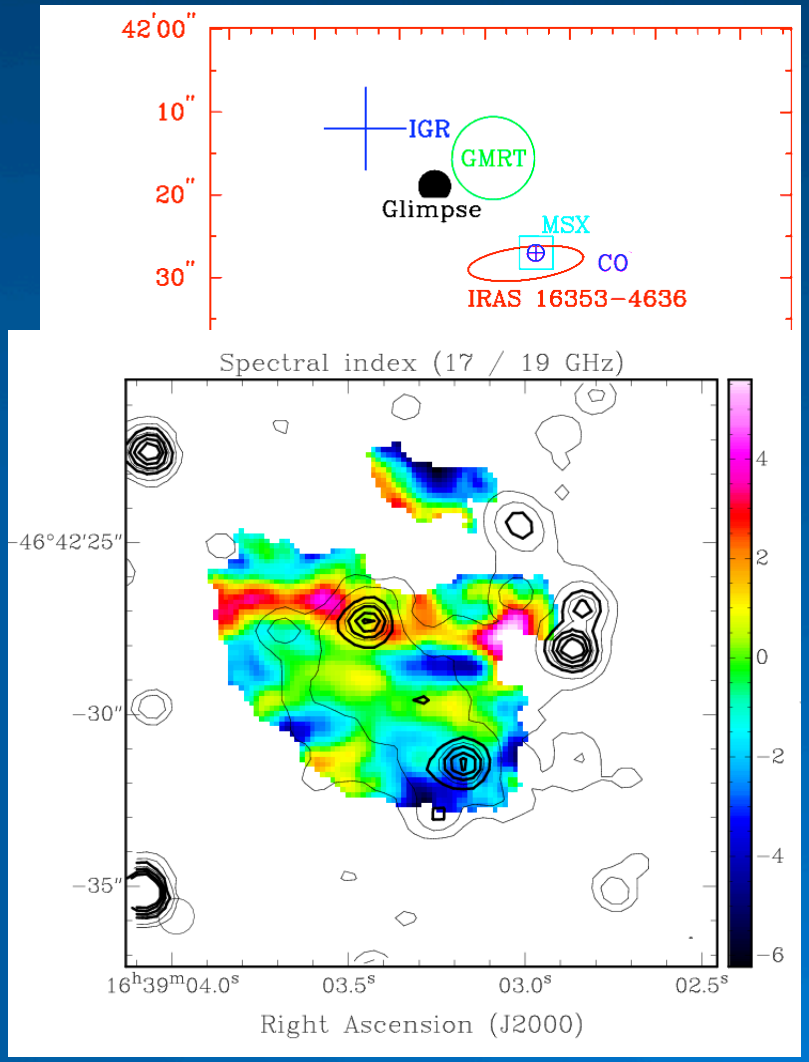

Benaglia, Rodríguez, et al. 2010

Interaction with the ISM

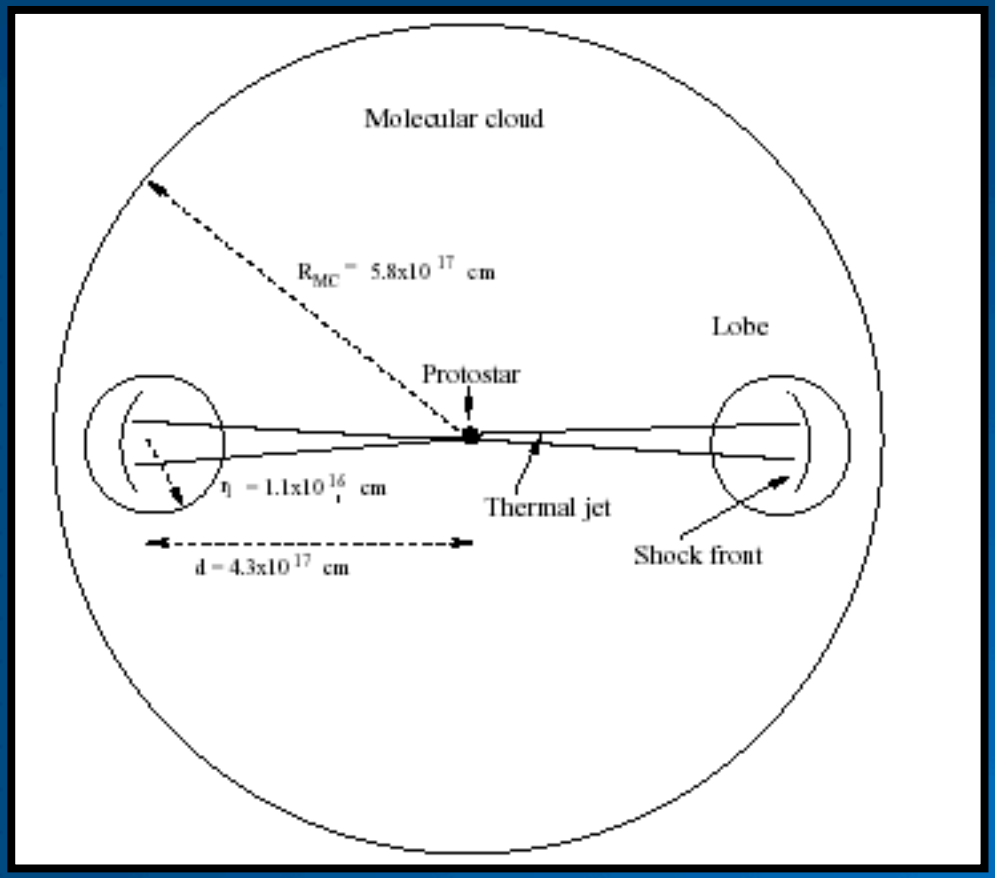

IRAS 16547-4247 : The whole source (protostar + jets) is embedded in the molecular cloud

Araudo, Romero, Bosch-Ramon & Paredes 2007, A&A 476, 1289

Particle acceleration and losses at the lobes

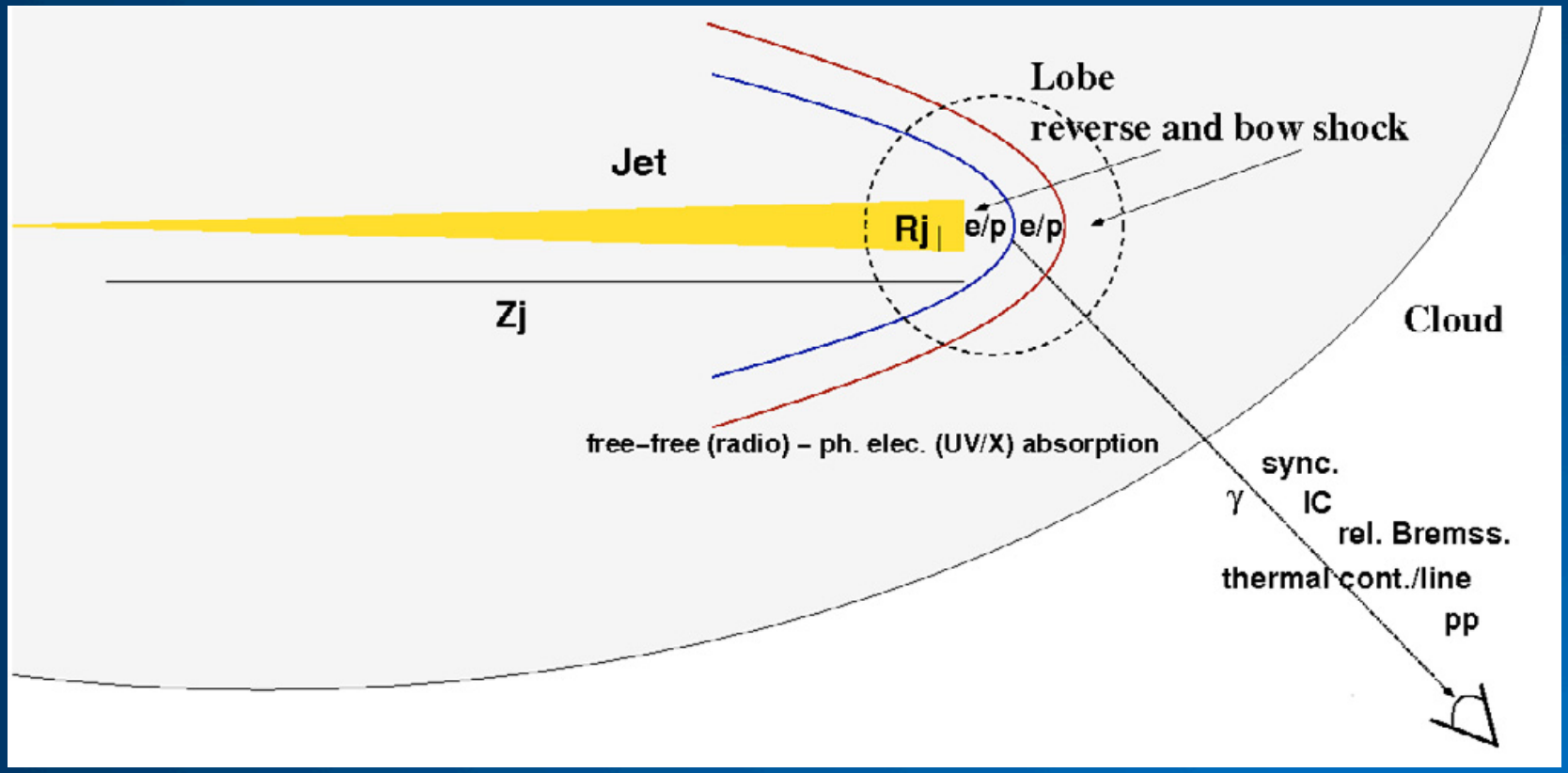

Bosch-Ramon, Romero, Araudo & Paredes A&A 511, A8 (2010)

Diffusive shock acceleration

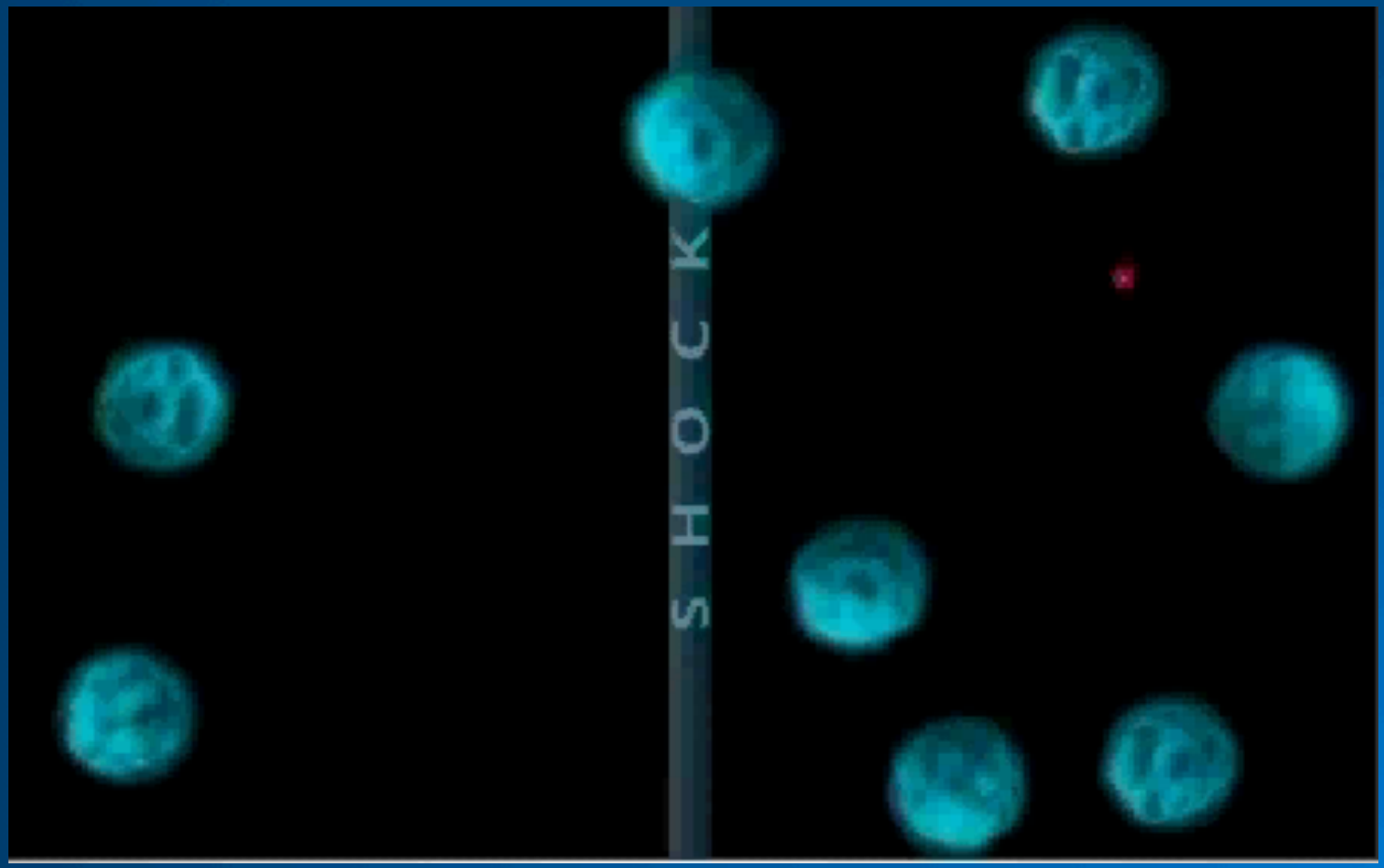

Particle acceleration and losses

$$\partial n(t,\gamma)/\partial t + \partial \dot{\gamma} n(t,\gamma)/\partial \gamma + n(t,\gamma)/\tau_{\rm esc} = Q(t,\gamma),$$

$$\dot{Q}(E) = \dot{Q}_0(E) E^{-\alpha}$$

$$\dot{\gamma}_{p,\ \rm gain} = \frac{\eta e B c}{m_p c^2}.$$

$$\dot{\gamma}_{e,\ \rm gain} = \frac{\eta e B c}{m_e c^2},$$

$$\dot{\gamma}_{\rm gain} = \dot{\gamma}_{\rm loss}.$$

$$\frac{B^2}{8\pi} = u_{e_1} + u_p + u_{e_2}.$$

Simplest case → $N(E) \propto (\mathrm{d}E/\mathrm{d}t)^{-1} \int_E Q(E)\mathrm{d}E$

pp, Bremss, ad.

$$\frac{dE}{dt} \propto E: \quad N(E) \propto E^{-\alpha}$$

Synchr., IC (Thompson)

$$\frac{dE}{dt} \propto E^2: \quad N(E) \propto E^{-(\alpha+1)}$$

Ionization

$$\frac{dE}{dt} \propto const: \quad N(E) \propto E^{-(\alpha-1)}$$

IC (K-N)

$$\frac{dE}{dt} \propto E^{-1}: \quad N(E) \propto E^{-(\alpha-2)}$$

Particle acceleration and losses

$$t_{\rm sync} \approx 4 \times 10^{11}\, B_{-3}^{-2}\, E_{\rm GeV}^{-1}\ {\rm s},$$

$$t_{\rm IC} \approx 1.6 \times 10^{13}\, u_{\rm IR-9}^{-1}\, E_{\rm GeV}^{-1}\ {\rm s},$$

$$t_{\rm Brems} \approx 3.5 \times 10^{10}\, n_{\rm j,c3}^{-1}\, F_{10}^{-1}\ {\rm s},$$

$$t_{\rm pp} \approx 5 \times 10^{10}\, n_{\rm j,c3}^{-1}\, F_{10}^{-1}\ {\rm s},$$

$$t_{\rm diff} \approx 1.5 \times 10^{12}\, d^{-1}\, R_{\rm j16}^{2}\, B_{-3}\, E_{\rm GeV}^{-1}\ {\rm s},$$

$$t_{\rm life} \approx 10^{11}\, Z_{\rm pc}\, v_{\rm bs8}^{-1}\ {\rm s},$$

$$t_{\rm gain} = E/\dot{E}_{\rm e,p\ gain} \approx 6.7 \times 10^{4}\, d\, v_{\rm r,bs8}^{-2}\, B_{-3}^{-1} E_{\rm GeV}\ {\rm s},$$

$$d = D/D_{\rm B},\ \text{with}\ D_{\rm B} = cr_{\rm g}/3$$

$$E_{\rm max\ sync} \approx 2.4 \times 10^{3}\, d^{-1/2}\, v_{\rm r,bs8}\, B_{-3}^{-1/2}\ {\rm GeV},$$

$$E_{\rm max\ IC} \approx 1.5 \times 10^{4}\, d^{-1/2}\, v_{\rm r,bs8}\, u_{\rm IR-9}^{-1/2}\, B_{-3}^{1/2}\ {\rm GeV},$$

$$E_{\rm max\ Brems} \approx 5.2 \times 10^{5}\, d^{-1}\, v_{\rm r,bs8}^{2}\, B_{-3}\, n_{\rm j/c3}^{-1}\, F_{10}^{-1}\ {\rm GeV},$$

$$E_{\rm max\ pp} \approx 7.5 \times 10^{5}\, d^{-1}\, v_{\rm r,bs8}^{2}\, B_{-3}\, n_{\rm j/c3}^{-1}\, F_{10}^{-1}\ {\rm GeV},$$

$$E_{\rm max\ diff} \approx 4.7 \times 10^{3}\, d^{-1}\, v_{\rm r,bs8}\, B_{-3}\, R_{\rm j16}\ {\rm GeV},$$

$$E_{\rm max\ life} \approx 1.5 \times 10^{5}\, d^{-1}\, Z_{\rm pc}\, v_{\rm r,bs8}\, B_{-3}\ {\rm GeV}.$$

Additional details of the model

- Effects of both the forward and reverse shocks are considered. The reverse shock is responsible for particle acceleration up to relativistic energies, and the forward shock sweeps matter while decelerates.
- Swept matter by the bow shock is a target for pp and ep interactions.
- Protons can escape from the acceleration region and diffuse into the molecular cloud.
- Several protostars can “light up” a giant cloud in gamma-rays.

HH 80-81: a partially embedded massive protostellar system

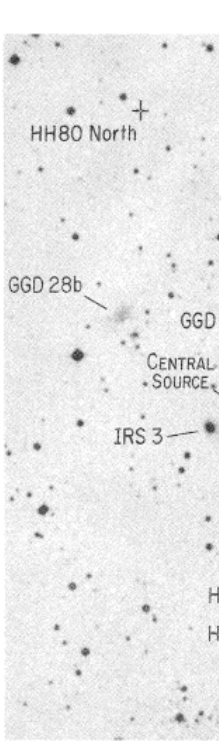

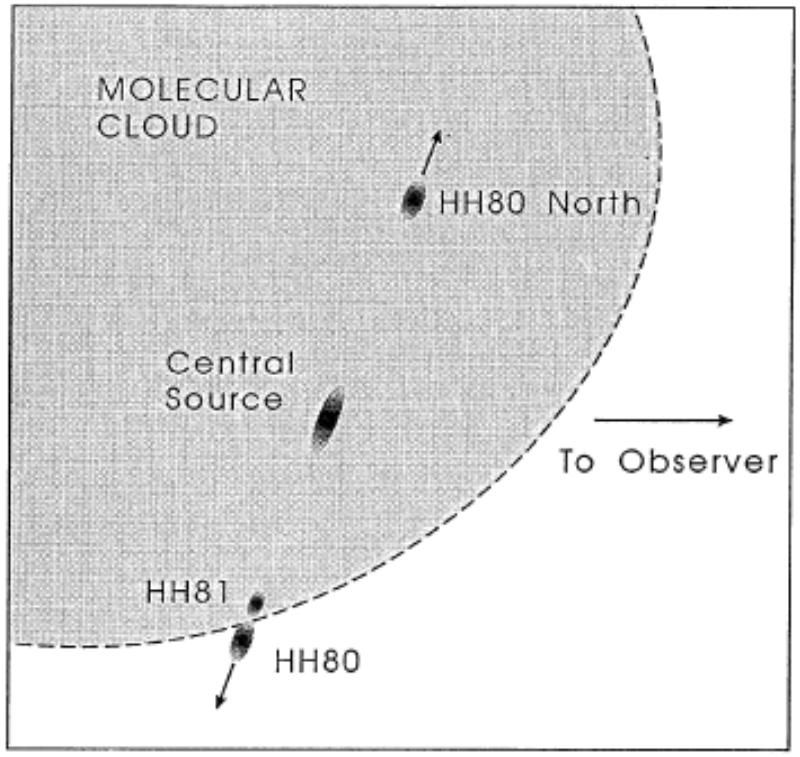

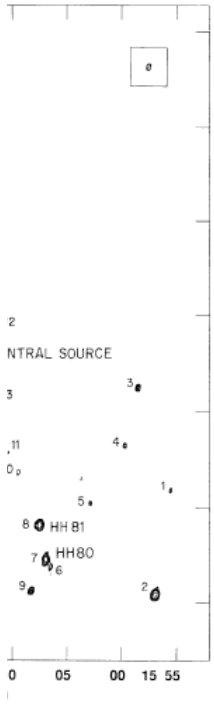

FIG. 1.—(*a*) The region of HH
arcseconds from the central source
east is left. (*b*) Composite VLA 6
northern counterpart of HH 80–8

FIG. 7.—A possible geometry proposed for the HH 80–81 system in order to account for the fact that the optically visible HH objects are redshifted.

) 27b is a reflection nebula a few
cal counterpart. North is up, and
ry beam response-corrected. The
lowing a slightly sinusoidal path.
This can be interpreted as evidence of jet precession. Contours are −3, 3, 4, 5, 7, 10, 20, 30, and 100 times 20 μJy per beam, the rms noise of the individual maps. The beam size is 7.0 × 4.9 with position angle of −18°.

Martí, Rodriguez & Reipurth (1993)

Some basic parameters for HH 80-81

- $v_j \sim 700$ km/s
- $n \sim 1000$ cm^{-3}
- $R_{HH} \sim 5\ 10^{16}$ cm
- $D \sim 1.7$ kpc
- $L_X \sim 4\ 10^{31}$ erg/s
- $B_{eq} \sim 5$ mG
- $E_{max,\,p} \sim 3\ 10^{14}$ eV - $E_{max,\,e} \sim E_{max,\,p}/12$

See Martí et al. (1993), Pravdo et al. (2004), and Bosch-Ramon et al. (2010) for details on the source.

SED for HH 80-81

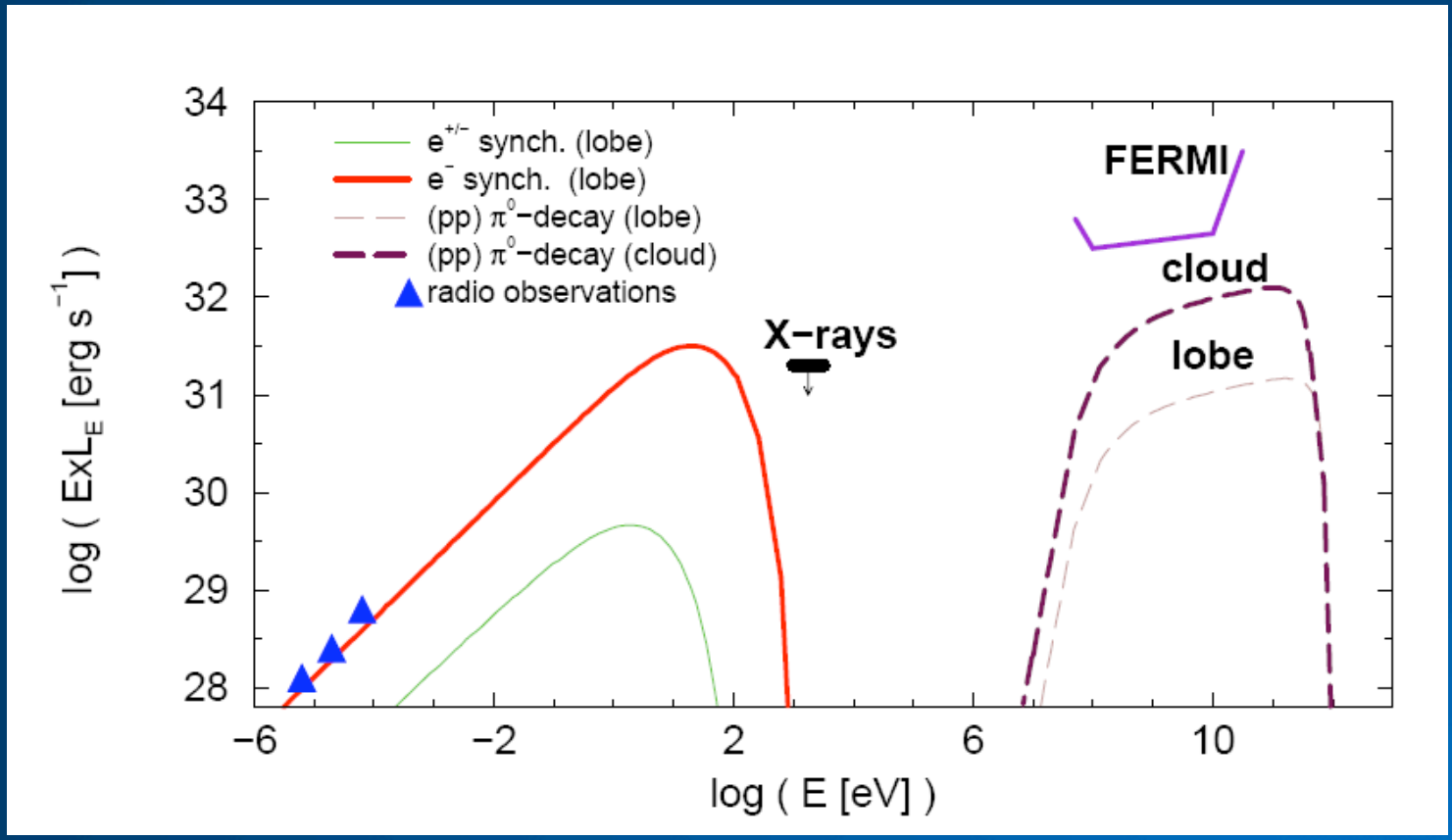

a=100

The massive protostar IRAS 16547-4247

Southern lobe:

S=cte $\mathbf{n}^{a}$,
a~ -0.6

d=2.9 kpc

B~10^{-3} G

V_s~1000 km/s

Clear non-thermal emission

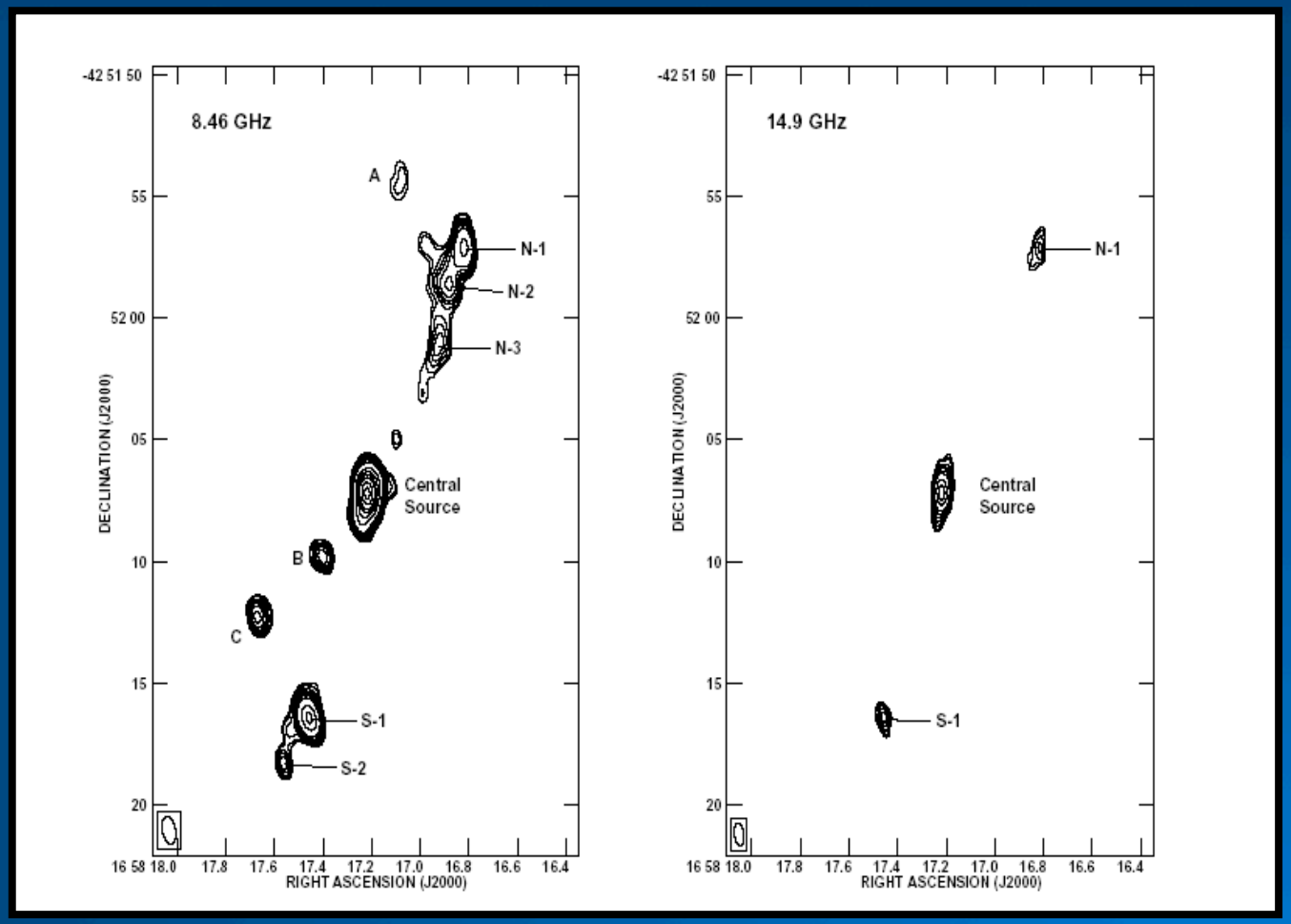

Rodríguez et al. (2005)

VLA

SEDs for **IRAS 16547-4247**

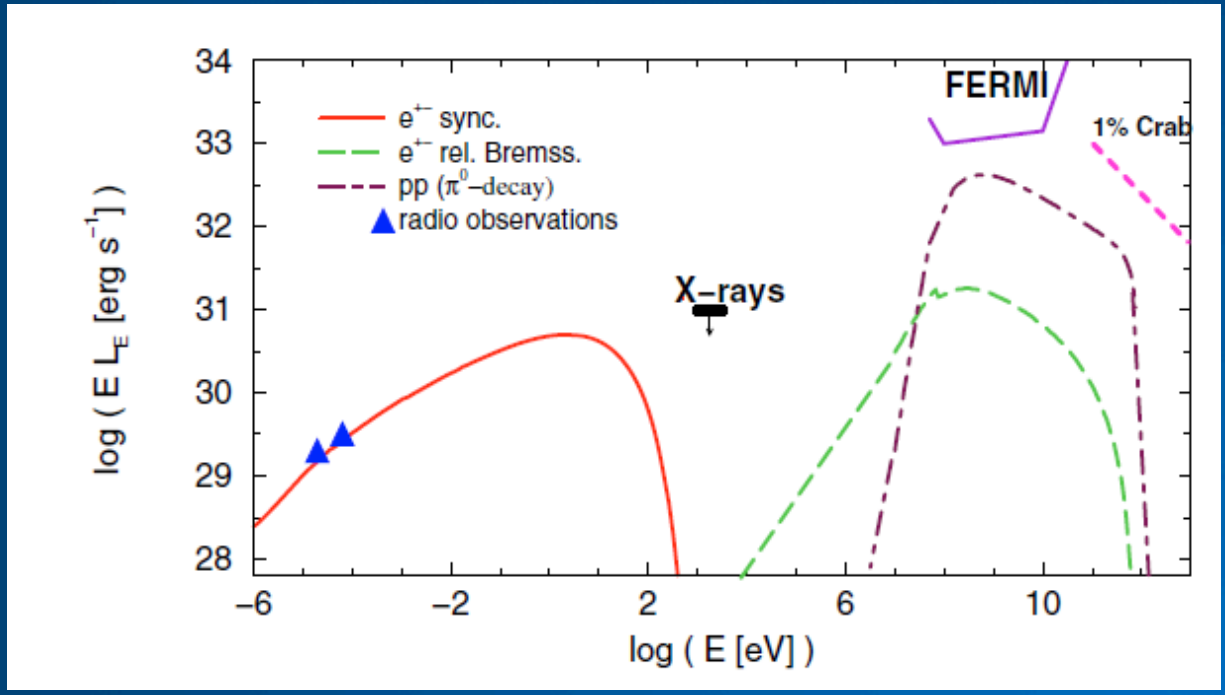

Bosch-Ramon et al. (2010)

Radio-gamma connection

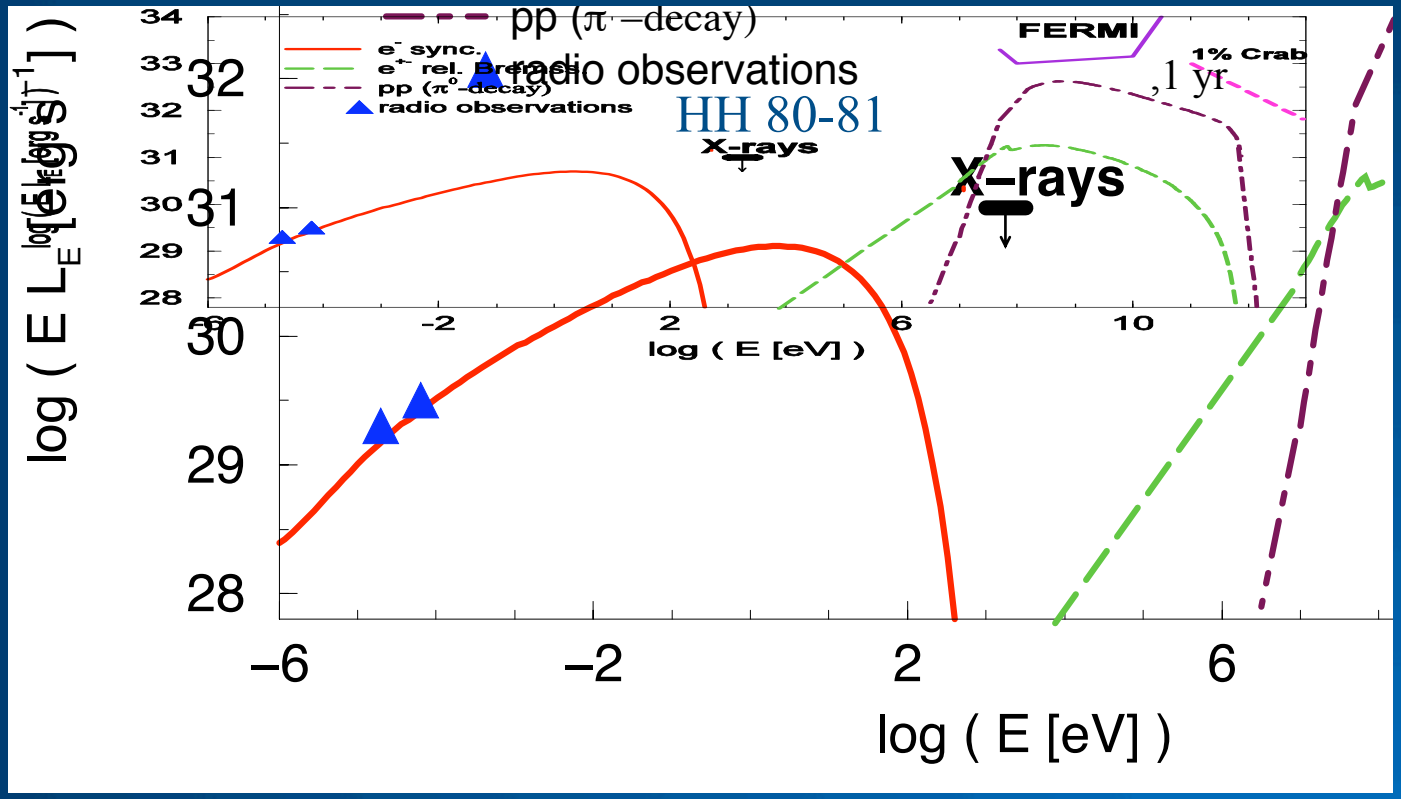

Spectral energy distribution of the non-thermal emission for HH 80 (Bosch Ramon et al. 2010), $n_{cloud} = 10^3/cm^3$.

Gamma-ray astronomy can be used to probe the physical conditions in star-forming regions and particle acceleration processes in the complex environment of massive molecular clouds.

Low-mass proto-stars: T-tauri

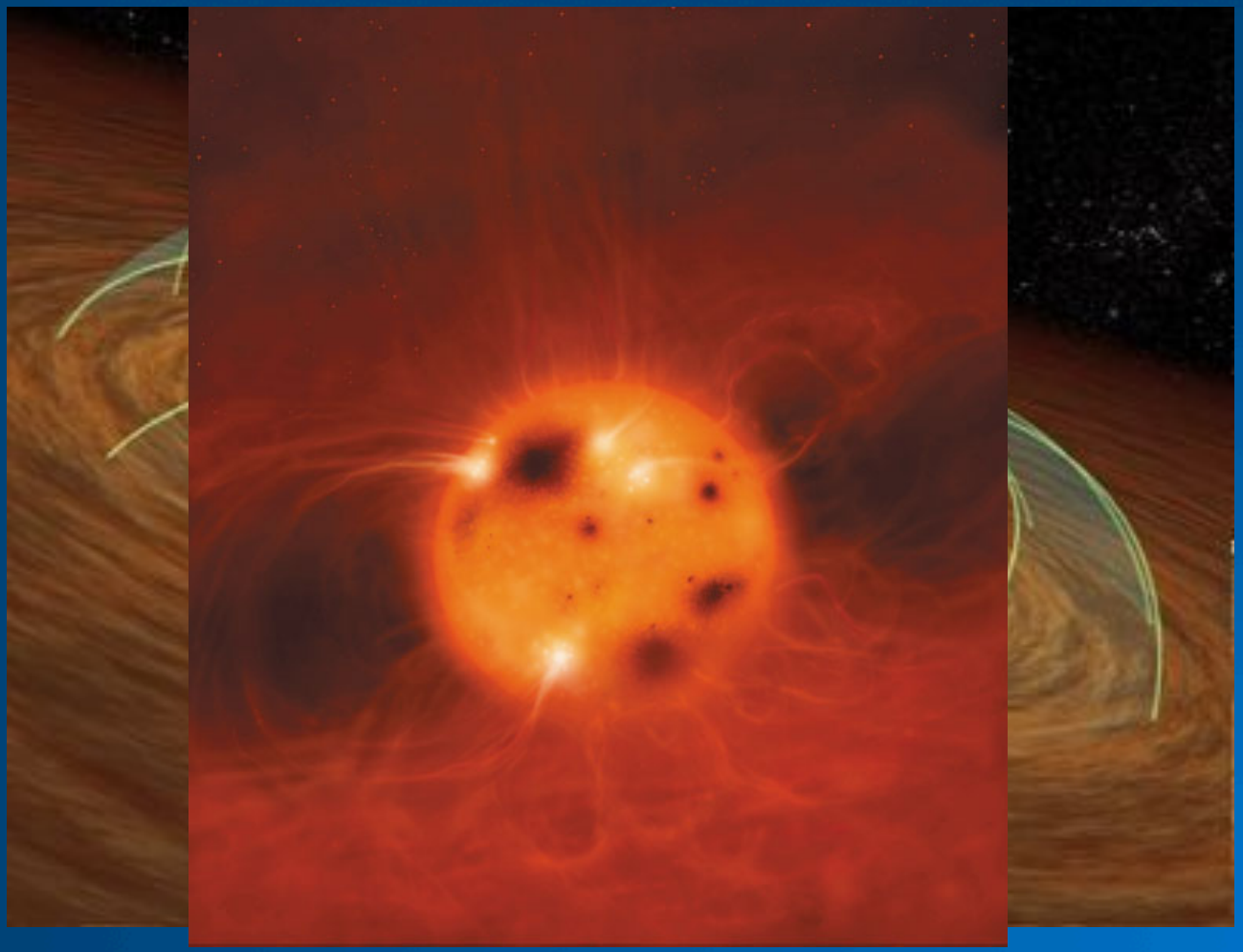

Magnetic reconnection in T-Tauri magnetospheres

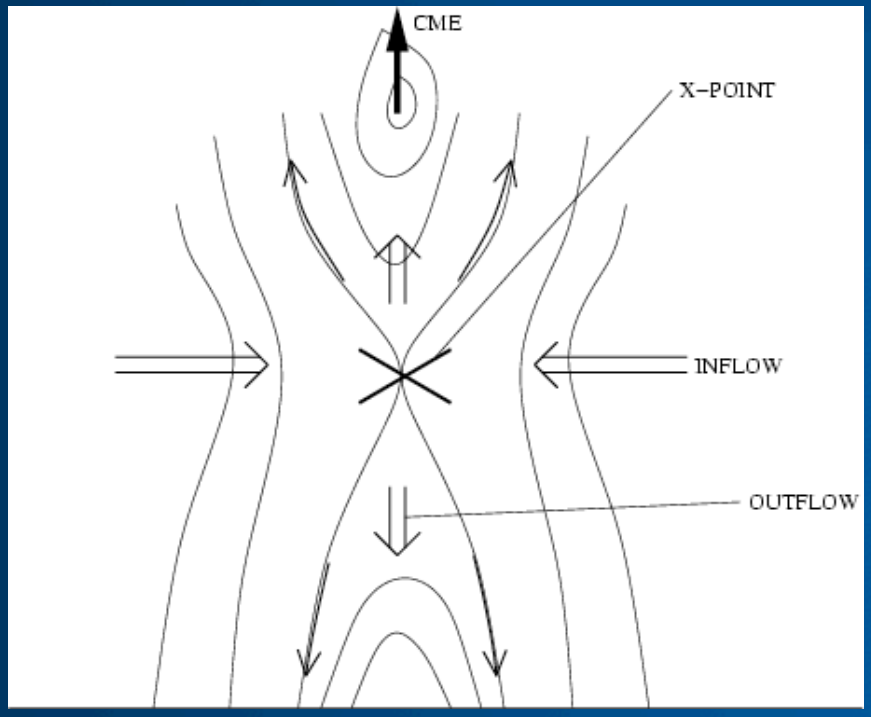

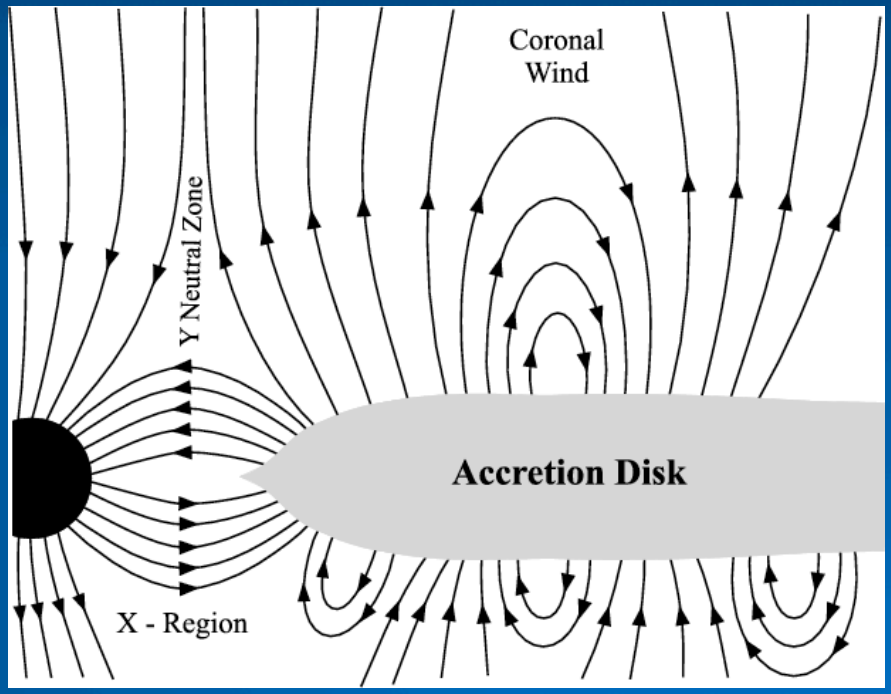

e.g. de Gouveia Dal Pino, E.M., Piovezan, P.P., & Kadowaki, L.H.S. 2010, A&A, 518, id. A5; Kowal, G., de Gouveia Dal Pino, E.M., & Lazarian, A. 2011, ApJ, in press.

The power available in the magnetized system is

$$L = \frac{B^2}{8\pi} A\, v_{\rm A},$$

The efficiency of non-thermal acceleration in the magnetized plasma is

$$\eta \sim 10^{-1} \frac{r_{\rm g} c}{D} \left(\frac{v_{\rm rec}}{c}\right)^2,$$

$v_{\rm rec} = 0.6 v_{\rm A}$, that gives an efficiency $\eta \sim 10^{-6}$.

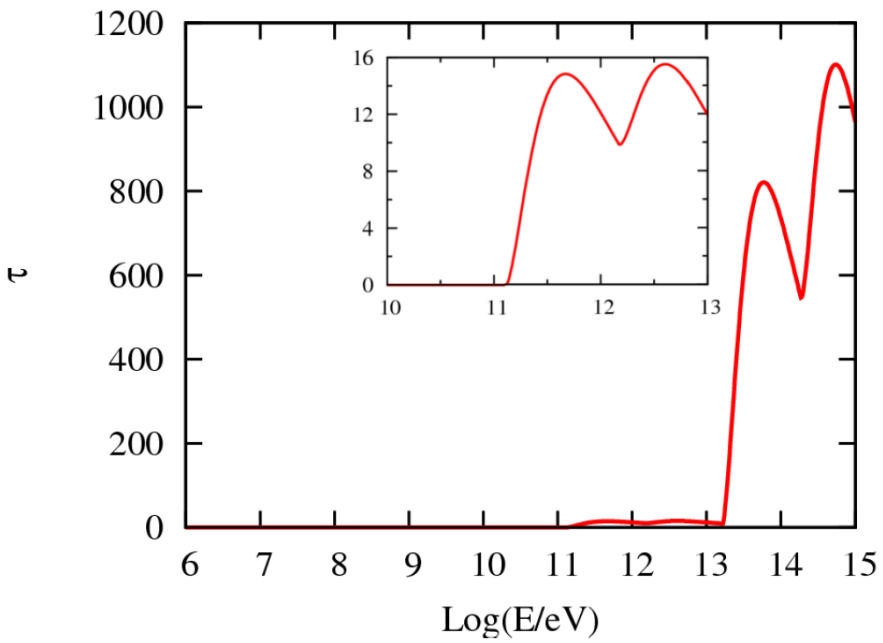

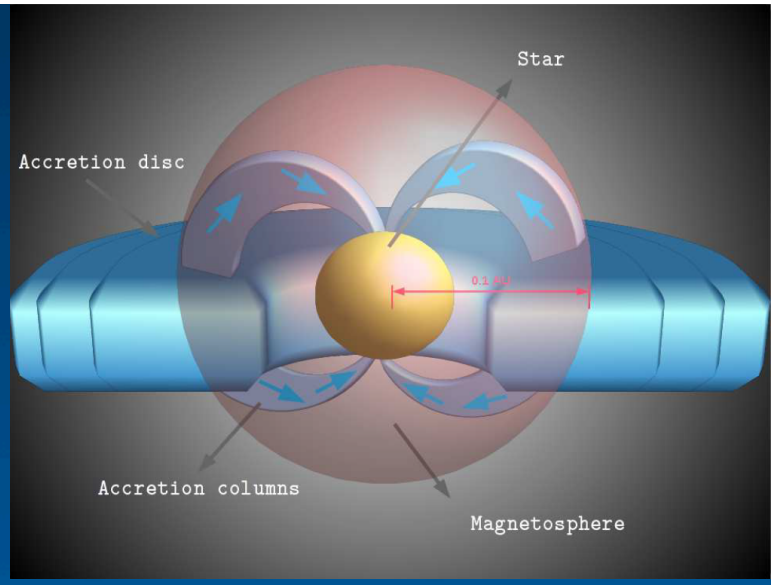

Del Valle, Romero, Martí, et al. ApJ, 2011, in press

Absorption

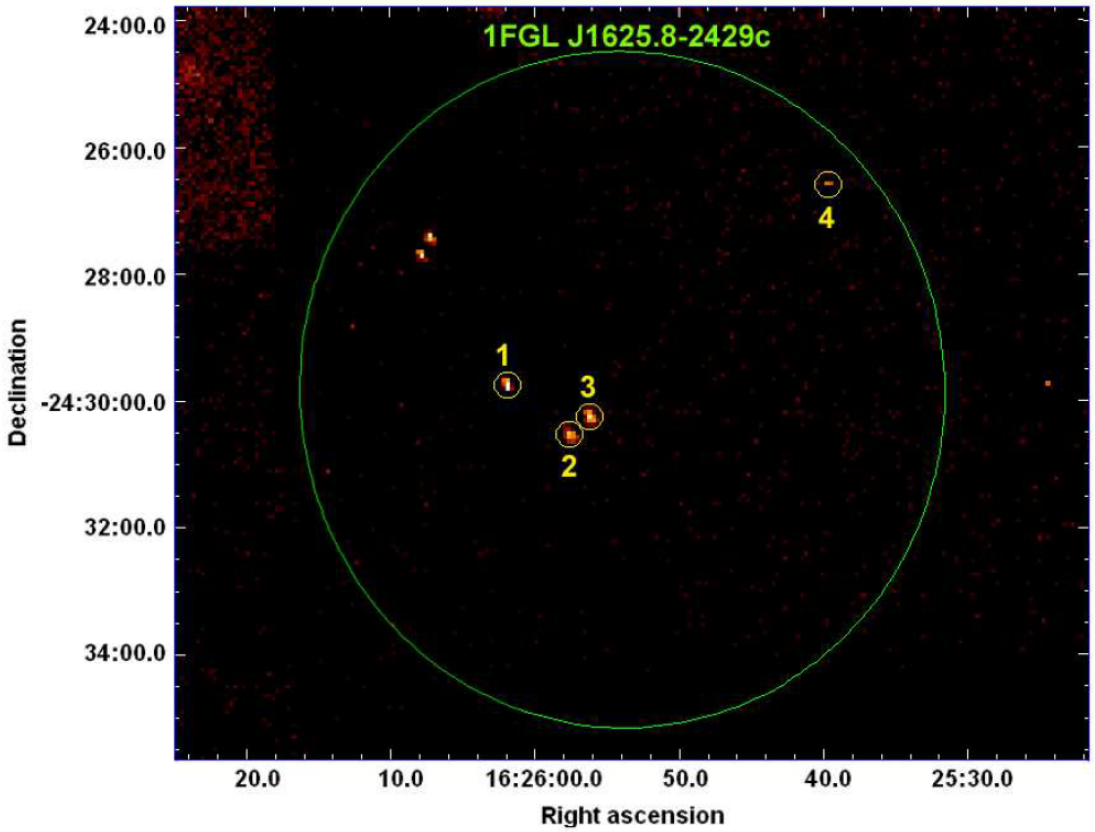

Fig. 8.— Composite X-ray image of the 1FGL J1625.8−2429c error circle obtained with the *Chandra* ACIS camera in the energy range 0.1-10 keV (Dataset identifier: ADS/Sa.CXO#obs/00618). Numbers indicate the T Tauri stars consistent with this *Fermi* source in decreasing order of right ascension. All of these stars are X-ray emitters.

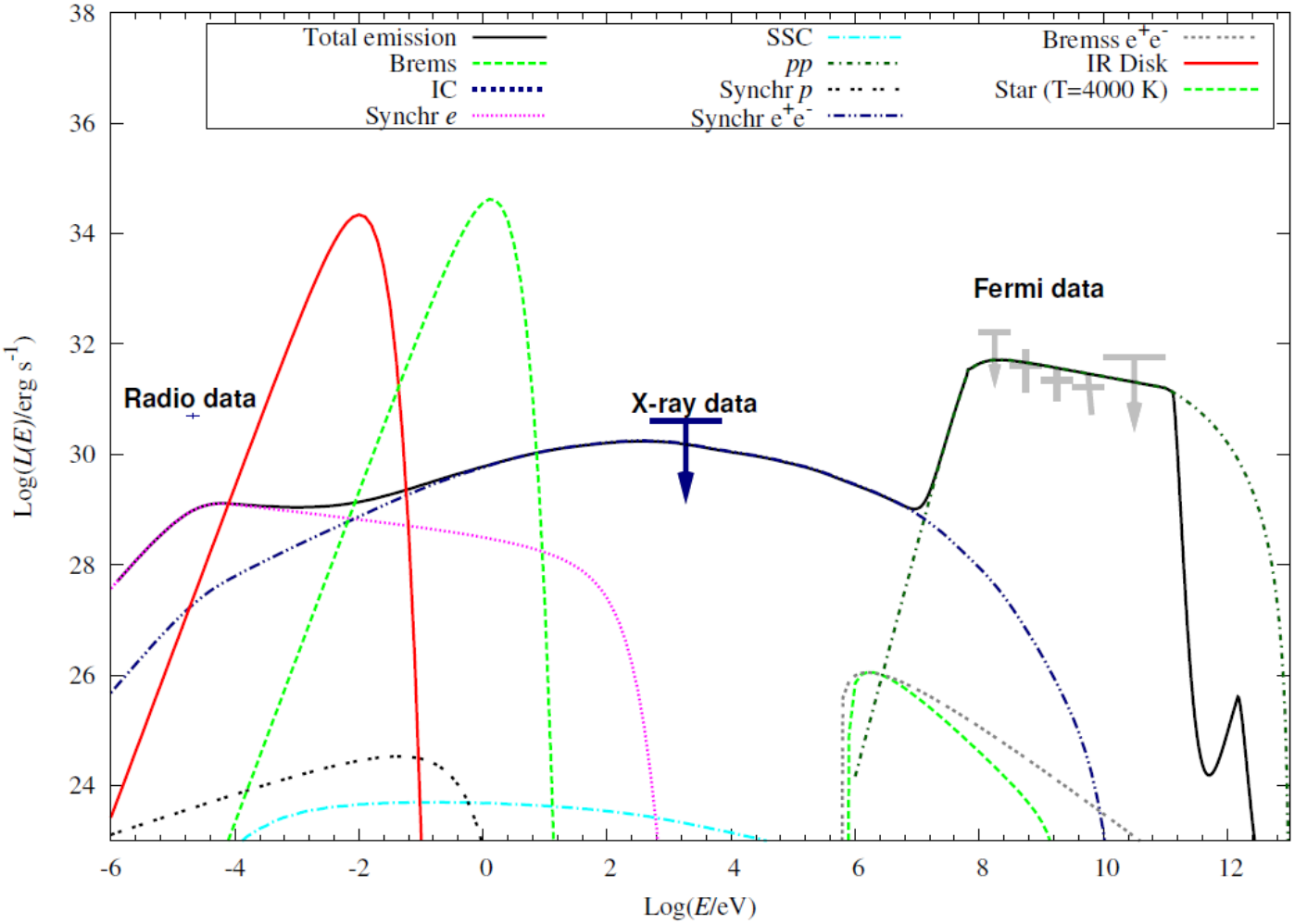

Fig. 10.— Computed non-thermal luminosity and *Fermi* upper bounds for the four T Tauri stars, assuming a distance of 120 pc. The spectral energy distribution is corrected by photon absorption.

Association of gamma-ray sources with SFRs: a long story

THE ASTROPHYSICAL JOURNAL, 231:95–110, 1979 July 1

ON GAMMA-RAY SOURCES, SUPERNOVA REMNANTS, OB ASSOCIATIONS, AND THE ORIGIN OF COSMIC RAYS

THIERRY MONTMERLE
Section d'Astrophysique, Centre d'Etudes Nucléaires de Saclay, France
Received 1978 July 26; accepted 1979 January 5

ABSTRACT

Although supernova explosions are widely thought to give rise to cosmic rays (nucleons), there is, as yet, no direct evidence from individual objects to support this view. A possible tool in this respect is the detection of γ-rays emitted by supernova remnants (SNRs) via π^0 decay, which results from high-energy cosmic ray interactions with the ambient matter. However, the accumulating γ-ray data (in particular from the *Cos B* satellite) show that SNRs as a class are not γ-ray sources, but rather that γ-ray sources are, in general, closely linked with young objects. Bearing in mind the cosmic-ray production problem, we examine, among other possibilities, if a *restricted* class of SNRs are actually γ-ray sources; we restrict the class to those SNRs physically linked with extreme Population I objects.

Along these lines, spatial coincidences between SNRs and OB associations or H II regions (SNOBs) are sought by various methods, and this yields a list of about 30 objects (which is certainly incomplete). From the *Cos B* data, one finds that five (perhaps six) out of 11 as yet unidentified γ-ray sources (above 100 MeV) are associated with SNOBs, and there is a hint that as much as three-fourths of the best identified SNOBs are seen in γ-rays. The associated probabilities of chance coincidence are $\sim 10^{-4}$. Angular and other statistical considerations also support this association.

Pending confirmation, if a substantial proportion of the observed γ-rays does come from π° decay, SNOBs appear to be a major source of galactic cosmic rays, in which cosmic-ray (≥ 2 GeV) energy densities in the range $\sim$ 10–100 times the solar neighborhood value are found. To lead the way toward a possible model for the origin of cosmic rays consistent with the γ-ray data, a phenomenological scenario is suggested. In this scenario, cosmic rays are produced by a two-step process, in which low-energy (MeV range) particles are injected by young stars pertaining to an OB association, and are subsequently accelerated by the shock wave of a neighboring supernova explosion.

In this context, we discuss such items as the case of "isolated" SNRs, the possible links with light-element production, further observational tests, and the links between SNOBs and other astronomical objects.

Subject headings: clusters: associations — cosmic rays: general — gamma-rays: general — nebulae: supernova remnants — stars: flare

Positional coincidences of EGRET sources with OB Assoc.

γ-source (3EG J)	F_γ (10^{-8} ph cm^{-2} s^{-1})	Γ	OB Assoc.	$\Delta\theta$ (deg)	r (kpc)	Size (deg)	L (10^{34} erg s^{-1})	Other coincidences
0229+6151	37.9±6.2	2.29±0.18	Cas 6	1.44	2.01	0.95	11.1 ± 1.6	Of
0617+2238	51.4±3.5	2.01±0.06	Gem 1	2.07	1.34	1.94	6.7 ±0.4	SNR
0634+0521	15.0±3.5	2.03±0.26	Mon 2A	1.27	1.63	0.84		Of/SNR
			Mon 1B	1.27	1.48	0.60	2.4 ± 0.6	
0824-4610	63.9±7.4	2.36±0.07	VELA 2	4.75	0.49	4.14	1.1 ± 0.1	SNR
0848-4429*	20.1±7.7	2.05±0.16	VELA 1B	1.62	1.41	1.00	2.3 ± 1.7	
1027-5817*	65.9±7.0	1.94±0.09	Car 1A	1.17	2.40	0.80		
			Car 1B	1.98	2.14	1.61	21.8 ±2.3	
1048-5840*	61.8±6.7	1.97±0.09	Car 1B	1.78	2.14	1.61	20.5± 2.2	
			Car 1E	1.72	2.64	1.55		
			Car 1F	0.72	2.76	0.55		
1102-6103	32.5±6.2	2.47±0.21	Car 1-2	1.17	2.62	0.56		WR/SNR
			Car 2	3.15	2.16	2.54	10.1 ± 3.0	
1308-6112	22.0±6.1	3.14±0.59	Cen 1B	1.15	1.76	0.44	5.0 ±1.3	
			Cen 1D	1.46	1.87	0.75		
			Sco 2A	8.89	0.16	8.18	0.04 ±0.01	
1410-6147	64.2±8.8	2.12±0.14	CLUST 3	1.12	1.51	0.76	10.6 ±1.4	Of/SNR
1420-6038*	44.7±8.6	2.02±0.14	CLUST 3	1.08	1.51	0.76	7.4 ± 1.4	
1639-4702	53.2±8.7	2.5±0.18	Ara 1A A	1.95	1.59	1.39	9.8 ± 1.5	SNR
			NGC 6204	2.11	1.94	1.55		
1655-4554	38.5±7.7	2.19±0.24	Ara 1A B	1.13	1.35	0.47	5.1 ± 1.0	WR
1718-3313	18.7±5.1	2.59±0.21	Sco 4	1.84	1.23	1.30	2.0 ±0.6	
1734-3232	40.3±6.7	–	Tr 27	1.63	1.31	1.14	5.0 ±0.8	SNR
1809-2328*	41.7±5.6	2.06±0.08	Sgr 1B	0.47	1.94	0.31	11.3 ± 1.7	
1823-1314	42.0±7.4	2.69±0.19	Sct 3	1.45	1.48	1.16	6.7 ± 1.2	
1824-1514	35.2±6.5	2.19±0.18	Sct 3	1.68	1.48	1.16	5.6 ± 1.0	SNR
1826-1302*	46.3±7.3	2.00±0.11	Sct 3	1.62	1.48	1.16	7.3 ± 1.2	
2016+3657	34.7±5.7	2.09±0.11	Cyg 1,8,9	5.49	1.17	4.94	3.4 ±0.6	WR/SNR
2020+4017	123.7±6.7	2.08±0.04	Cyg 1,8,9	5.10	1.17	4.94	12.3 ±0.6	SNR
2021+3716	59.1±6.2	1.86±0.10	Cyg 1,8,9	5.24	1.17	4.94	5.9 ± 0.7	WR
2022+4317	24.7±5.2	2.31±0.19	Cyg 1,8,9	5.66	1.17	4.94	2.4 ±0.5	WR
2027+3429*	25.9±4.7	2.28±0.15	Cyg 1,8,9	5.71	1.17	4.94	2.9 ±0.1	
2033+4118	73.0±6.7	1.96±0.10	Cyg 1,8,9	5.22	1.17	4.94	7.2 ±0.7	Of
2227+6112*	41.3±6.1	2.24±0.14	Cep 2 B	4.06	0.77	3.60	1.8 ±0.2	

* Pulsar candidate?.

The probability of chance association is negligible Romero et al. A&A 348, 868 (1999

Positional coincidences of *Fermi* sources with OB Assoc.

Object type	Coincident γ-ray sources	Simulated $1^\circ - bin$	Probability $1^\circ - bin$	Simulated $2^\circ - bin$	Probability $2^\circ - bin$
YSO	12	4.4±2.0	1.8×10^{-4}	3.6±1.8	5.6×10^{-6}
WR	2	1.3±1.1	2.9×10^{-1}	1.2±1.1	2.9×10^{-1}
Of-type	5	2.9±1.7	1.1×10^{-1}	2.9±1.7	1.1×10^{-1}
OB assoc.	107	72.5±8.0	4.2×10^{-6}	72.8±8.0	5.5×10^{-6}

The probability of chance association is still negligible

Munar-Adrover, Paredes & Romero, A&A, 530 (2011) A72

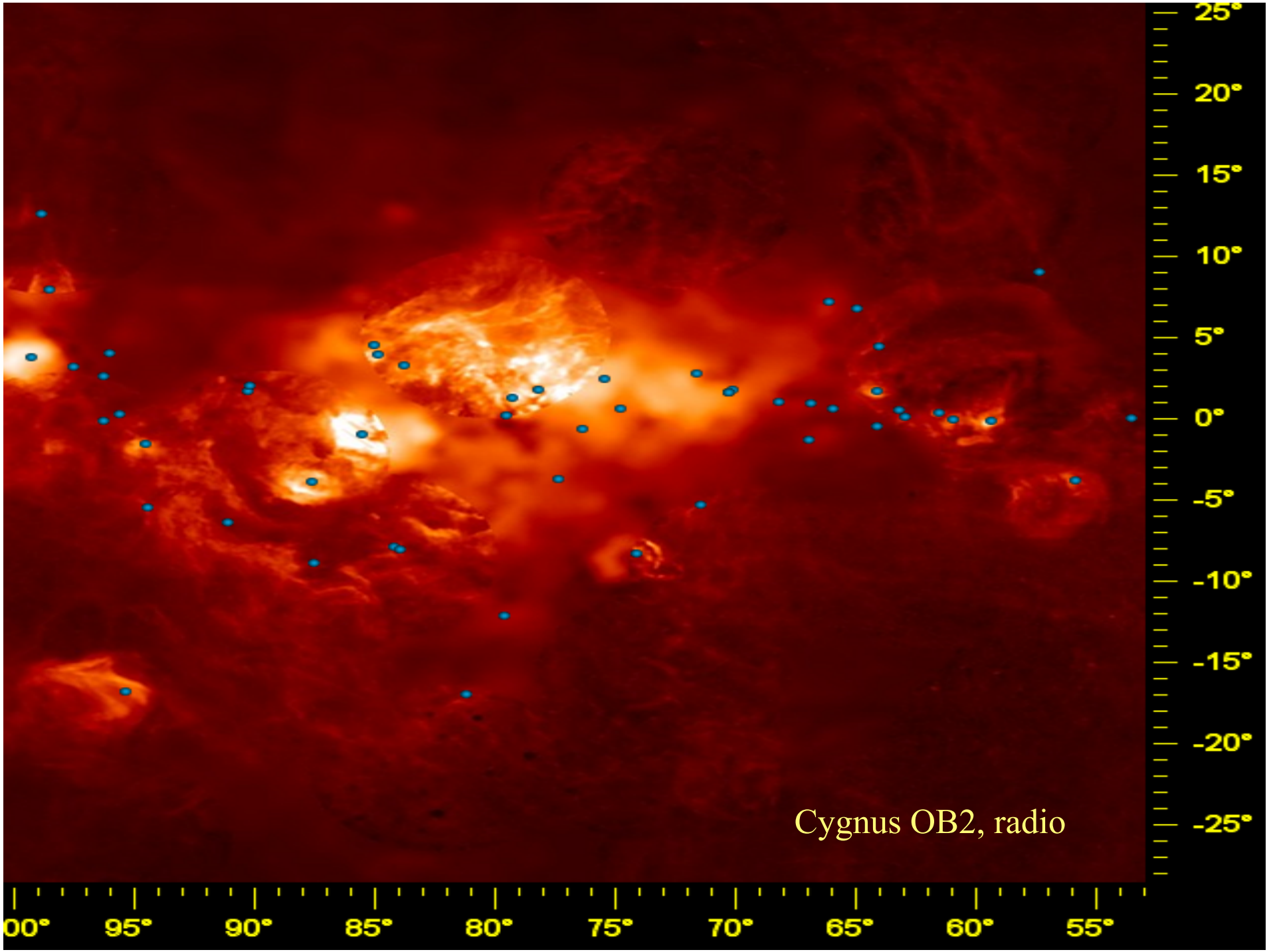
25°
20°
15°
10°
5°
0°
-5°
-10°
-15°
-20°
-25°
00°
95°
90°
85°
80°
75°
70°
65°
60°
55°
Cygnus OB2, radio

MAGIC OBSERVATIONS OF TeV J2032-4130

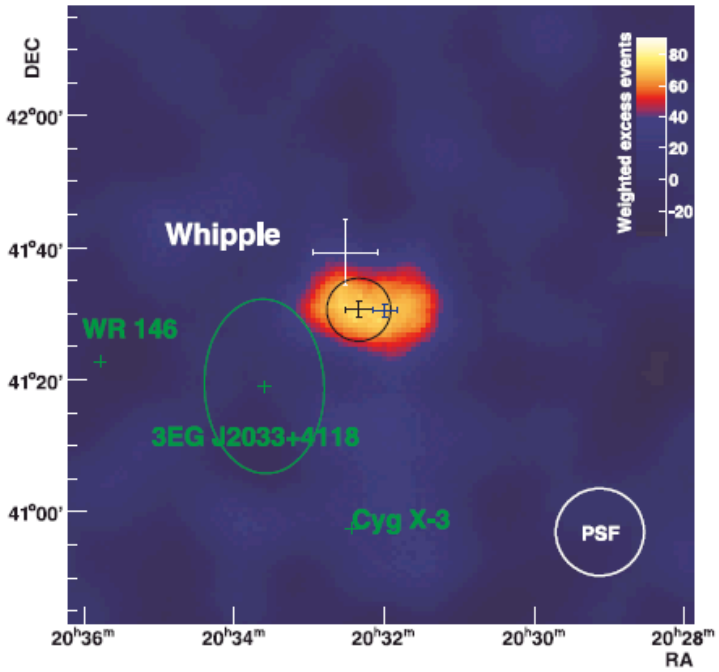

FIG. 2.—Gaussian-smoothed ($\sigma = 4'$) map of γ-ray excess events (background subtracted) for energies above 500 GeV. The MAGIC position is shown with a black cross. The surrounding black circle corresponds to the measured 1 σ width. The last position reported by Whipple is marked with a white cross while the HEGRA position is shown with a blue cross in the center of the field of view. The error bars, in all cases, correspond to the linear sum of the statistical and systematic errors. The green crosses correspond to the positions of Cyg X-3, WR 146, and the EGRET source 3EG J2033+4118. The ellipse around the EGRET source marks the 95% confidence contour.

Albert et al. 2008, ApJ, 675, L25

Westerlund 2 detected by HESS

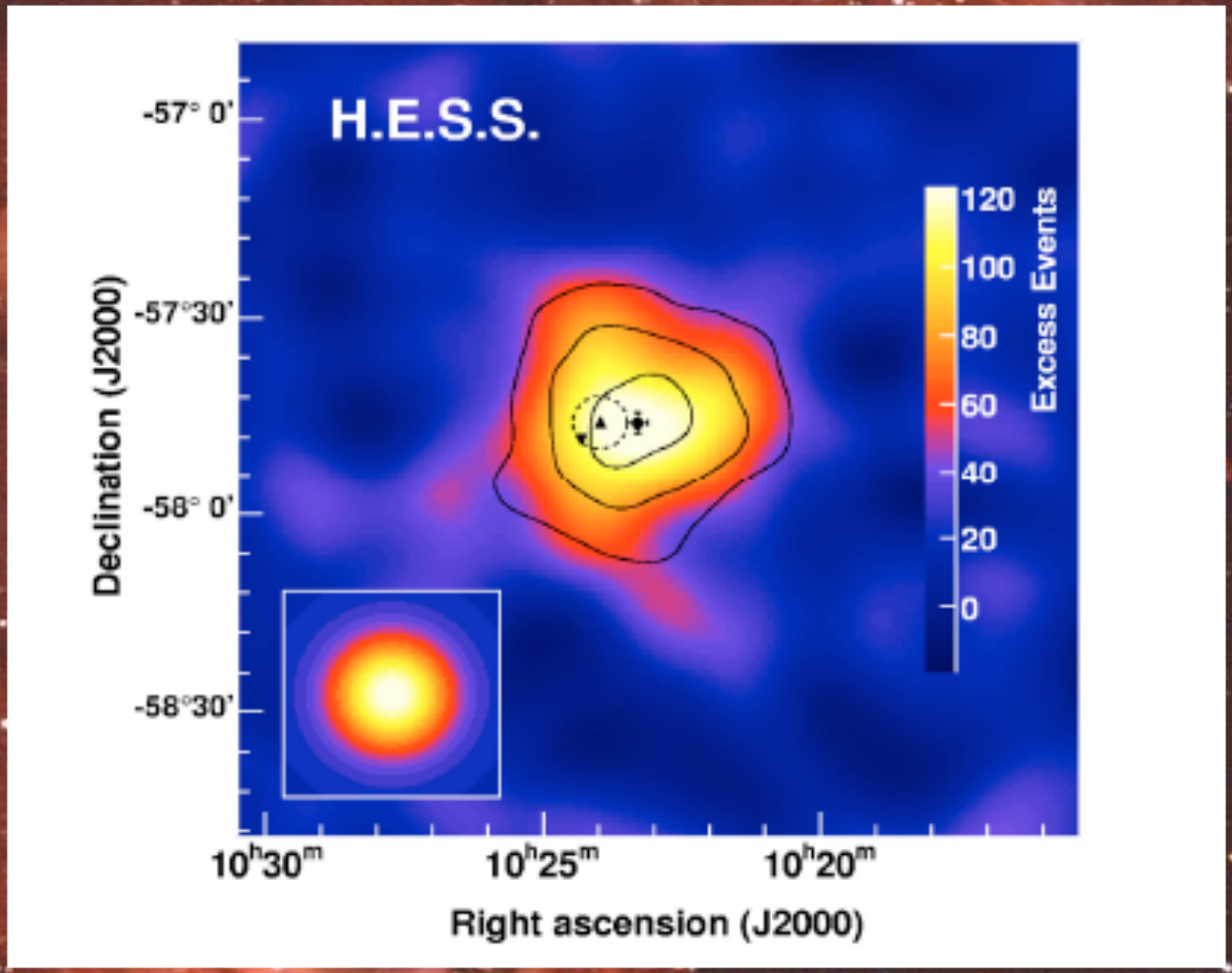

Aharonian et al. 2007, A&A 467, 1075

Gamma-rays from SFRs in other galaxies

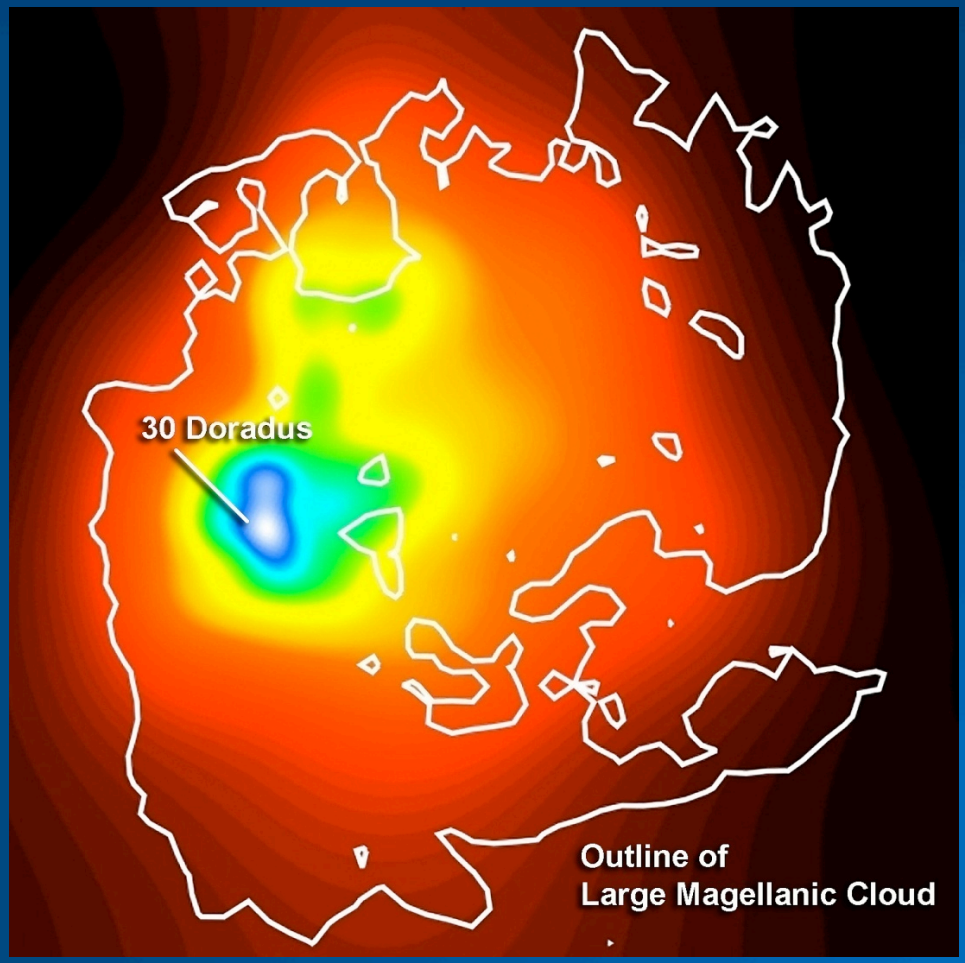

Fermi

NGC 253: An archetype of starburst galaxy

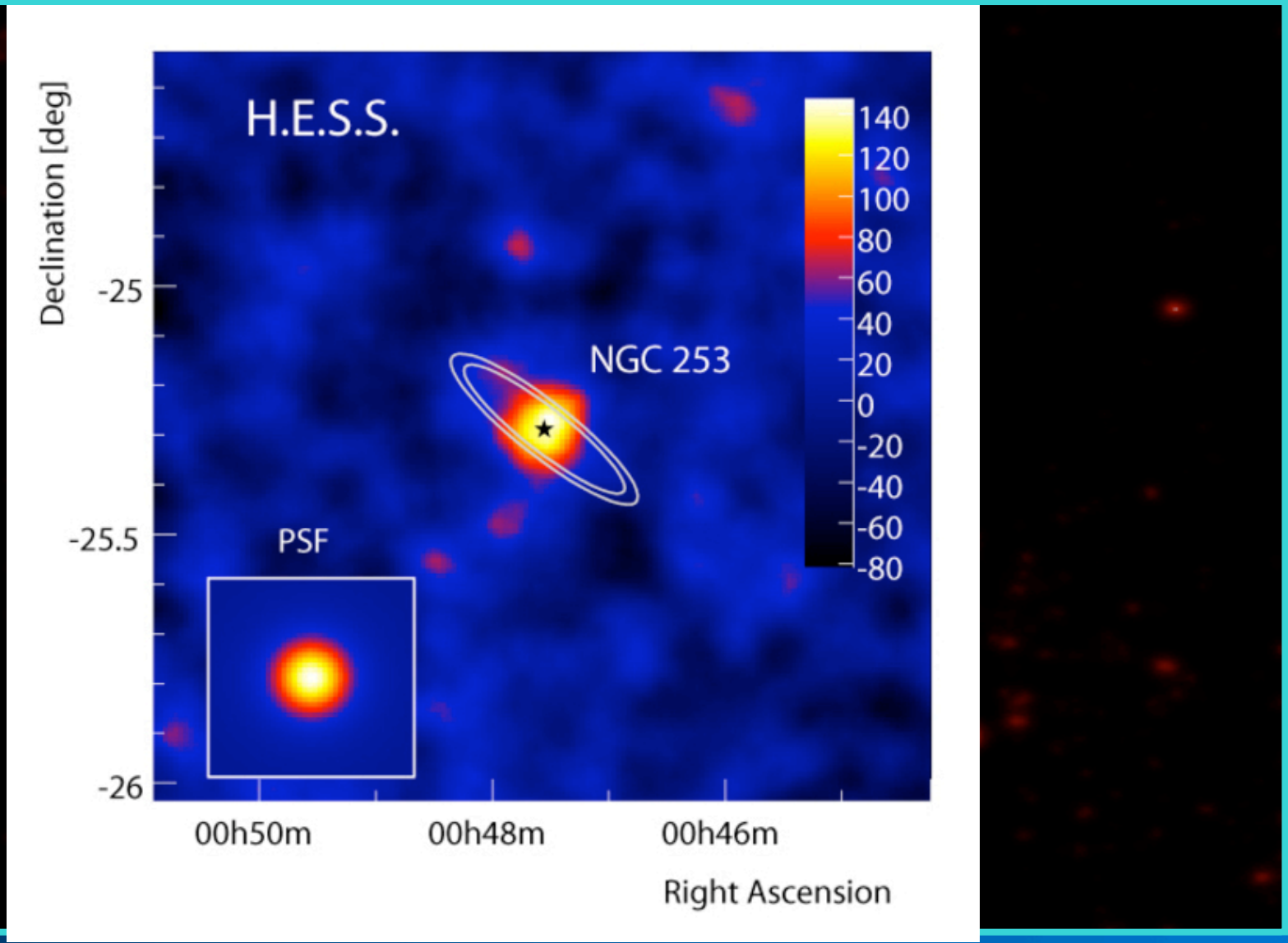

M 82

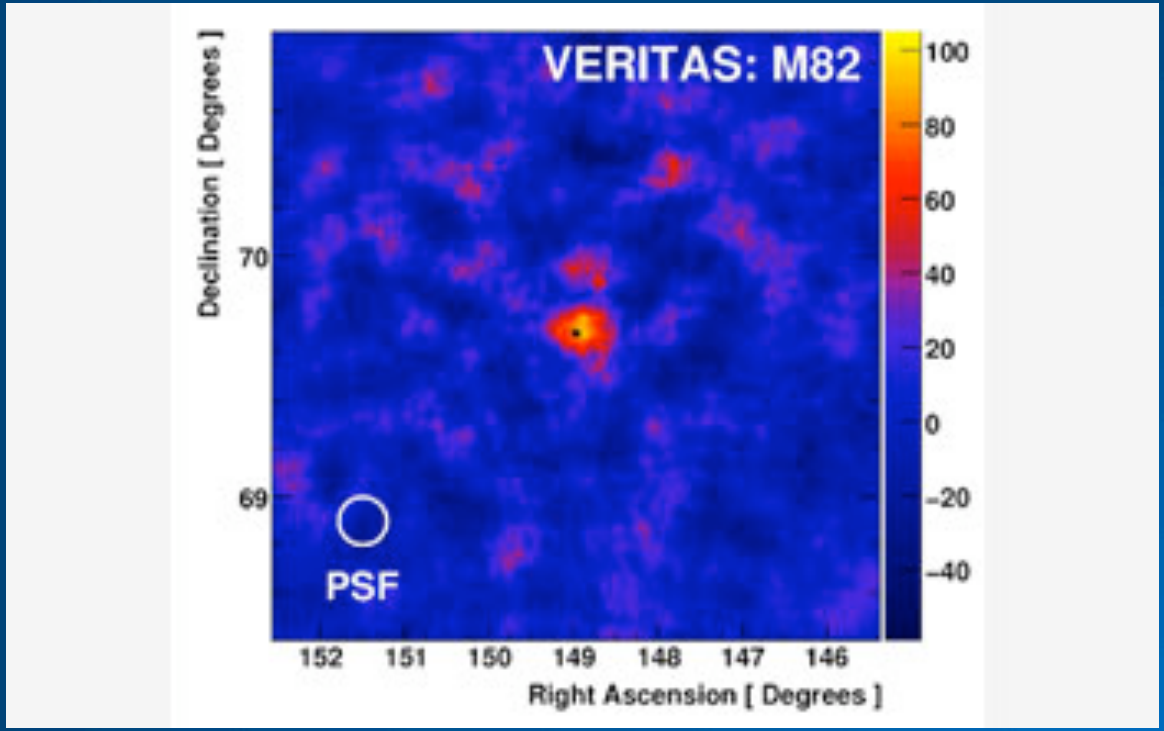
VERITAS: M82
Declination [Degrees]
70
69
PSF
152
151
150
149
148
147
146
Right Ascension [Degrees]
100
80
60
40
20
0
−20
−40

What does produce the gamma rays in SFRs?

- If the OB association had time to age, then SNRs and compact objects might be present, injecting high energy particles in a rather dense medium (e.g. Montmerle 1979, Aharonian & Atoyan 1996, Gabici & Aharonian 2007).

- In a rather young OB association, collective effects of the stellar winds of hot stars might play an important role (e.g. Bykov & Fleishman 1992; Bykov 1999; Torres, Domingo-Santamaría & Romero 2004; Bednarek 2007), as well as contributions from colliding wind binaries (Eichler & Usov 1993, Benaglia & Romero 2003, Reimer et al. 2006, Pittard & Dougherty 2006).

- If the SFR is very young then massive protostars can produce high-energy emission, a possibility almost not explored so far (Araudo, Romero, Bosch-Ramon & Paredes 2007, 2008; Bosch-Ramon et al. 2010)

Conclusions

- Protostars in young SFRs can be gamma-ray sources when embedded in the original molecular core.
- The typical luminosities are ~ 10^{33} erg/s at E>100 MeV.
- The cumulative effect of several protostars in a SFRs can make a source detectable by *Fermi* and MAGIC II / HESS II.
- Candidates should be found through a combination of IR, high-resolution radio, and molecular line observations.
- Gamma-ray astronomy can open a new window to the study of massive star forming processes. Excellent prospect for CTA.

Thank you!

Jet-launching: Disk winds II

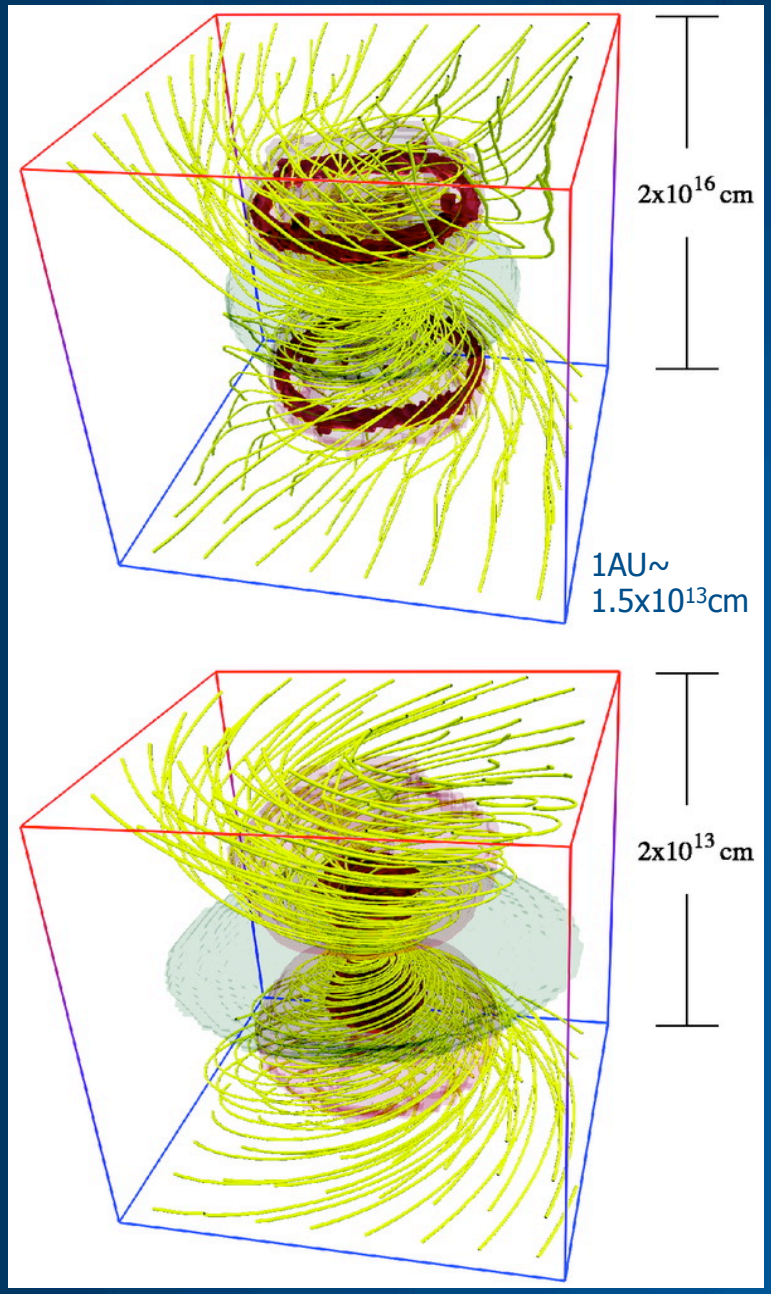

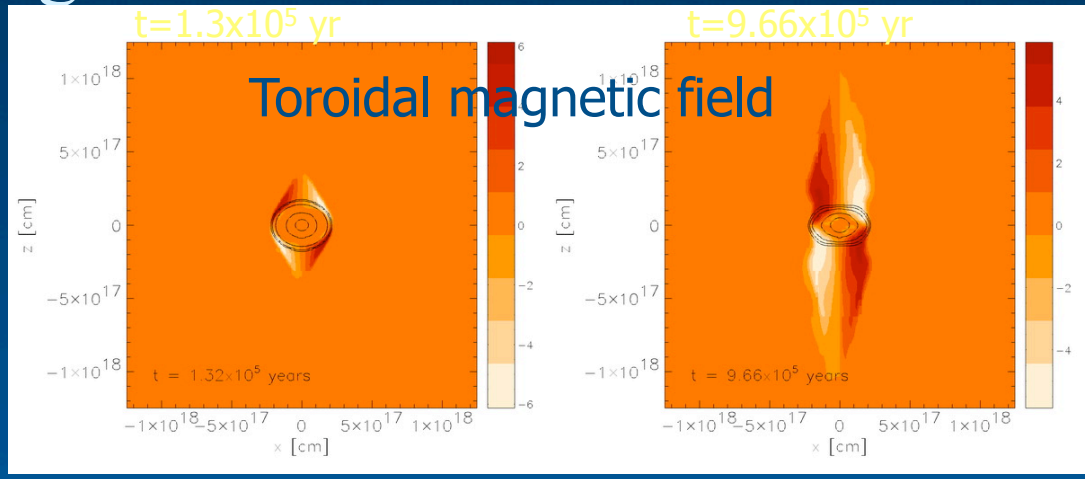

- On larger scales, a strong toroidal magnetic field builds up during collapse.

- At large radii (outside Alfven radius r_A, the radius where kin. energy equals magn. energy) B_f/B_p much larger than 1
  --> collimation via Lorentz-force $F_L \sim j_z B_f$

Banerjee & Pudritz 20

HH 80-81: the central source

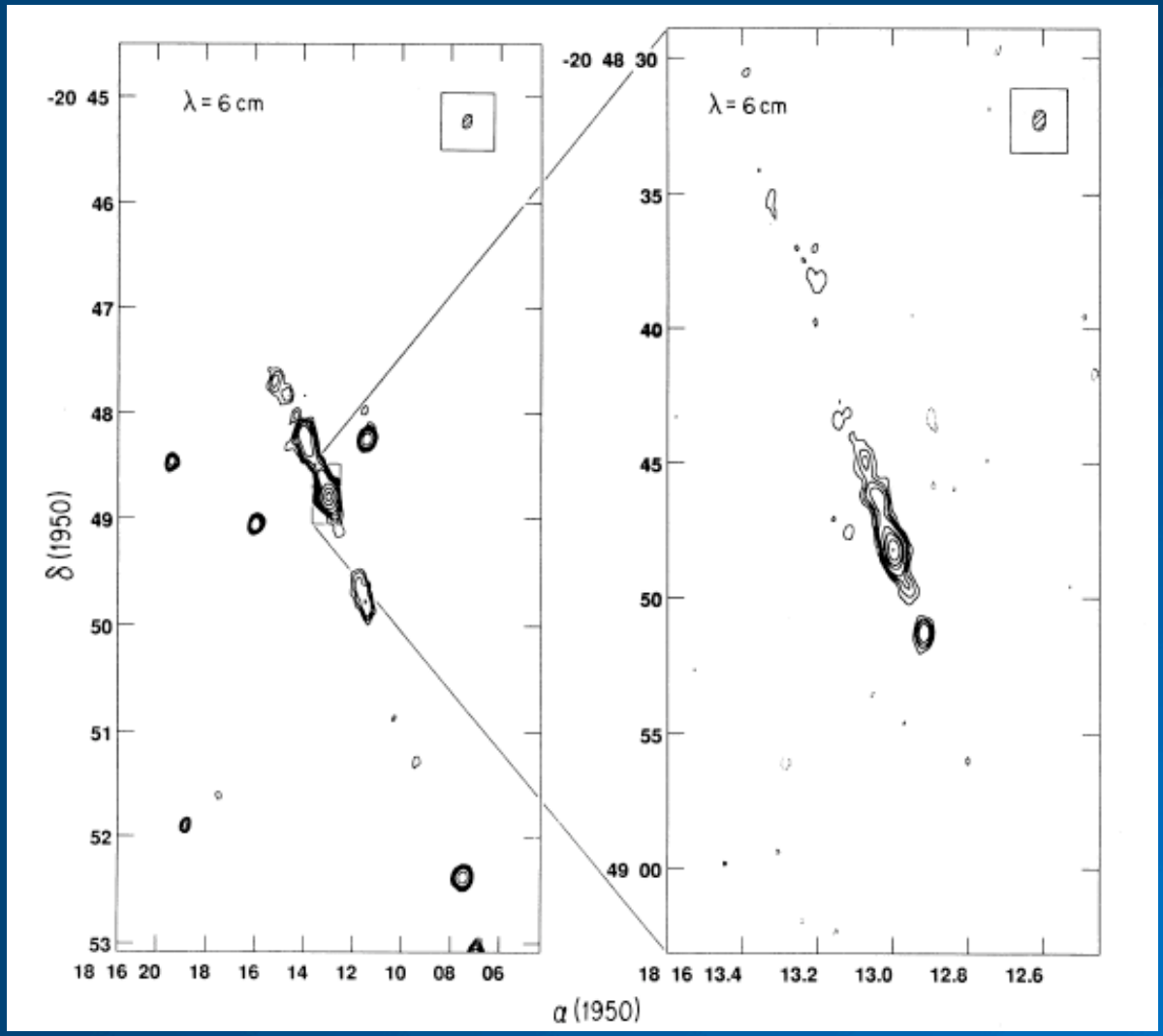

Martí, Rodriguez & Reipurth (1993)

IRAS 16359-4635

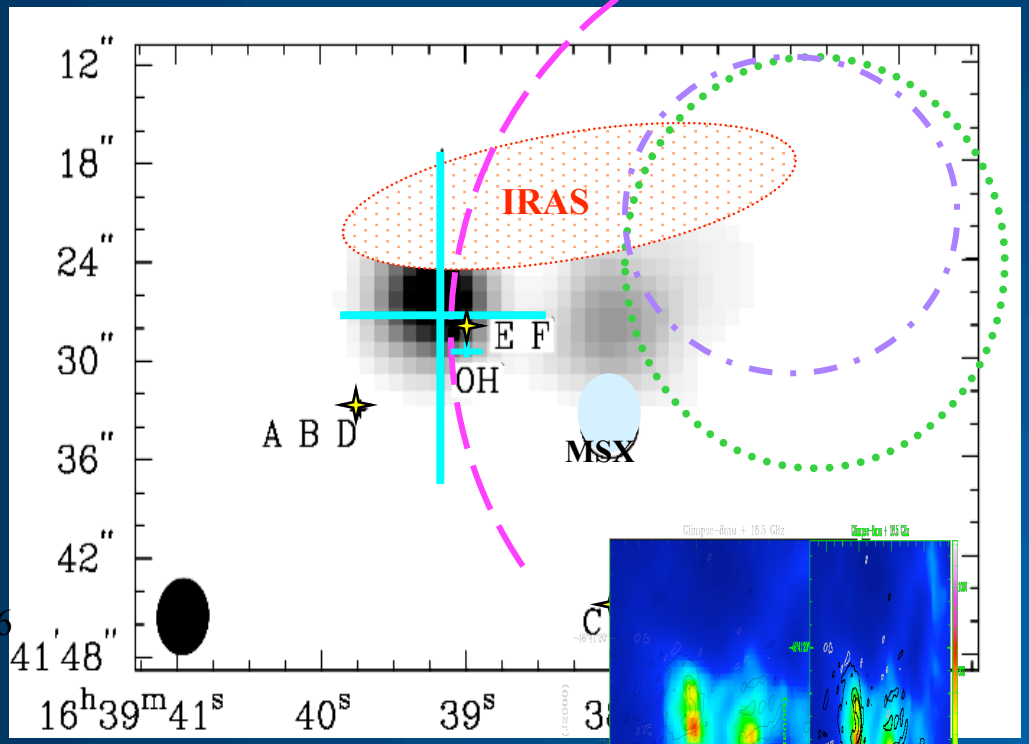

$d_1 \sim 3.5$ kpc

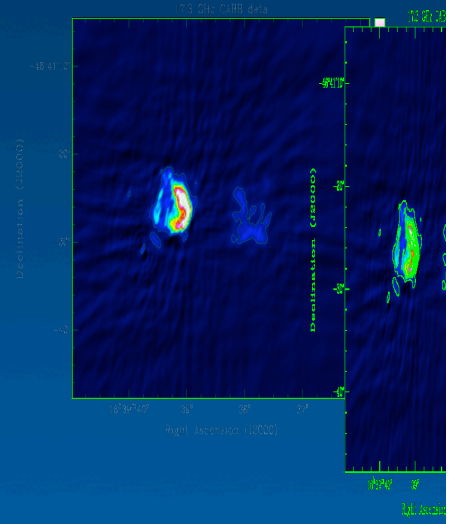

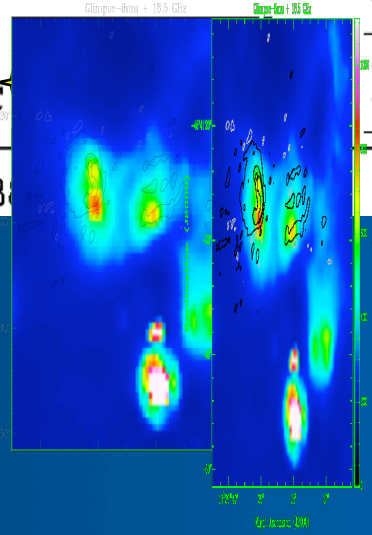

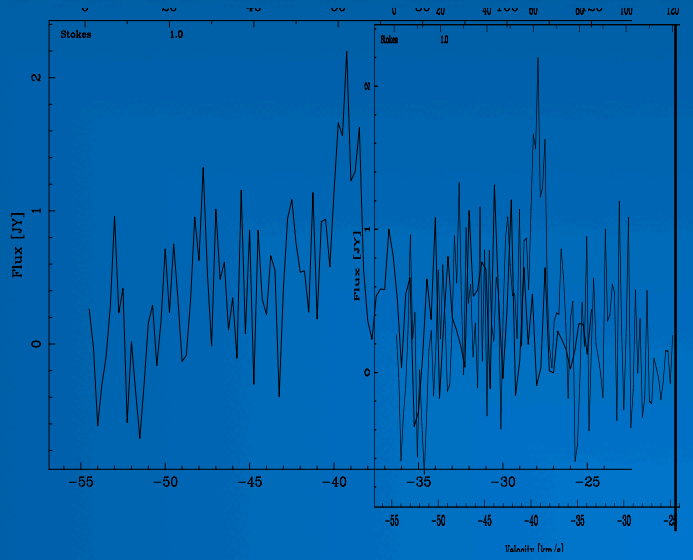

Benaglia & Koribalski 2011